UNIVERSITÀ
DEGLI STUDI
DI PADOVA

Sede Amministrativa: Università degli Studi di Padova

Dipartimento di Biologia

SCUOLA DI DOTTORATO DI RICERCA IN: BIOSCIENZE E BIOTECNOLOGIE

INDIRIZZO: GENETICA E BIOLOGIA MOLECOLARE DELLO SVILUPPO

CICLO XXVI

In vivo analyses of morphogen signalling pathways using Zebrafish transgenic reporter lines

Direttore della Scuola: Ch.mo Prof. Giuseppe Zanotti

Coordinatore d'indirizzo: Ch.mo Prof. Rodolfo Costa

Supervisore:Ch.mo Prof. Francesco Argenton

Dottorando : Alessandro Casari

TABLE OF CONTENTS

ABTRACT

Cells movements and cell fate decision occurring during embryonic development are ruled by several chemical signals genetically encoded. Some of them are known as morphogens, because they create a gradient along the embryo and stimulate a different cell response depending on the concentration detected by each cell. BMP, TGFb, Wnt and Shh are actually recognized as chemical signals acting as morphogens. In the responsive cells, these extracellular signals trigger a signal transduction pathway that leads to the activation of specific transcription factors. In adult, they are also important to maintain the tissue homeostasis and to regulate the regeneration processes. It has been demonstrated that their deregulation is associated to some diseases, such as cancer and some pathologies associated to an altered inflammatory response.

Zebrafish can be a useful tool to study these pathways. The transparency of the embryo and the external fertilization that make possible both chemical and genetic manipulations are some of the advantages of this experimental model. Our lab has developed some transgenic reporter lines to study *in vivo* morphogens signalling. The aim of this thesis has been to characterize and validate these reporter lines, especially the smad3/TGFb-responsive line.

After having demonstrated that these lines are faithfully responsive to the correspondent pathway, they have been used for two main projects:

- to understand the role of smad3 during the central nervous system (CNS) development
- to study the interaction occuring among the morphogens together with Notch and FGF signalling in early larval development

It has been demonstrated that smad3-associated reporter expression is localized in the inner part of the CNS, where neural progenitor cells are situated. Notably, colocalization measurment with reporter genes expressed in various neural markers have demonstrated that smad3 is active in both glial and neuronal precursor cells. Furthermore, both chemical inhibition and smad3 knock-down cause a decrease of precursors accompanied to an increase of progenitor, and a reduction of mature cells, such as motor neurons and oligodendrocytes. EdU proliferation assay has confirmed that smad3 is active in post-mitotic, non proliferating cells and smad3/TGFb inhibition leads to an increase of cell proliferation and an altered epithelial-to-mesenchymal transition that can be responsible of the observed motor neuron misalignment. Both Zebrafish smad3 paralogues, smad3a and 3b, seem to play a similar role in the CNS development as knock-down of each isoform impairs neural differentiation.

To study epistatic interactions, reporter lines embryos have been treated at 24 hpf with drugs specifically acting on the 4 studied morphogen pathways, Notch and FGF signalling. The effects of treatments have been initially recorded with the epifluorescent microscope. Results have been associated to those inferred by GFP mRNA *in situ* hybridization performed on the reporter larvae treated with the same drugs as before. To have reliable data, fluorescence levels have been quantified for each group of treatment through ImageJ software. Results obtained have been used to infer possible interactions among the observed chemical signals at early larval development. A confocal analysis of double reporter transgenic larvae has confirmed the relative expression of the signalling pathways.

As a further demonstration of the possibility of an *in vivo* use of Zebrafish transgenic lines, a preliminary study concerning the role of morphogens on pancreas development has been performed. Crossing the morphogens lines with transgenics expressing a reporter gene in endocrine or exocrine pancreas, in either progenitors or precursors, it has been possible to reveal a new involvement of Shh signalling in the pancreatic islet at early larval development and the activity of BMP pathway in pancreatic vasculature, where it seems to play a role in the correct positioning of the main islet and control angiogenesis, as demonstrated by functional studies.

In conclusion, the morphogen reporter lines here described can represent interesting experimental models in different biological fields. They permit to follow dynamic processes both in physiological and pathological conditions in vivo. They are faithfully responsive to the studied signalling and can be a complementary tool to the current *in vitro* studies.

INTRODUCTION

1. Zebrafish as a model for *in vivo* study: developmental biology, genetics, pharmacology and physiopathology

In the last decades Zebrafish (*Danio renio*) has become a useful model for studies of genetic, developmental biology and pharmacology. Its small size, short generation time (roughly three months), relatively easy breeding and reproduction and the large amount of embryos obtained from each female (roughly 200 eggs per female) represent some of the positive aspects that make Zebrafish a fascinating model for physiological and pathological processes (Moro et al., 2013).

Another of the biggest advantages of Zebrafish is represented by the external fertilization that makes possible any genetic and chemical manipulations. Furthermore, due to its extra-uterine development and its tissues transparency any morphological modifications of the organs can be follow *in vivo* at the microscope using either transient or stable reporter expression (Moro et al., 2013).

1.a Transgenic reporter lines: how to study gene activity *in vivo*

The transparency of Zebrafish embryo and the relatively easy genetic manipulations have permitted the generation of several transgenic lines. By cloning a reporter gene (i.e., GFP, CFP, mCherry, YFP and so on) under the control of a gene promoter it is possible to study *in vivo* how the expression of this target gene change temporally and spatially in a living animal. Furthermore, the reporter gene expression can be directed by repeated sequences that are responsive to a specific transcription factor. This let us study a dynamic process in normal and altered conditions (mutant background, drug treatment, morpholino knock-down) and in relation with other processes (creating double transgenics).

Our lab has produced some transgenic reporter lines to study four morphogens: BMP, TGF-beta, Wnt and Shh.

Briefly, a polymerized repeated sequence corresponding to the *cis* element bound by the transcription factor acting at the bottom of the signal is cloned upstream to a minimal promoter and a reporter gene. These sequences have been cloned in a Tol2-vector, a transposone-donor plasmid, that is microinjected in Zebrafish embryos at 1-2 cell stage together with mRNA enconding for a transposase necessary for excision and recombination of the Tol2-vector into the host genome (Fig. 1). The efficacy of this method of transgenesis can reach 70 % (Moro et al.,

2013).

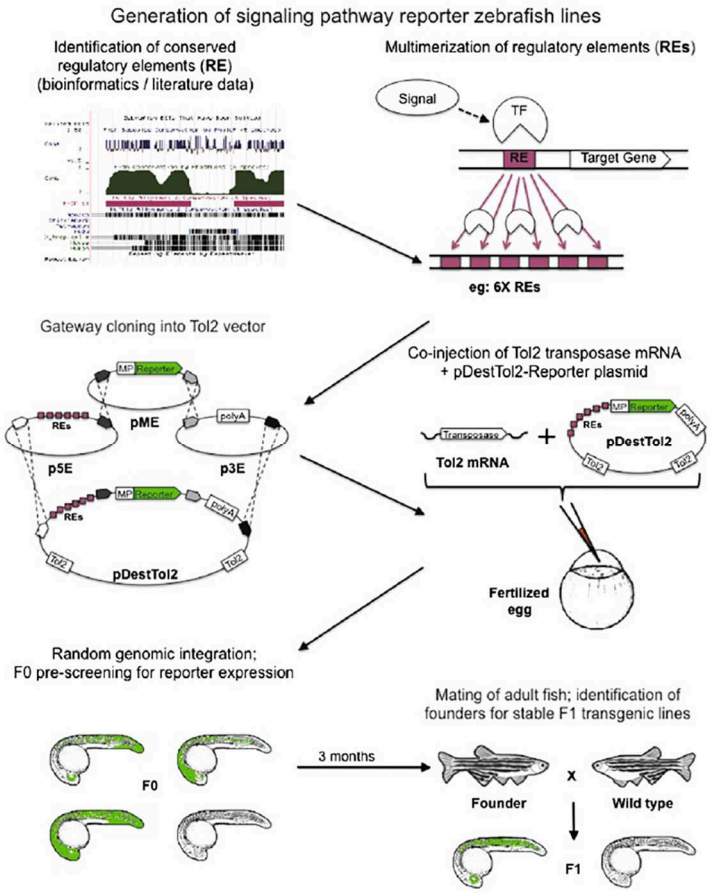

Fig. 1. Rappresentative scheme of the generation of a transgenic reporter line. Regulatory elements (RE) can be found in litterature and/or through *in silico* analysis. These sequence are polymerized to increase the sensibility of the future reporter line and cloned upstream of a reporter gene together with a minimal promoter and a poly-A site. For Tol-2 transgenesis, a pDestTol2 vector is injected into fertilized eggs with a transposase mRNA. The injected embyos are selected for the reporter expression and grown to adulthood. These fishes are then screened to find a founder of a stable reporter integration (Moro et al., 2013).

Here follows a description of the chemical signal transduction pathways studied in this thesis. The corresponding reporter lines will be presented on the next chapter (*Results*).

2. Genetic signals involved in embryonic development: BMP, TGF-beta, Shh, Wnt and Notch

2.1 Morphogens

The concept of morphogen has been introduced some decades ago to explain how cells migrate during the embryonic development and why they adopt a cell fate instead of another one.

Morphogens are also important for a proper tissue patterning (Charron and Tessier-Lavigne, 2007). The concept of morphogen relies on the presence of a chemical extracellular signal released by a group of cells called organiser (Kodjabachian, 2001). This signal forms a concentration gradient along the embryo body triggering a different response in the receiving cells depending on their distance from the emitting organiser. Nowadays, four chemical signals have been identified as morphogens: Transforming Growht Factor-beta (TGFb)/Bone Morphogenetic Proteins (BMP), Sonic hedgehog (Shh) and Wnt (Charron and Tessier-Lavigne, 2007).

2.1a TGFb superfamily: BMP and TGFb

TGFb and BMP signalling belong to the TGFb-superfamily. Both morphogens show a similar transduction pathway. The secreted ligands interact with type I and II transmembrane serine-threonine kinases receptors. The type II receptors phosphorylate type I receptor, which in turn permits the binding of receptor-regulated transcription factors smads (r-smads) and their following phosphorylation at the C-terminus. Activated r-smads can interact with a common mediator smad or co-smad (smad4) and then translocate into the nucleus to direct target gene expression (Fig. 2).

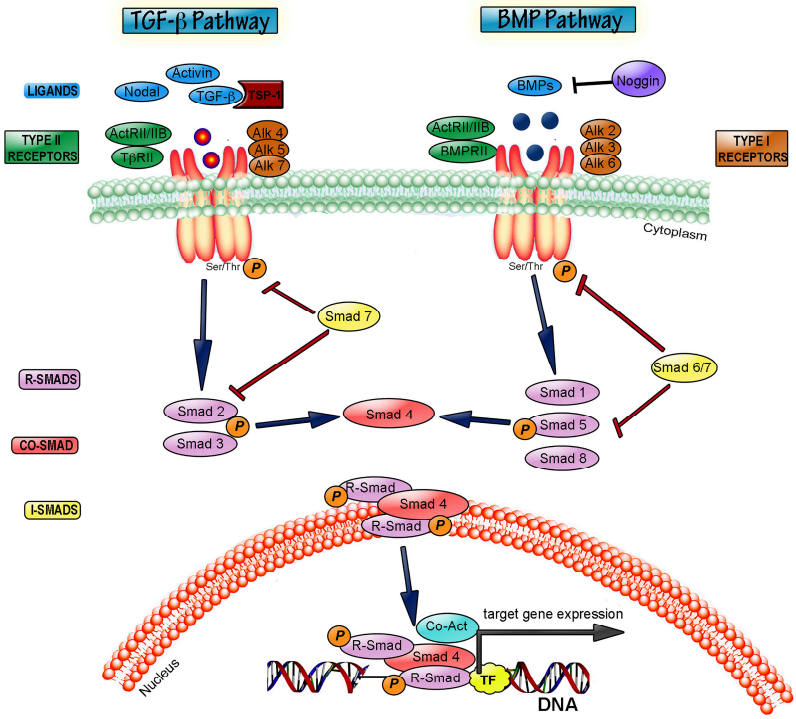

Fig. 2. TGFb and BMP signalling pathways. BMP and TGFb share a similar transduction pathway Secreted ligands bind to type II serine/treonine kinase receptors that activate type I receptors. This

receptor complex activate r-smads transcription factors, that together with smad4 transcription factor translocate to the nucleus where they coordinate the target gene expression. Both BMP and TGFb can activate smad-indipendent cascades (MAPK signallling) (Villapol et al., 2013).

BMP pathway

Bone Morphogenetic Proteins (BMPs) were initially identified for their ability to induce bone regeneration. They are a large subgroup (more than 20 members) of the transforming growth factor-beta (TGFb) super family. They are expressed in many tissues under physiologic conditions and are regulated through extracellular antagonists, like noggin, chordin, follistatin and DAN. BMPs are divided into several subgroups according to sequence similarities and homology (Wen et al., 2009). The action of BMP is mediated by heterotetrameric serine/threonine kinase receptors. There are two specific BMP receptor subunits, BMPRI (BMP Receptor Type-I) and BMPRII, which are required for high-affinity binding. The binding of BMP ligands leads to BMPRI activation and then smad1, 5 and 8 phosphorylations. The phosphorylated BMP-specific smads form a complex with the co-smad or smad4 and then translocate into the nucleus to activate transcription of specific genes by binding with the GCCG motif in the promoter regions of many BMP-responsive genes (Wen et al., 2009). They are also recruited to the promoters of BMP-responsive genes by cofactors such as OAZ, which binds to the promoter of STAT3, leading to the transactivation of the glial fibrillary acidic protein gene (GFAP), a marker for astroglial differentiation (Wen et al., 2009).

BMPs are involved in many developmental processes, including cell proliferation, differentiation, apoptosis and intercellular interactions during morphogenesis. In the ectoderm, BMPs activate two biochemical pathways, one mediated by smads and the other mediated by the p38/MAPK (mitogenactivated protein kinase) pathway downstream of TAK1 (TGFb activated kinase-1) (Wen et al., 2009).

During embryogenesis, BMP signalling forms an antero/posterior and dorso/ventral gradients along the embryo body (Hashiguchi and Mullins, 2013) and it also regulates the left to right asymmetry (Luo and Su, 2012). BMP is important at the end of gastrulation to specify the ventral-posterior patterning, that in zebrafish leads to the formation of the cloaca (Pyati et al., 2006).

TGFb pathway

BMP and TGFb signalling require different ligands (GDF and BMP ligands for BMP, activin,

nodal and properly-said TGFb ligands for TGFb), type II receptors (Alk1, 2, 3 and 6 for BMP and Alk4, 5 and 7 for TGFb) and r-smads (smad1, 5 and 8 for BMP and smad2 and 3 for TGFb) (Hinck, 2012). As a consequence, r-smads-recognized gene sequences are different for the two signalling.

For Zebrafish two smad3 isoforms are known: smad3a and 3b. They are the results of the genome duplication occurred during teleost evolution. These two genes show a partially overlapping expression: they are both expressed in tail bud and lateral stripes of the forming mesoderm, however, smad3a is also produced in an additional area that surrounds the tail bud (Dick et al., 2000). Their general cellular mechanisms of action are similar and they are expressed in overlapping and not overlapping tissues (Pogoda and Meyer, 2002) displaying additive genetic effects.

All the receptor-regulated smads and smad4 are ubiquitously expressed since blastula stage as a consequence of their maternal origin (Dick et al., 2000). During gastrulation, all the receptor-activated smads are either present at very low level (smad2), or quite undetectable (smad3a and 3b) (Dick et al., 2000) (Pogoda and Meyer, 2002). In contrast, smad4 expression is maintained at a high rate in all this stage (Dick et al., 2000). From tail bud smad3a and 3b production rises up (Hsu et al., 2011). At late somitogenesis (16 hpf) smad3a is confined to the eyes and tail region, although it is present throughout the embryo at low level. Smad3b is expressed in the same areas, but it has a higher ubiquitous expression. Both smad2 and 4 are present in the entire embryo with a higher level in tail region, eye and brain (Hsu et al., 2011). However, smad2 and 3 expression is necessary but not sufficient for a function since a signal transduction cascade leading to their phosphorylation is needed (Liu et al., 1997).

R-smads activity is regulated by inhibitory-smads (i-smad). For TGFb smad7 functions as negative signalling regulator. The inhibitory transcription factor smad7 is induced by smad3 and provides a negative feedback loop to the pathway. Smad7 shows a pattern of expression similar to that observed for smad3b, underlying the reciprocal functional connection between the 2 genes. Smad7 is ubiquitously present as maternal transcript until gastrula stage, when its expression falls down, becoming limited to the ventral side of the embryo, while its expression increases in the tail bud (Pogoda and Meyer, 2002). Smad7 can act in different ways: it can compete to r-smads for binding type I receptors; it can recruit E3-ubiquitine ligases (Smurf1 and 2) to the activated type I receptors causes its degradation (ten Dijke and Hill, 2004).

TGF-beta signalling is involved in a wide range of physiological and pathological processes both in embryonic and adult stage. It acts as a morphogen through Nodals and Activins directing the

patterning of the three germ layers (Watabe and Miyazono, 2009). A disregulation of this pathway is associated to tumorigenesis, fibrosis, allergy and neurodegenerative diseases. Both in physiological and pathological conditions, its effects depend on its tight regulation of the cell cycle (Fleisch et al., 2006).

TGFb signalling is a well-known pro-apoptotic signal and promotes epithelial-to-mesenchymal transition (EMT), too (Song, 2007). However, these events seem to be mutually exclusive. It has been demonstrated that TGF-b1-induced G1/S phase growth arrest may provide cells a precondition for undergoing EMT, whilst TGF-b1 induces apoptosis in cells at G2/M phase (Song, 2007). As a matter of facts, smad4 is a powerful tumour suppressor in pancreatic tumours (Herman et al., 2013).

2.1b Shh signalling

Sonic hedgehog (Shh) is a member of the hedgehog family together with Indian hedgehog (Ihh) and desert hedgehog (Dhh). Before to be secreted, Shh precursor protein is cleaved to yield a ~19 kDa N-terminal domain (signaling domain; N-Shh) and a ~25 kDa C-terminal domain (catalytic domain). The canonical Hedgehog signalling is mediated by two transmembrane proteins, a twelve-pass membrane protein Patched (Ptc) and a seven-pass membrane protein Smoothened (Smo). When Shh is absent, Ptc acts as a transcriptional repressor, interacting with Smo. When Shh binds Ptc, this transmembrane receptor releases Smo, leading to the nuclear translocation of Gli proteins as transcriptional activators (Fig. 3). There are three Gli genes with different functions in vertebrates. The target genes of Shh signalling include proliferation-related genes N-Myc, cyclin D1, E2f1 and E2f2 and those involved in *de novo* vascularization during embryonic development such as all three VEGF-1 (vascular endothelial growth factor-1) isoforms and angiopoietins-1 and -2 (Oliver et al., 2003).

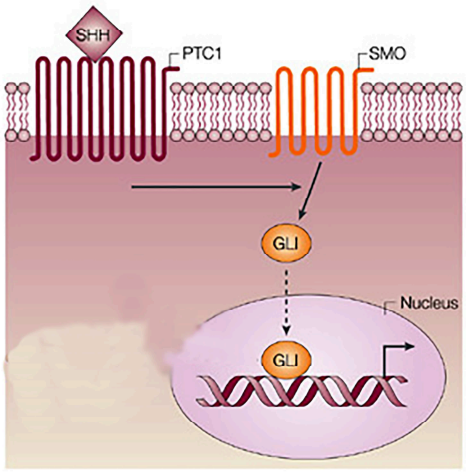

Fig. 3. Shh signalling pathway. HH ligands bind to patched 1 (PTC1) that releases repression of smoothened (SMO), enabling Gli translocation to the nucleus where it acts as a transcription factor to induce gene expression (Baker and McKinnon, 2004).

Shh is involved in the determination of cell fate and embryonic patterning during early vertebrate development. It patterns the ventral side of neural tube and somites and it is involved in the left to right asymmetry (Howie and Fisher, 2008)

2.1c Wnt/beta-catenin signalling

Three different Wnt signalling transduction pathways can be distinguished: the canonical Wnt pathway, the noncanonical planar cell polarity pathway and the noncanonical Wnt/calcium pathway.

In canonical Wnt pathway, interactions of Wnt proteins with other components, beta-catenin, adenomateous polyposis coli (APC), glycogen synthase kinase-3β (GSK-3β), Axin and Conductin, orchestrate cell proliferation and differentiation during embryogenesis. If Wnt pathway is not active, the excess of β-catenin in cytoplasm is phosphorylated by a complex formed by GSK-3β, Axin, Conductin and APC, and leads to degradation by the ubiquitin proteasome system. Activation of Wnt signalling pathway leads to inhibition of GSK-3β, resulting in accumulation of β-catenin, that enter to the nucleus. Wnt signalling activation is achieved if β-catenin moves into the nucleus and complexes with T-cell factors (TCFs) and/or lymphocyte enhance factors (LEFs) to activate transcription of target genes (Fig. 4).

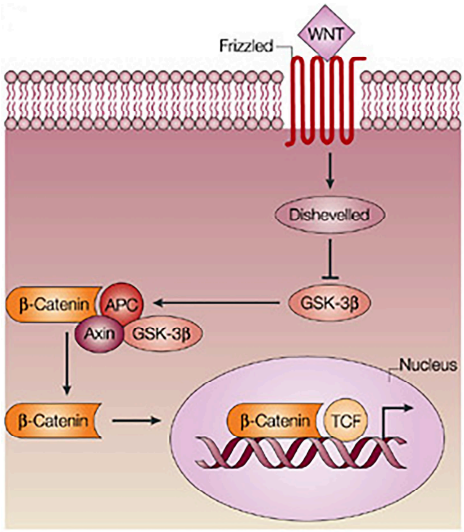

Fig. 4. Wnt signalling pathway. In the canonical Wnt/β-catenin signalling, Frizzled (Fz) binds Wnt ligands and activates Dishevelled (Dsh). Then Dsh inhibits blocks the beta-catenin destruction complex (adenomatous polyposis coli (APC), axin, and glycogen synthase kinase-3 (GSK-3)), which phosphorylates β-catenin in the absence of the ligands. beta-Catenin is stabilized and translocated to the nucleus, where it recruits transactivators proteins of the lymphoid enhancer factor/T cell factor (LEF/TCF) family. (Baker and McKinnon, 2004).

The noncanonical planar cell polarity (PCP) pathway is one of the two Wnt pathways that does not involve β-catenin. As in the canonical Wnt pathway, the PCP pathway is activated via the binding of Wnt to Fz and its co-receptor. The receptor then recruits Dishevelled (Dsh), which forms a complex with Dishevelled-associated activator of morphogenesis-1 (Daam1). Daam1 then activates the small G-protein Rho through a guanine exchange factor. Rho activates Rho-associated kinase (ROCK), which is one of the major regulators of the cytoskeleton. Dsh also forms a complex with rac1 and mediates profilin binding to actin. Rac1 activates JNK and can also lead to actin polymerization (Sugimura and Li, 2010).

The noncanonical Wnt/calcium pathway is the last Wnt pathway that does not stimulate accumulation of β-catenin. Its role is to help regulate calcium release from the endoplasmic reticulum (ER) in order to control intracellular calcium levels. Like other Wnt pathways, upon ligand binding, the activated Fz receptor directly interacts with Dsh and activates specific Dsh-protein domains. Unlike the other Wnt pathways, the Fz receptor also directly interfaces with a trimeric G-protein. This co-stimulation of Dsh and the G-protein can lead to the activation of either phospholipase C (PLC) or cGMP-specific PDE. If PLC is activated, the plasma membrane component phosphatidyl inositol 2-phosphate (PIP2) is cleaved into diacyl glycerol (DAG) and

inositol-3 phosphate (IP3). When IP3 binds its receptor on the ER, calcium is released (Komiya and Habas, 2008).

Wnt pathway is one of the most studied posteriorizing signals (Caneparo et al., 2007). In fact, increase of Wnt signalling in embryos at gastrula stage impairs the development of rostral neural identity and causes a posterior transformation of the anterior neural plate (Caneparo et al., 2007). A variety of molecules, acting as secreted antagonists of the Wnt pathway, have been identified in the Spemann Organizer. Most of them are related to the extracellular domain of the Wnt receptor Frizzled and act by direct binding to Wnt proteins (Caneparo et al., 2007).

2.2 Notch signalling

The Notch proteins are 300-kDa transmembrane receptors, which function in CNS development by guiding cell fate determination. Four Notch receptors (Notch1-Notch4) and five structurally similar Notch ligands, Delta 1, Delta 3, Delta 4, Jagged 1 and Jagged 2, have been identified in mammals. The extracellular domain of the two transmembrane ligands, delta and serrate (jagged), interacts with the extracellular domain of Notch receptor on the adjacent cell. This ligand binding induces a sequence of proteolytic events that leads to the cleavage of Notch and, consequently, the generation of Notch intracellular domain (NICD). NICD translocates into the nucleus and then associates with the constitutive DNA binding protein CSL (CBF1, Suppressor of hairless, Lag-1), that is switched from a transcriptional repressor to a transcriptional activator (Fig. 5).

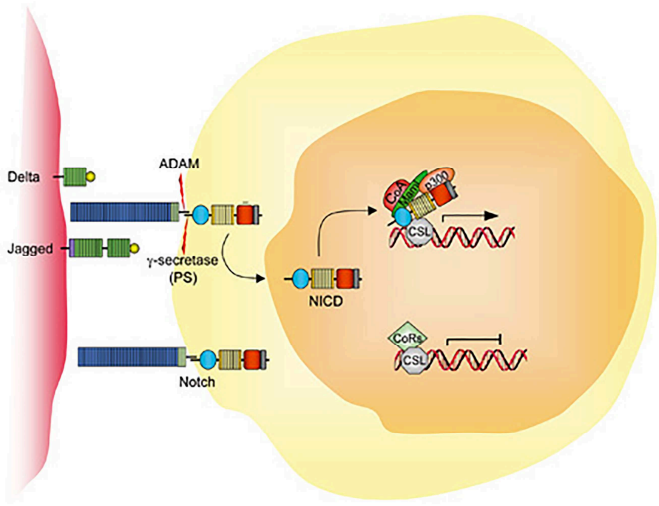

Fig. 5. Notch signalling pathway. Notch ligands (Delta and Jagged) bind to Notch receptors causing a

double proteolytic cleavage. The first is mediated by ADAM family metalloprotease, that cut the extracellular domain of the receptor. Then, another enzyme, gamma-secretase or presenilin (PS) cleaves the intracellular domain (NICD), that can enter the nucleus and direct the gene expression with various transcription factors (revfrost.files.wordpress.com).

The Notch signalling involves adjacent cells communicating with each other. Its effects do not depend on a concentration gradient, therefore it cannot be considered a morphogen. It is considered as a juxtacrine pathway that defines borders between cells and tissue types and it is possible that regulates the subdivision of the endoderm and mesoderm during gastrulation (Miazga and McLaughlin, 2009). All multicellular animals utilize this pathway, which contributes to the embryogenesis. In fact, it promotes different processes, such as neurogenesis, somitogenesis, myogenesis, and so on.

3. Neurogenesis in Zebrafish

The development of CNS begins as a sheet of cells made up of primary progenitors known as neuroepithelial cells. These cells are then substituted by different neural stem cells (NSCs). Nowaday, it is known that both embryo and adult contain NSCs. Mammalian NSCs produce different cell types at different developmental stages. Three models have been proposed for the origins of cells in the CNS (Wen et al., 2009). According to the first model, NSCs might generate two progenitor groups: neural restricted progenitors (NRPs) and glial restricted progenitors (GRPs). Then these two groups give origin to neuronal and glial cell types, respectively. Another theory predicts that neurons and glial cells arise from the same progenitors located in different areas of the nervous system. The last model suggests that in the motor neuron progenitor (pMN) domain NSCs might sequentially differentiate into olig-positive motor neurons, oligodendrocyte and olig-negative astrocyte precursors. A temporal regulated activation of specific genes may coordinate these events. The mechanisms of mammalian NSC commitment are largely unknown and might involved extrinsic and intrinsic mechanisms, such as changes of signal environment, transcription factor expression patterns and epigenetic modifications.

In Zebrafish neurogenesis shows several similarities with that of mice and chicken. Once more, the external embryonic development makes Zebrafish nervous system accessible for any kind of experimental manipulation. Notably, it has a greater neurogenic ability and this has made it an

interesting vertebrate model for neurogenesis.
As seen in other species (fruit fly, Xenopus, chicken, mouse), a complex network of chemical signals is implicated in each step of the nervous system formation.
Following some of these pathways are presented.

BMP signalling

In addition to promoting bone formation, BMPs, especially BMP2 and BMP4, exhibit diverse activities in brain development (Wen et al., 2009). They act at different stages of neural development and in different regions of the CNS to regulate proliferation and determine the cell fate and the manner of differentiation. BMP signalling also inhibits the transformation from primitive ectoderm into neural ectoderm and, once the neural tissue is established, BMP signalling promotes the regulation of dorsal neural cell type formation. Moreover, BMP signalling cross-talks with other developmental pathways, such as Wnt and Shh to coordinate cell proliferation and patterning allowing the formation of the appropriate numbers and types of differentiated neurons. In the developing neural tube, BMPs induce astrocyte specification rather than proliferation of pre-existing astrocyte precursors and inhibit oligodendrocyte specification (Wen et al., 2009).

TGFb signalling

In neural pathologies, the role of smad3/TGFb signal is not so clear. TGFb signalling disruption is correlated to several motor neuronal diseases, because of the neuroprotective and anti-inflammatory effects of this pathway (Katsuno et al., 2011). Its over-activation is associated to the formation of β-amyloid plaques in Alzheimer's disease (Town et al., 2008). Studies regarding axons development report that TGFb-like neurotrophic factors, such as GDNF and nodal, have neurotrophic effects on dopaminergic neurons. Notably, GDNF is able to induce axon-regeneration (Ho et al., 2000). It seems to be involved in glia differentiation and extracellular matrix (ECM) components production to constitute a scaffold for neuron localization in the neural tube, but also as a source of neurotrophic factors that stimulate neurogenesis and axon growth (Gomes et al., 2005).

Shh signalling

Shh is able to promote proliferation of both neural and non-neural tissues. It stimulates neural stem cell proliferation by regulating the expression of N-Myc, cyclin D1, E2f1 and E2f2 (Wen et

al., 2009). In addition to the roles in proliferation and differentiation, Shh signalling seems to control cell death, because some of its downstream genes such as N-Myc and cyclin D1 are involved in the regulation of cell survival. Shh pathway has been involved in the specification and development of oligodendrocytes (Wen et al., 2009). Alterations of Shh signalling are closely associated with neuroectodermal tumor formation.

Wnt signalling

Wnt signalling is implicated in the control of cell growth and differentiation during CNS development. Many studies show that this signalling induces neuronal and astroglial differentiation, but suppresses oligodendroglial differentiation (Wen et al., 2009). In early embryonic development, Wnt signalling promotes proliferation of early neural progenitor cells (NPCs), whilst it stimulates neural differentiation on late NPCs.

Notch signalling

In the nervous system, Notch signals stimulate the expression of HES (hairy and enhancer of split paralogues) genes, like Hes1 and Hes5, and the HES-related genes Hesr1 and Hesr2 which belong to basic helix-loop-helix (bHLH) transcriptional repressor. Both N-Myc and c-Myc are targeted by Notch, which play several roles in regulating cell cycle (Wen et al., 2009). These evidences show the importance of Notch signalling in the developmental processes such as stem cell self-renewal, cell fate determination and differentiation. Notably, during mammalian CNS development, Notch signalling maintains neuronal progenitor renewal, inhibits neuronal commitment, promotes astrocyte formation, prevents oligodendrocyte formation.

4. Pancreas development in Zebrafish

The pancreas is both an endocrine and exocrine organ: it controls the blood glucose level and secretes some digestive enzymes. The endocrine pancreas synthesizes glucagon (alpha-cells), insulin (beta-cells), somatostatin (delta-cells), pancreatic polypeptide (PP-cells) and ghrelin (epsilon-cells) (Pauls et al., 2007) (Prado et al., 2004) (Wierup et al., 2004). The exocrine pancreas consists of exocrine glands called acini that produces digestive enzymes such as trypsin amylase and carboxypeptidase A and a branched network of ducts that guides them to the gut (Fig. 6).

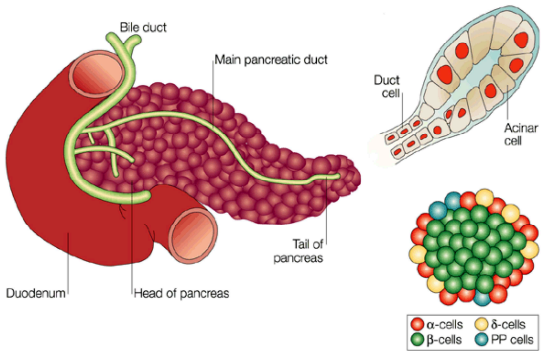

Fig. 6. Pancreas morphology. The pancreas is both an endocrine and exocrine organ. It produces digestive enzymes, that are secreted by the acinar cells into the gut via the pancreatic duct. The endocrine pancreatic cells include: alpha, beta, delta, PP cells and (not shown) epsilon-cells. These cells produce glucagon, insulin, somatostatin, pancreatic polipeptide and grelin, respectively (Edlund, 2002).

The mammalian pancreas emerges from the duodenum as a ventral and a dorsal bud that eventually fuse to form the organ (Slack, 1995). Both buds contain precursors for all pancreatic cell types, but they give rise to different parts of the pancreas. The human pancreas can be subdivided in a head and a tail region referring to the proximal and the distal part of the organ. Precursors of the ventral bud give rise to the posterior part of the head, whilst the dorsal bud contains precursors for the anterior part of the head and the tail.

The transcription factors involved in the pancreas formation can be divided in two groups (Edlund, 2002) (Jensen, 2004; Schwitzgebel, 2001) (Wilson et al., 2003). A group is represented by those factors expressed in the pancreatic anlage and necessary for both endocrine and exocrine part developments. Pdx1, Ptf1a and Mnx1 belong to this category. The other group of transcription factors is involved in the differentiation of pancreatic endocrine cell types. Some of them are NeuroD, Pax6, Pax4 and Nkx2.2 (Jensen, 2004) (Wilson et al., 2003).

In Zebrafish, pancreas develops from two buds: one placed dorsally to the gut, the other one located ventrally and anterior to the first. The posterior dorsal bud is formed by two cell populations that converge at the midline of the forth somite between 14 and 18 somite stages to form a single pancreatic bud (Field et al., 2003). The anterior ventral bud develops near the liver and emerges at 40 hpf. It seems to give rise to pancreatic duct and exocrine tissue, whilst the posterior bud forms the islet. At 44 hpf the two buds keep contact and at 52 hpf they are completely fused (Field et al., 2003).

Many of the transcription factors discovered in mammals are also expressed in the zebrafish pancreas. Transcription factors such as pdx1, nkx2.2a and pax6b are expressed in the endoderm

shortly before or in parallel to the onset of insulin expression at 12 somites (Biemar et al., 2001). Insulin expression is followed by somatostatin at 16 somites and glucagon at the end of somitogenesis (24 hpf) (Argenton et al., 1999) (Biemar et al., 2001). The mRNAs for the first digestive enzymes are detectable at 48 hpf (Biemar et al., 2001) (Yee et al., 2005). The entire exocrine pancreas and late differentiating endocrine cells are generated from ptf1a-positive precursors situated in the so-called anterior pancreatic bud (Field et al., 2003) (Lin et al., 2004), (Yee et al., 2005), (Zecchin et al., 2004). For Zebrafish nkx2.2 two homologues have been identified. Nkx2.2a a is expressed in the ventral CNS and in the pancreas (Barth and Wilson, 1995) and (Biemar et al., 2001). Nkx2.2b is also expressed in the central nervous system but was not detected in the endoderm (Schafer et al., 2005). At the 10 somite stage nkx2.2a is first detectable in the pancreatic primordium and thereafter in the mature pancreatic duct (Pauls et al., 2007).

The expression of these transcription factors is ruled by chemical signals emanating from the surrounding tissues. For instance, Shh and Ihh are absent in the foregut region, which will give origin the posterior bud. Ectopic expression of Shh in the developing pancreatic endoderm of mice and chicken abolishes Pdx1 expression. On the other hand, Shh signalling inhibition produces extra pancreatic buds and an increase of pancreas size and beta-cell number (Tehrani and Lin, 2011). Blocking Shh in early development leads to a sever reduction of endocrine cells in Zebrafish, too (diIorio et al., 2002). Nevertheless, the same signalling seems to play a different role after gastrulation. In fact, a later Shh inhibition causes an ectopic expression of beta-cells (diIorio et al., 2002). It has been proposed a dual role for this pathway: at early gastrulation it promotes migration and differentiation of pancreas progenitors (both exocrine and endocrine cells). By late gatrulation, it switch to a negative role antagonizing retinoic acid and, therefore, inhibiting endocrine pancreas specification, but still stimulating exocrine (Tehrani and Lin, 2011).

BMP is another important signalling for pancreas formation. It promotes the hepatic fate at the expense of the pancreatic one (Zahra Tehrani and Shuo Lin, 2011). It also promotes the budding of the anterior ventral bud, whilst it inhibits beta-cells induction (Chung et al., 2009).

Wnt signalling has been suggested to exert a role during early and late stages of gastrointestinal development. In mouse, Wnt4 expression was observed in the late pro-endocrine cells and differentiated endocrine cells as well as the intestinal and stomach epithelia. At later stages of development, Wnt4 expression became restricted to the islets with preferential high expression in non–β-cells. Wnt7b expression was also expressed in the pancreatic epithelium at later stages.

Frz3 is expressed in the early pancreatic buds, but appears reduced at later stages. These data suggest a role for Wnt signalling in the pancreatic epithelium proliferation during the major phase of pancreatic growth (Papadopoulou and Edlund, 2005). Furthermore, some polymorphisms of the transcription factor TCF7L2 impair glucose-stimulated insulin secretion in humans, suggesting that perturbations in the Wnt signalling may contribute to the pathogenesis of type 2 diabetes (Liu and Habener, 2010).

5. Angiogenesis and BMP

During embryonic development, formation of vasculature system consists of two sequential steps: vasculogenesis and angiogenesis. *de novo* development of blood vessels (vasculogenesis) is followed by remodelling and growth of new vessels from the pre-existing ones (angiogenesis) (Moser and Patterson, 2005).

In vivo and *in vitro* experiments have demonstrated the importance of BMP pathway in both processes. For example, (Boyd et al., 2007) and bmp2 overexpression leads to neoangiogenesis in tumor mass (Langenfeld and Langenfeld, 2004). The inhibition of BMP signal impairs gastrulation and vascular differentiation in mice (Moser and Patterson, 2005). Conditional knockout of the mouse BMP type 1a receptor (ALK3) after initial embryonic patterning decrease the vessel formation and alters the recruitment of smooth muscle cells to the vasculature (Park et al., 2006).

It has been also demonstrated that in Xenopus the removal of dorsal aorta blocks endocrine cell differentiation (Lammert et al., 2001). Furthermore, in the absence of this vessel the murine prepancreatic endoderm fails to express the endocrine marker ins (Lammert et al., 2001). On the other hand, Field et al. have demonstrated that both endocrine and exocrine pancreas develop normally in Zebrafish lacking most endothelial cells. The authors have tried to explain this difference envisaging the presence of other tissues that might provide inducing signalling for the pancreas.

6. Aim of the study

In this thesis I will show how the reporter lines produced in our lab can be used for *in vivo* study of the morphogenetic signalling pathways: BMP, TGFb, Wnt and Shh.

As first, I will explain how these transgenics have been validated through chemical treatment and microscope observation and latter focusing my attention on smad3/TGFb reporter line, not yet characterized and published. Molecular and genetic approaches have completed the analysis of the smad3-responsive line.
These analyses were needed to demonstrate that each reporter is faithfully responsive to the corresponding chemical signal and, therefore, the data obtained through them are perfectly reliable.

Then, I will present two different projects that take advantage of the use of Zebrafish transgenic lines:
- smad3 and neurogenesis: the role of smad3-mediated TGFb during the nervous system development is not well cleared. Since this signalling is impaired in cancer (Schiavone Marco et al., 2014) as well as in many pathologies with an altered inflammatory process (Lan, 2011) (Fiocchi, 2001) (Anthoni et al., 2007), it is important to understand how this signalling work in physiological conditions
- morphogens epistasis. The interactions among chemical signals are very important to direct the cell proliferation, differentiation and movement during embryogenesis. This network is impaired in many pathologies. Our study wants to offer a new approach for evaluating *in vivo* these mechanisms, both in physiological and pathological conditions.

As further example of the use of these reporter lines, it will be illustrated a preliminary study regarding the pancreas development and the role of morphogens in early larval development. Many studies have been done on the relation between each morphogen and pancreas. Nevertheless, most of them analyse these pathways in early embryonic development (till gastrulation and/or early somitogenesis). Less is known about the role of these pathways during organogenesis (after 24 hpf). For this reason, the four reporter lines have been crossed to other transgenics with a pancreas-specific expression and observed *in vivo* during the first month of development at the confocal microscope. I will conclude this analysis with a functional study to understand the role of BMP in pancreatic angiogenesis

MATERIALS AND METHODS

Animals

Zebrafish (*Danio renio*) is a tropical fish, native to the Himalayan region, belonging to the minnow family (Cyprinidae) of order Cypriniformes.

Animals were staged and fed according to methods and rules described by Kimmel C.B. et al. (Kimmel et al., 1995). The project was examined and approved by the Ethics Committee of the University of Padua with protocol number 18746. Fish are maintained in large scale acquaria systems (Aquarienbau Schwarz, ZebTech, TECNIPLAST and Mueller-Pflegger)Recericluation systems with biological filters and a reverse osmosis supply guarantee the high-quality water and a regular water exchange rate. These systems allow to raise and maintain a large amount of fishes. Water is sterilized by UV radiation before distribution to the tanks in order to reduce the risk of diseases spread.

Fish are kept in overflow tanks with different volume depending on the number of the individuals: 1 liter tank for single animal, 5-10 liters containers for 2 up to 30 fish.

pH, temperature and saline conditions are maintained constant: pH of about 7, temperature of 28.5°C and conducibility between 200 and 400 μS. Timers regulate the dark/light cycle (12 hours light, 12 hours dark).

Animals are fed once with dry food (TetraMin) and twice with living *Artemia salina* nauplia. Artemia is a species of small shrimps. It is bought as cysts and then raised to nauplia stage into some hatcheries. These hatcheries consist of inverted cones lighted with a neo lamp. 80 ml of cysts are dispersed into 8 liters of water containing 192 g of NaCl. A porous stone inflates air and mix Artemia keeping them alive. After two days, they are completely hatched and nauplia can be harvested. Aeration is stopped to separate the nauplia (on the bottom) from the cyst shells (floating on the water). Then, nauplia are filtered to remove not-hatched cysts and the excess of salt. The nauplia are resuspended in fresh water and distributed to the fish.

Zebrafish are mated on late afternoon using suitable mating boxes (Westerfield, 1995) These boxes consist of a plastic tank with an internal removable container with a grid on the bottom. This grid avoids fishes to eat eggs. Sometimes a small bundle can separate fish pair till the mating to reduce fish aggression. Fishes mate on the morning when the light turns on. Eggs are harvested with a tea net and transferred in Petri dishes containing embryo medium (fish water). Eggs are then controlled at the dissection microscope to separate living embryos from

unfertilized eggs and dead embryos. Embryos are incubated at temperature between 25 and 33°C and then can be either fixed for immunohystochemistry or mRNA in situ hybridization (ISH) or raised to the adulthood. 5 dpf larvae are transferred in 1 liter tanks and maintained in an incubator at 28.5°C until they reach two weeks, when they are moved to the ZebTech, TECHNIPLAST acquaria. Zebrafish larvae are fed twice with dry Artemia powder (Novotom, JBL) from 5 dpf.

We used wild-type (wt) UMBRIA and Giotto-Leo Zebrafish (*Danio renio*) strains in all the experiments.

Screening of oep^{m134} and din^{tt250} lines

Oneeyedpinhead (*oep*^{m134}) (Schier et al., 1996) and chordin (*din*^{tt250}) (Schulte-Merker et al., 1997) mutant carriers have been identified both by PCR analysis and phenotypes screening of their offspring at 24 hpf.

Tail fin clipping

1. Fill small fish tanks with system water
2. Fill a 50 ml becker with 48 ml system water and 2 ml of 25x tricaine
3. Move a fish into the tricaine solution and wait for the fish to stop moving
4. Take the fish with a spoon and put it on a clean glass Petri dish
5. Cut 1/3 of the tail with surgical scissors
6. Place the fish into the previously prepared tank and label with the same number both the fish and the corresponding tail sample

Genomic DNA extraction

1. Put the tail sample in 100 µl of lysis buffer (10 mM tris pH 8.2: 10 mM EDTA; 200 mM NaCl; 0.5 % SDS)
2. Vortex for 30 seconds
3. Add 10 µl of Proteinase K (10 mg/ml) and incubate O/N at 55°C. Stop the reaction incubating at 98°C for 10 minutes
4. Store the lysate at -20°C
5. For PCR dilute the sample with nuclease-free water (1:20) and use 2.5 µl of this dilution

Genotyping of oep^{m134} and din^{tt250} lines

For *oep* PCR screening, the following primers have been used: oepm134-wtFw (5'-GGCTCCCTCAGAACACTGTC-3'), oepm134-mutRv (5'-GGCTCCCTCAGAACACTGTA-3') and oepm134-Rv (5'-CTCTTGGGCACAAAAGAGAA-3'). The annealing temperature is: 58°C.
For *dino* PCR screening, the following oligonucleotides have been used: dino-Fw (5'-GACACAAATGCGGGGTAAAC-3'), dino-Rv (5'-ATGTTGCAACTCAGCAGCAG-3'), dino-wtRv (5'- CTGTGCACAACTCAC-3') and dino-mutRv (5'- ACTGTGCACAACTCAC-3').
The annealing temperature is: 52°C.

Zebrafish transgenic lines

For functional *in vivo* studies we have used the following transgenic lines: tg(Ngn1:GFP)^{sb1}, tg(gfap:GFP)^{mi2001}, tg(mnx1:GFP)^{ml2} and tg(Nkx2.2a:mGFP)^{vu17}. For NeuroD, we used a transgenic line, tg(-2.4kb neurod:EGFP), previously produced in our Lab.
For smad7 overexpression, we used tg(hsp70:smad7/YFP) line, gift of Prof Dirk Meyer.
For pancreas studies the following transgenic lines have been mated: tg(nkx2.2a:mEGFP)^{vu17}, tg(-1.2ins:HSV.UL23-GFP)^{ia8}), tg(ins:dsRED)^{m1018}, tg(gcga:GFP)^{ia1}, tg(−5.5Ptf1a:DsRed)^{ia6}, tg(Ptf1a:GFP) and tg(kdrl:GFP)^{la116}.
For all the *in vivo* studies, the following reporter lines have been created in our lab:
- smad3/TGFb: tg(12xSBE:EGFP)^{ia16} and tg(12xSBE:nls-mCherry)^{ia15} lines
- BMP: tg(BMPRE:EGFP)^{ia18} and tg(BMPRE:nls-mCherry)^{ia17} lines
- Shh: tg(12xGli-Hsv.Tk:GFP)^{ia11} and tg(12xGli-Hsv.Tk:nls-mCherry)^{ia10} lines
- beta-catenin/Wnt: tg(7xTCF-Xla.Siam:GFP)^{ia4} and tg(7xTCF-Xla.Siam:nls-mCherry)^{ia5} lines
- Notch: tg(Tp1bglob:eGFP) and tg(Tp1bglob:nls-mCherry) lines

Generation of tg(12xSBE:EGFP)^{ia16} and tg(12xSBE:nls-mCherry)^{ia15} lines

12 repeats of a smad3-binding sequence, so called CAGA box (Dennler et al., 1998), have been amplified together with major late promoter Adenovirus (MLP) with the attB4cagafor (5'-GGGGACAACTTTGTATAGAAAAGTTGGCCCGGGCTCGAGAGCCAG-3') and attB1cagarev (5'-GGGGACTGCTTTTTTGTACAAACTTGTTGGAAGAGAGTGAGGACGAA-3') oligonucleotides and then cloned into a pDONOR^{TM} P4-P1R according to the manifacturer's guideline (Invitrogen Multisite Gateway System, CA). The resulting Gateway 5' entry vector has been recombined with a middle entry vector containing a reporter gene (EGFP, nls-mCherry,

CFP), pME vector, and a 3'entry vector containing SV40 poly A sequence. 25-50 pg of the obtained Tol2 vector containing smad3-responsive sequences has been co-injected together with 25 pg of *in vitro* synthesized Tol2 Transposase mRNA into one-cell stage wild-type embryos. Mosaic transgenic fishes have been selected at roughly 24 hour post-fertilization (hpf) for fluorescent expression and grown up to the adult stage for screening. Positive founders have been selected for the fluorescence level of their offspring in areas of known Smad3 activity and by checking responsiveness of reporter expression to SB-431542 (S4317, Sigma, MO), a known Alk4- Alk5-inhibitor (Fig. S3). A founder for EGFP, nls-mCherry and CFP reporter lines has been selected and used to follow *in vivo* smad3-mediated TGF-beta signalling.

Chemical treatments

The following drugs were used to modify chemical signals:

- SB431542 (S4317, Sigma, MO): Alk4 and 5 inhibitor; stock solution 100 mM; final concentration 100 µM
- LY364947 (L6293, Sigma, MO): Alk5-inhibitor; stock solution 6 mM; final concentration 40 µM. For treatment at 2 hpf, a final concentration of 10 µM in zebrafish fish water has been utilised
- LDN193189 (SML0559, Sigma, MO) Alk2 and 3 antagonist; stock solution 10 mM; final concentration 10 µM
- Dorsomorphine (S7306, Selleckchem, TX) inhibitor of Alk2, 3 and 6 and AMP-activated protein kinase (AMPK); stock solution 10 mM; final concentration 20 µM
- DAPT (D5942, Sigma, MO): gamma-secretase inhibitor; stock solution 100 mM; final concentration 100 µM
- SU5402 (SML0443, Sigma, MO): FGFR antagonist; stock solution 10 mM; final concentration 10 µM
- Purmorphamine (S3042, Selleckchem, TX): Smoothened agonist; stock solution 100 mM; final concentration 60 µM
- Cyclopamine (S1146, Selleckchem, TX): Smoothened antagonist; stock solution 100 mM; final concentration 100 µM
- BIO (13123, Cayman CHEMICAL, MI): inhibitor of glycogen synthase kinase-3β (GSK-3β); stock solution 5 mM; final concentration 5 µM
- IWR-1 (I0161 Sigma, MO): agonist of glycogen synthase kinase-3β (GSK-3β); stock solution 20 mM; final concentration 10 µM

All substances have been solubilised in pure DMSO, except for cyclopamine that has been solubilised in ethanol. The drugs have been diluted in zebrafish fish water containing 2 mM 1-phenyl-2-thiourea (PTU) for treatment at 24 hpf. For treatment at 2 hpf no PTU was added. The chorion around the embryos is often not permeable to the drugs. Therefore, it has been manually removed with dissection needles before each treatment.
Treatments have been done in 6 or 24 well-plates. Embryos and larvae have been fixed in 4% paraformaldehyde (PFA)/PBS overnight at 4°C and then stored in pure methanol at - 20°C.

WISH: whole mount RNA *in situ* hybridization

Whole mount RNA *in situ* hybridization has been performed as described before (Thisse et al., 1993).

Transformation of E.coli

Vector containing EGFP sequence (pME:EGFP from Tol2 kit) have been introduced in bacterial E. coli cells (One Shot® TOP10 Chemical Competent E. coli, Invitrogen). Chemical competent bacteria have been thawed on ice. 10-50 ng of plasmid DNA have been added to the bacteria and left on ice for 30 minutes. Heat-shock has been performed at 42°C for 30 seconds and followed by incubation on ice for 2 minutes adding 200 µl of S.O.C. medium (Invitrogen™). The transformed bacteria have been incubated at 37°C on a shacker for 45 minutes. Then, cells can be plated on agar containing ampicillin for the antibiotic-resistance selection. After an O/N incubation positive colonies can be selected and cultured in Luria-Bertani medium with ampicillin.

Purification of plasmid DNA

Extraction and purification of plasmid DNA have been performed using a commercial kit provided by Qiagen (QIAprep Spin Miniprep kit). High-quality DNA plasmid has been eluted in 100 µl of nuclease-free water.

Anti-sense probe synthesis

Plasmid has been linearized using ApaI restriction enzyme. Linearization reaction has been done in a total volume of 50 µl, using 1.2 µl of the restriction enzyme and the corresponding buffer and BSA:

- plasmid DNA 5 µg
- 10x Buffer 2 µl

- 100x BSA 0.5 µl
- HindIII 1.2 µl
- ddH2O up to 50 µl

The reaction mix has been incubated at 37°C O/N. The linearized plasmid has been then purified using Phase Lock gel tubes (Eppendorf):
- centrifuge column tube for 1 minute at max speed
- add nuclase free water to 100 µl to the sample and transfer the volume in a Phase Lock column
- add 50 µl phenol and 50 µl of chloroform
- centrifuge for 5 minutes at mx speed
- add 100 µl of chlorophorme and centrifuge at max speed for 5 minutes
- transfer the aqueous phase containing the linearized plasmid in a new 1.5 ml tube
- add 2.5 ml of absolute ethanol, 2 µl of glycogen and 0.2 M NaCl
- mix well and precipitate O/N at -80°C
- centrifuge 15 minutes at max speed
- remove the surnatant and wash the pellet 3 times with 200 µl of 70% ethanol centrifuging 2 minutes at max speed
- remove the surnatant and dry the pellet
- resuspend the pellet in 20 µl of nuclease-free water
- run an electrophoresis on 1.55 agarose gel, loading 1 µl of the purified linearized plasmid

Synthesis of RNA probe has been done in a 20 µl reaction volume at 37°C for 2 hours:
- linearized plasmid 1µg
- 10x transcription buffer (Roche) 2 µl
- DIG-RNA Labelling Mix (Roche) 2 µl
- RNAsin® Ribonuclease Inhibitor (Promega) 1 µl
- T7 RNA Polymerase (Roche) 2 µl

After the transcription, the template plasmid DNA is digested with 2 µl of DNAse (RNAse-free DNAse, Promega) at 37°C for 20 minutes.
The purification of the anti-sense RNA probe has been performed using a commercial kit (MEGAclear™, Ambion®). The purified probe is stored at -80°C. To control and quantify the transcription, an electrophoresis has been performed on 1.5% agarose gel. Prior to be loaded on

gel, the probe has been denatured at 65°C for 5 minutes.

WISH protocol

Solutions:

Hybridization mix (HM)
60% formamide
4.6 µM citric acid, pH 6
5x SSC
50 µg/ml heparin
500 µg/ml torula yeast total RNA (tRNA)
0.1% Tween-20
dH20 up to 100 ml

Washing mix
HM without tRNA and heparin

1x PBS
150 mM NaCl
10 mM Na2HPO4
ddH2O up to volume

1x PBT
1x PBS
0.1 % Tween-20

PFA
4% paraformaldehyde in 1x PBS

Antibody anti digoxigenin
The antibody used to recognize the digoxygenin was conjugated to alcaline phosphatase (AP) (Roche). It has been diluted 1:1000 in PBT/2% sheep serum/200 mg/ml BSA.

NBT/BCIP staining buffer
100 mM Tris-HCl, pH 9.5
50 mM MgCl2
100 mM NaCl
0.1% Tween-20
ddH2O

FAST RED staining buffer
100 mM mM Tris-HCl, pH 8.2
0.1% Tween-20

FAST RED staining solution
1 tablet of FAST RED (Roche) in 2 ml of the corresponding staining buffer. Filter the solution before to use it.

Protocol

- progressive rehydratation of the embryos (75%, 50%, 25% methanol in PBS): 5 minutes for each wash
- 4 washes in PBT for 5 minutes
- digest with Prtoteinase K (10 mg/ml): 7 minutes for 24 hpf embryos, 20 minutes for 48 hpf larvae. This step can be skipped for embryos younger than 24 hpf
- briefly wash with PBT and then post-fix the digested embryos with 4% PFA for 20 minutes at RT
- 4 washes PBT for 5 minutes
- prehybridize the embryos in HM for 3 hours at 65°C
- incubate at 63°C O/N with HM containing 100-200 ng/ml of the anti-sense probe
- remove the probe and washes for 15 minutes with gradually decreasing solutions of HM (100%, 75%, 50%, 25%) in 1x SSCT pre-warmed at 65°C
- wash twice with 2x SSCT at 65°C for 15 minutes
- wash twice with 0.2x SSCT at RT for 15 minutes
- wash for 15 minutes with gradually decreasing solutions of 0.2% SSCT (100%, 75%, 50%, 25%) in 1x PBT
- wash twice for 15 minutes at RT with PBT

- blocking with the blocking solution for at least 2 hours
- incubate with anti-DIG antibody O/N at 4°C
- wash 6 times at RT with PBT
- wash 3 times for 15 minutes with the appropriate staining buffer
- incubate embryos at RT in the dark in staining solution
- monitor the reaction with the stereomicroscope and stop it with 4% PFA

Morpholinos injections

To generate a loss-of-function phenotype for a known zebrafish gene it is possible to transiently inhibit the protein function by injecting anti-sense oligos, namely morpholinos, into fertilized eggs (Nasevicius and Ekker, 2000). The morpholonos are 20-25 bases chemically modified oligos that bind specifically to the 5' UTR region or early coding sequence of a give mRNA and block the translation. Morpholinos can also be drawn to overlap splice site and to block splicing (Draper et al., 2001; Nasevicius and Ekker, 2000). Stability and, therefore, efficacy of a specific morpholino can be quite different, but they usually cannot block translation beyond 4 dpf.
Smad2, 3a and 3b knock-down have been carried out injecting morpholinos previously tested by Jia S. et al. (Jia et al., 2008):

MO-Smad2 5'-TTACCCTTCCTACGAAAAGCGTTCT-3'
MO-Smad3a 5'-TTCAGTTCAGCGTTCCTTCCTCTATTGC-3'
MO-Smad3b 5'-TTGTCCACGAGTCACATCACCGCAT-3'

For Smad4, GeneTools, LLC, OR has synthesized 4 different morpholinos targeting this gene at either the start-codon or 3 different splicing sites:

MO4(1) 5'- TCTCGCCCACCTGAACGTCCATCTC-3'
MO4(2) 5'- TACTGATGTTGACGCTCTACCTCGC-3'
MO4(3) 5'- GCAGTCTGAAAACAGAGAAGTCAGA-3'
MO4(4) 5'- GTGTATGTGTTTCTCACCTTGATGT-3'

Morpholinos were delivered as a sterile, salt-free lyophilized powder. The stock solution has been prepared adding nuclease-free water to have a final concentration of 8 mg/ml and then store at RT.

Morpholino working solutions have been prepared by diluting the stock solutions in 1x Danieau Buffer (58 mM NaCl; 0.7 mM KCl; 0.4 mM MgSO4; 0.6 mM Ca(NO3)2; 5 mM HEPES, pH 7.6) with 0.5% Phenol Red (Sigma) to make the solution visible during the injection.

All morpholinos for Smad4 have been injected at 1 mM concentration in tg(12xSBE:EGFP)^{ia16} line. Effects on embryo morphology and EGFP expression have been observed at 24 hpf. MO4(3) has been adopted for *in vivo* experiments at lower concentration (0.5 mM). To verify its ability of control BMP signalling, it has been also tested in tg(BMPRE:EGFP)^{ia18} line.
As control of each injection, we have injected a morpholino with the following scrambled sequence (MO-CTL) 5'-TTGTTGTTGTTGTTGTTGTTGTTGG-3'

Before the injection, embryos have been collected and alligned along the border of a glass slide in the lid of a Petri dish. Injections have been performed under a dissecting microscope using a micromanipulator attached to a microinjector (Leica Microsystem). Both morpholino solutions and plasmid DNA dilutions have been loaded into the injection needles. The tip of the needle has been broken using a dissecting forceps. Embryos have been injected into the yolk sac at 1-2 cell stage and then incubated in 1x fish water at 28.5°C.

Heat-shock induced overexpression of smad3b and smad7

To validate tg(12xSBE:nls-mCherry)^{ia15} line, we have elicited overexpression of smad3b and smad7. For TGFb-associated transcription factor, we have injected 1-2 cell stage embryos of 12xSBE line with a plasmid containing smad3b sequence in frame to YFP sequence under the control of heat-shock 70 promoter (hsp70). For TGFb general inhibitor smad7, tg(12xSBE:nls-mCherry)^{ia15} line has been crossed to tg(hsp70:smad7/YFP) line. Heat-shock has been performed 3 times at 37°C each 12 hours starting at 24 hpf. Larvae have been observed at confocal microscope 2 hours after the third heat-shock.

Confocal analysis and colocalization measurements

Fluorescence has been visualized at the Leica M165FC dissecting microscope and then at Nikon C2 H600L confocal microscope. For *in vivo* analyses embryos and larvae have been anesthetised with tricaine and mounted in 0.7% low melting agarose gel. EGFP and mCherry fluorescence have been visualized by using 488 and 561 nm lasers, respectively, through 20x and 40x immersion objectives (Nikon). All images have been analysed with Nikon software.

Colocalization has been measured with Volocity 6.0 software, whilst statistical analyses have been done with Prism GraphPad software. For analysis of smad3/TGFb evolution at 24 hpf, we have mated tg(12xSBE:nls-mCherry)^{ia15} to the following transgenics: tg(Ngn1:GFP)^{sb1}, tg(-2.4kb neurod:EGFP), tg(gfap:GFP)^{mi2001}, tg(mnx1:GFP)^{ml2} and tg(Nkx2.2a:mGFP)^{vu17}. Confocal stacks of 6 tails at 24 hpf for each group of double transgenics have been recorded. Since 2 somites are formed each hour between 15 and 24 hpf, each tail has been divided in pairs of somites and a time-point value has been associated to each of them (hours of development). Colocalization has been expressed as Manders' coefficient referred to mCherry/TGFb and it has been measured in 4 somites pairs. Resulting values have been plotted on a graph in function of the corresponding somite/time (hours of development).

Fluorescence quantification

GFP expression level has been measured through ImageJ software. Photos of 3 dpf treated larvae have been acquired with a Leica DMR microscope and saved as TIFF files. Each photo has been visualized as a color image (RGB). Therefore, it is splitted in the 3 colour components: green, red and blue. The green one has been used to quantify fluorescence level. A threshold has been set to highlight all the fluorescent areas in the picture and to decrease the auto-fluorescence of the embryo tissues. The same threshold is set for all the pictures. Fluorescence has been quantified and expressed as integrated density. Since some drugs (BIO and SU5402) cause an aspecific fluorescence effect, the integrated density has been measured for 3 not-fluorescent larvae treated with these drugs or DMSO. The mean value of these "aspecific fluorescence" has been subtracted to each integrated density value obtaining the real fluorescence value. For each group of treated larvae the mean value of "real" integrated density has been calculated together with the corresponding standard deviation using the GraphPad Prism Software. Data have been normalized respect to the integrated density of the control larvae.

Whole-Mount Immunohistochemistry

Embryos and larvae have been fixed in 4% PFA/PBS overnight and then stored in 0.15% TritonX-100 in PBS (PBTr) at 4°C.

Protocol

- tissues have been permeabilized through incubation with 10 µg Proteinase K at room temperature
- 4 washes of 5 minutes in 1xPBS

- block with 4% BSA in PBTr for 2 hours at room temperature
- specimens were immunostained with antibodies anti-phospho-smad3 (ab52903, Abcam, Cambridge, UK), anti-GFP (A10262, Lifetechnology, CA) and anti-phospho-histone H3 (06-570, Millipore, MA), according to standard procedures: 4°C O/N on a shaker
- 4 washes of 5 minutes in 1xPBS
- block with 4% BSA in PBTr for 2 hours at room temperature
- incubate in the dark at 4°C O/N with the following secondary antibodies: Goat Anti-Rabbit IgG, AP conjugate (Secondary Antibody Millipore™, 112448, Upstate™, MA), Alexa Fluor® 488 Goat Anti-Chicken IgG (H+L) Antibody (A1-1039, Lifetechnology, CA) and Polyclonal Swine Anti-Rabbit Immunoglobulins/TRITC (R0156, DakoCytomation, Glostrup, Denmark)
- 3 washes of 5 minutes with 1x PBS in the dark before to watch the results at the confocal microscope

EdU proliferation assay

Cell proliferation has been evaluated on embryos at 20 and 24 hpf.

The Click-iT® EdU Alexa Fluor® 594 Imaging Kit (C10339, Life Technology). In this assay the modified thymidine analogue EdU is efficiently incorporated into newly synthesized DNA and fluorescently labelled with a bright, photostable Alexa Fluor® dye. This fluorescent labelling of proliferating cells is accurate and compatible with immunohistochemistry.

Protocol

- chill 10 mM EdU solution on ice
- move 10-20 embryos in a 2 ml eppy and remove fish water as much as possible
- add 50 µl of 10 mM EdU solution and put the embryos immediately on ice
- incubate on ice on a shaker (20 minutes for 24 hpf embryos, 10 minutes for 20 hpf embryos) to allow EdU uptake into the embryos (pulse)
- 1 wash (1 minute) with cold fish water
- 3 washes (5 minutes) with RT fish water to completely remove EdU
- incubate embryos at 28.5°C for at least 30 minutes to permit the incorporation of EdU into the DNA of proliferating cells. The incubation time depends on the developmental stage and the tissues (chase)
- fix embryos in 4% PFA and then dehydrate them with increasing concentration of methanol (25, 50, 75 and 100% methanol in PBS)
- store in pure methanol at 20°C for at least 1 night

- rehydrate embryos with decreasing concentrations of methanol (75, 50 and 25% methanol in PBS)
- 3 washes with 1xPBS
- permeabilize embryos with 10 mg/ml proteinase K (20 minutes for 24 hpf embryos)
- stop the reaction incubating with 4% PFA at RT
- 3 washes with 1xPBS
- incubate for 20 minutes with 1% DMSO in PBT (0.1% tween-20 in 1xPBS)
- remove the DMSO solution and incubate O/N at RT in the dark with 50 µl of Click-iT™ reaction cocktail
- remove the reaction cocktail and wash 3x for 10 minutes with PBT on a shaker
- proceed with the microscope analysis
- immunohistochemistry can follow this protocol

RESULTS

1. Validation of reporter lines

Our laboratory has developed a number of transgenic zebrafish lines expressing a reporter gene such as GFP, mCHERRY and CFP under the control of DNA elements responsive for specific cellular pathways involved in cell proliferation, stem cell maintenance and differentiation, tissue homeostasis and cancer (Wnt, BMP, TGFb, Shh). These responsive sequences have been found in literature and already validated *in vitro*.

For Wnt signalling, tg(7xTCF-Xla.Siam:GFP)^{ia4} line has been obtained cloning seven repeats of TCF/LEF binding sites followed by the siamois minimal promoter (Maretto et al., 2003) (Moro et al.., 2012).

For BMP pathway, two repeats isolated in the human Id1 gene has been cloned upstream to the Major Late promoter of Adenovirus to produce tg(BMPRE:EGFP)^{ia18} line (Lopez-Rovira et al., 2002).

For TGFb signalling, 12 repeats of smad3 specific sequence from the human PAI gene, namely CAGA box, have been cloned together with the major late promoter Adenovirus (MLP) to produce tg(12xSBE:EGFP)^{ia16} line (Dennler et al., 1998).

For Shh tg(12xGli-Hsv.Tk:nlsmCherry)^{ia10} line contains 12 repeats of Gli binding sites (from mouse hepatocyte nuclear factor-3beta or mHNF-3beta gene) together with the TK minimal promoter (Sasaki et al., 1997).

To prepare these reporter lines, a Tol2 vector containing the sequences specific for each morphogen has been co-injected together with Tol2 Transposase mRNA into one-cell stage wild-type embryos. Mosaic transgenic fishes have been selected at roughly 24 hour post-fertilization (hpf) and grown up to the adult stage for screening (Moro et al., 2013). Positive founders have been selected for the fluorescence level of their offspring in areas of known morphogen activity and by checking responsiveness of reporter expression to known specific inhibitor. Founders for EGFP, nls-mCherry and CFP lines have been positively selected and used to follow *in vivo* morphogens signalling.

Before to use for our *in vivo* experiments, we have validated these transgenic lines in order to demonstrate their specificity. All of them have been treated with known specific drugs at 24 hpf: BIO and IWR1 for Wnt, LDN193189 for BMP, SB431542 for TGFb and cyclopamine for Shh. Fluorescence expression has been checked at epifluorescent microscope after two days of

treatment (Fig. 7a-b-c-d).

For Wnt, BMP and TGFb we have evaluated the decrease of GFP mRNA through mRNA *in situ* hybridization (ISH). For this aim, 24 hpf embryos of these reporter lines have been treated with the appropriated inhibitor and fixed after 2, 4, 6 and 8 hours of treatment. GFP mRNA degradation shows a similar kinetic: within 8 hours the reporter transcript is completely eliminated (Fig. 7d, 8a and b). On the other hand, reporter protein is more stable than the corresponding transcript and, consequently, needs more time to be almost completely abolished.

Since TGFb/smad3 reponsive line was the only unpublished line, we have performed a more detailed validation by chemical, genetic and molecular approaches on it.

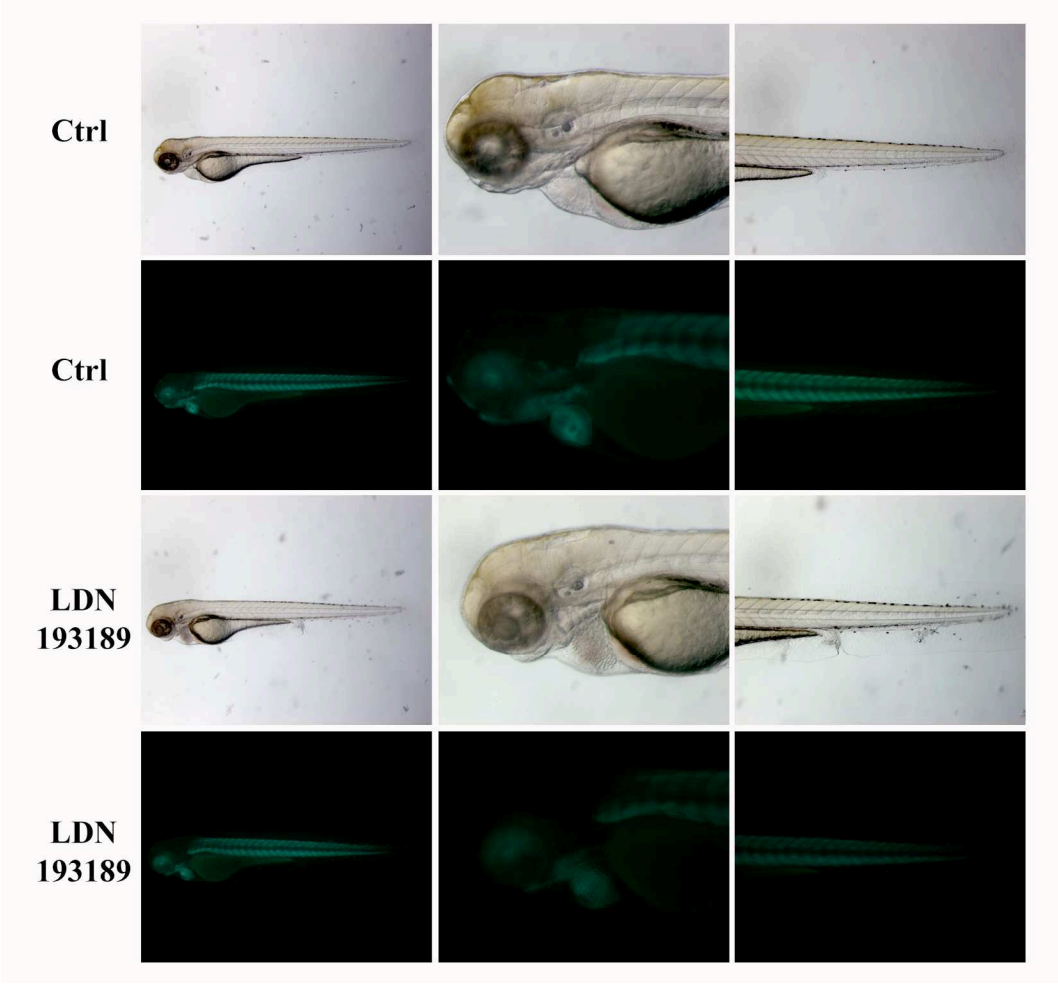

Fig. 7a. tg(BMPRE:EGFP)^{ia18} line: chemical validation. Brightfield and fluorescent images of 3 dpf larvae of tg(BMPRE:EGFP)^{ia18} from epifluorescent microscope,lateral views, left to right. Larvae have been treated with an Alk2 and 3 inhibitor.

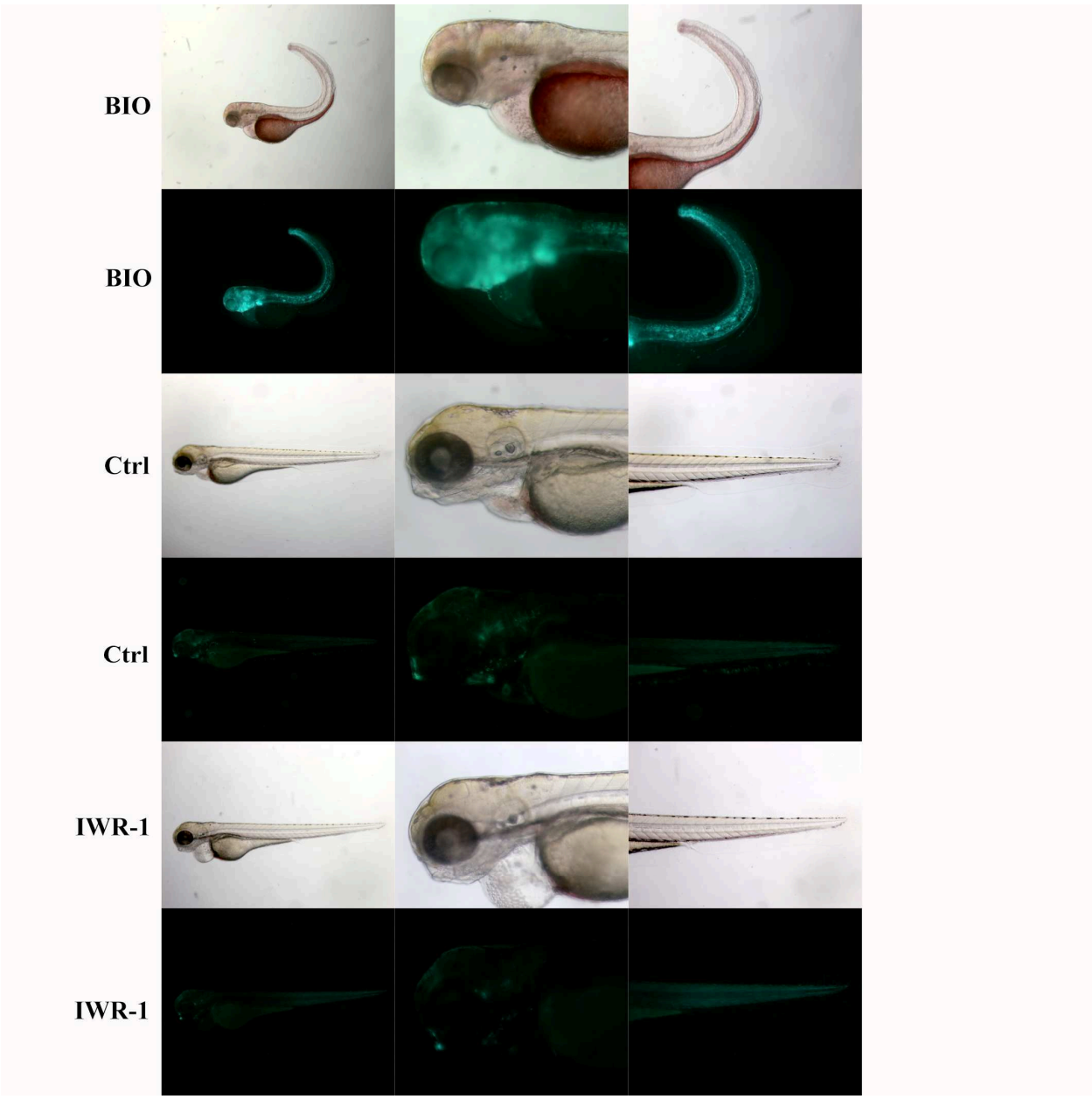

Fig. 7b. tg(7xTCF-Xla.Siam:GFP)ia4 line: chemical validation. Brightfield and fluorescent images of 3 dpf larvae of tg(7xTCF-Xla.Siam:GFP)^{ia4} line from epifluorescent microscope,lateral views, left to right. Larvae have been treated with a GSK-3 inhibitor (BIO) and a GSK-3 agonist (IWR-1).

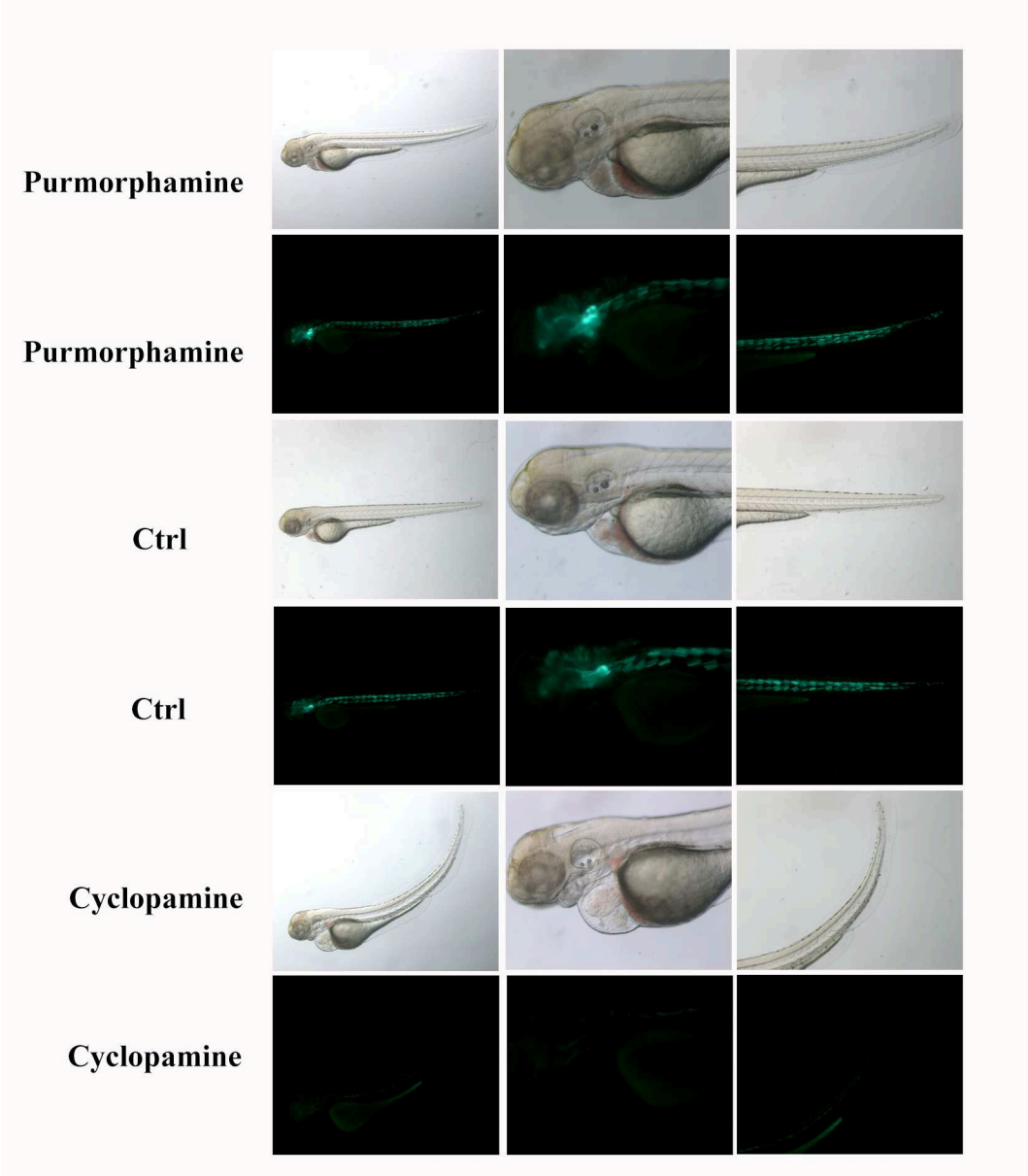

Fig. 7c. tg(12xGli-Hsv.Tk:GFP)^{ia11} line: chemical validation. Brightfield and fluorescent images of 3 dpf larvae of tg(12xGli-Hsv.Tk:GFP)^{ia11} line from epifluorescent microscope,lateral views, left to right. Larvae have been treated with a Smoothened agonist (purmorphamine) and a Smoothened antagonist (cyclopamane).

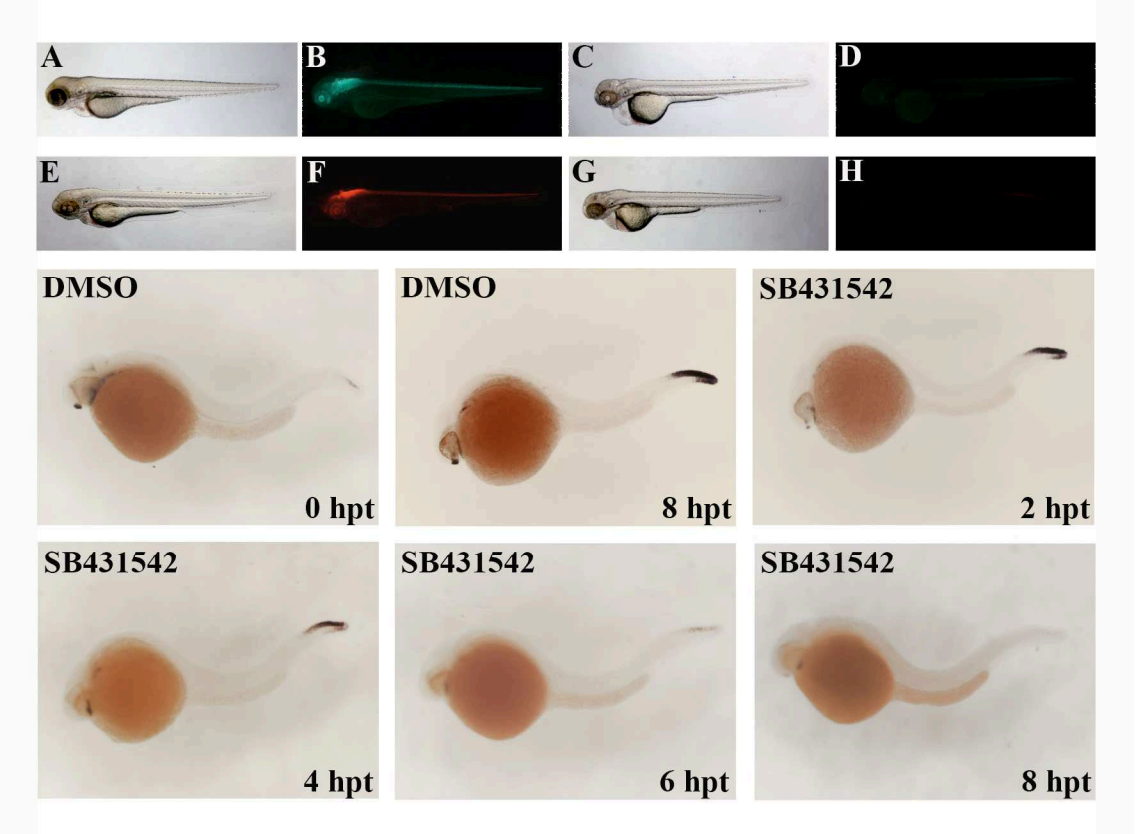

Fig. 7d. Chemical inhibition of TGFb signaling reduces reporter expression in 12xSBE lines. Brightfield and fluorescent images of 3 dpf larvae of Tg(12xSBE:EGFP)^{ia16}**, A-B',** and tg(12xSBE:nlsmCherry)^{ia15}, **C-D'**, lines from epifluorescent microscope,lateral views, left to right. **A-A', C-C'**, 3dpf larvae treated with DMO at 24 hpf and used as control; **B-B', D-D'**, 3 dpf lavae treated with SB-431542 at 24 hpf. **E,** RNA *in situ* hybridization for EGFP mRNA performed on 24 hpf embryos of Tg(12xSBE:EGFP)^{ia16} treated with the Alk4- and Alk5-inhibitor, SB-431542, at 24 hpf and fixed at different time points: 2, 4, 6, 8 hours post treatment (hpt).

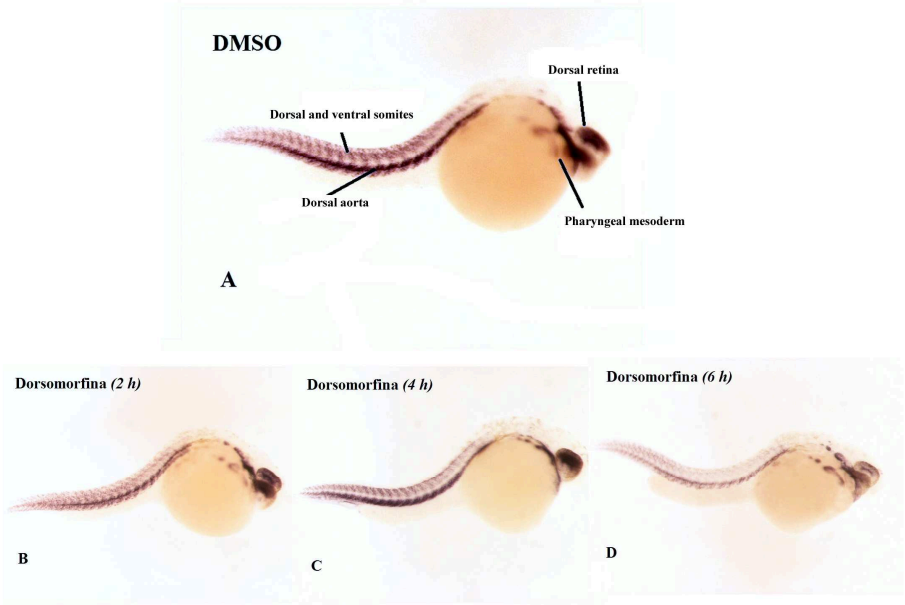

Fig. 8a. Chemical inhibition of BMP signalling reduces reporter expression in tg(BMPRE:EGFP)^{ia18} line. Brightfield images of RNA *in situ* hybridization for EGFP mRNA performed on 24 hpf embryos of tg(BMPRE:EGFP)^{ia18} line treated with dorsomorphine, at 24 hpf and fixed at different time points: 2 (B), 4 (C) and 6 (D) hours post treatment (hpt).

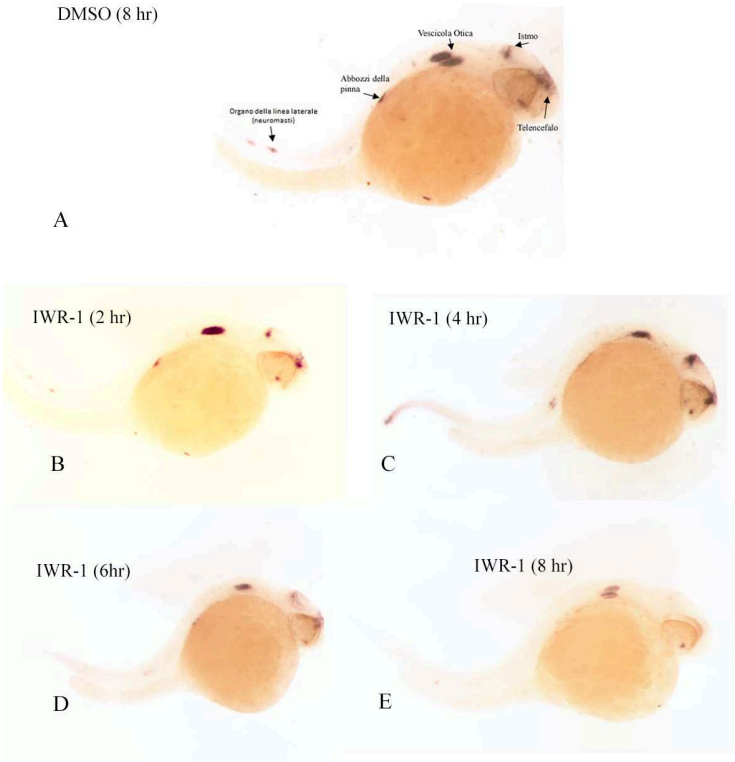

Fig. 8b. Chemical inhibition of Wnt signalling reduces reporter expression in tg(7xTCF-Xla.Siam:GFP)^{ia4} line. Brightfield images of RNA *in situ* hybridization for EGFP mRNA performed on

24 hpf embryos of tg(7xTCF-Xla.Siam:GFP)^{ia4} line treated with IWR-1, at 24 hpf and fixed at different time points: 2 (B), 4 (C), 6 (D) and 8 (E) hours post treatment (hpt).

1.a Genetic and molecular validation of the tg(12xSBE:EGFP)^{ia16} and tg(12xSBE:nls-mCherry)^{ia15} line

To demonstrate that reporter expression correlates with smad3 activation, expression of phosphorylated smad3 has been checked by immunohistochemistry in 24 hpf embryos and 48 hpf larvae (Fig. 9). At both stages, smad3 activation has been revealed in neural tube and tail mesoderm, with a decreasing rostro-caudal gradient, as seen in transgenic lines. Reporter-expressing cells colocalize with smad3-activated cells (Fig. 9).

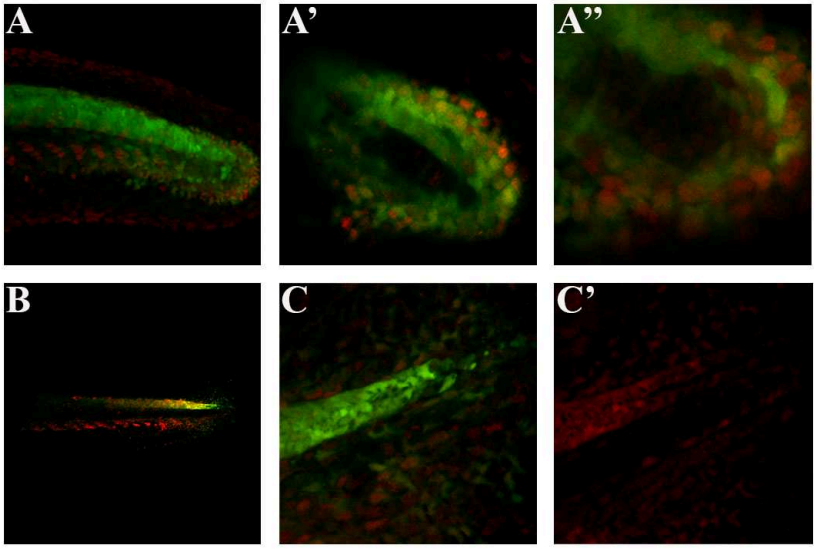

Fig. 9. Phosphorylated-smad3 correlates to reporter expression in 12xSBE line. A, B, C, confocal lateral views of double fluorescent immunohistochemistry for GFP (green) and phosphorylated smad3 on embryo tail at 24 hpf; **A'-A''**, zoom images of the edge of the tail of a 24 hpf embryo; **B-C'**, confocal images of double fluorescent immunohistochemistry for GFP (green) and phosphorylated smad3 on larva tail at 2 dpf; **C**, zoom view of the edge of the tail of a 2 dpf larva and, **C'**, the corresponding picture with the only red channel displayed.

For the genetic validation of the 12xSBE lines the tg(12xSBE:EGFP)^{ia16} line has been crossed with one-eyed-pinhead (*oep*) and chordin (*dino*) mutant lines (Fig. 10). One-eyed-pinhead (TDGF1 or CFC1) is a cofactor of Nodal signalling, a subset of TGF-beta family, involved in mesendoderm specification, left-right axis specification and anterior-posterior axis orientation.

Maternal and early zygotic oep mRNA are ubiquitously expressed. During gastrulation, oep expression is confined in the gastrula margin. In the later stages, it is present in the forebrain, lateral plate and nothocord. In absence of zygotic oep, our TGF beta-responsive line lacks GFP expression in cardiac mesoderm, underlying the role of oep-mediated TGF-beta signalling in mesendoderm specification. On the other hand, the reporter expression is unchanged in the nervous system (Fig. 10B-B'''). In fact, it is known that Nodal signalling is dispensable for neural induction (Jia et al., 2009).

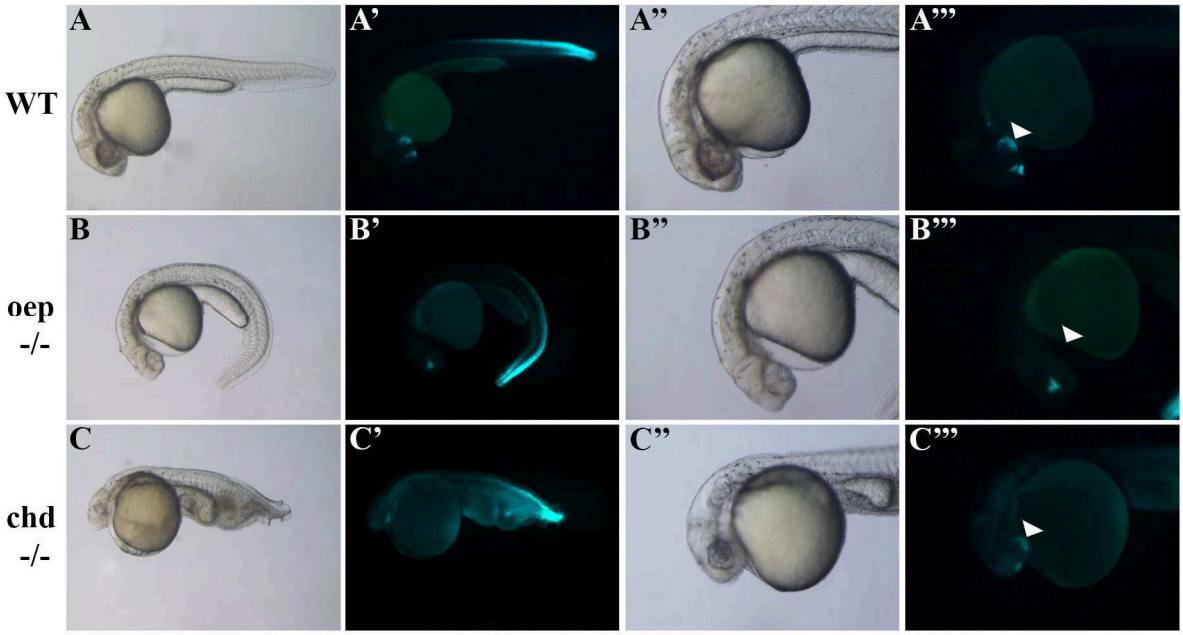

Fig. 10. smad3-induced EGFP expression is independent from smad1/5/8-BMP and partially dependent on nodal signalling. Brightfield and fluorescent lateral views of embryos at 24 hpf from epifluorescent microscope, left to right. **A-A'''**, wild type (WT) 24 hpf embryo of tg(12xSBE:EGFP)^{ia16} line. **B-B''',** oneyedpinhead (*oep*) mutant 24 hpf embryo of tg(12xSBE:EGFP)^{ia16} line. **C-C''',** chordin (*chd*) mutant 24 hpf embryo of tg(12xSBE:EGFP)^{ia16} line. **A'''**, **B''', C''',** white arrow-heads indicate in each picture the cardiac mesoderm region. GFP expression is absent only in *oep* mutant.

The effect of this mutant genetic background have also been evaluated in tg(BMPRE:EGFP)^{ia18} line. No change of fluorescence expression is appreciable on *oep* mutant (Fig. 10).

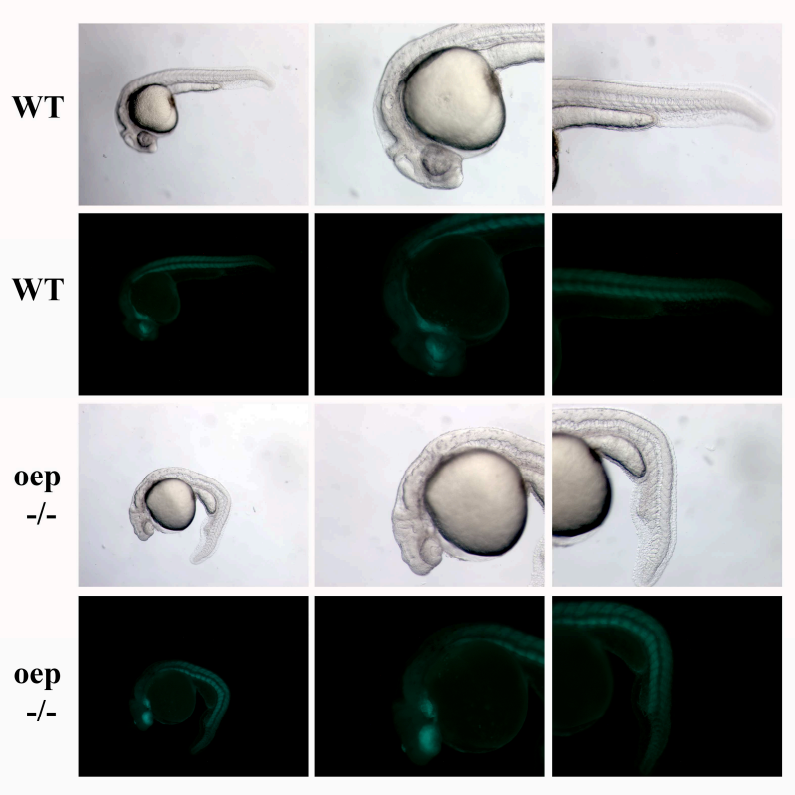

Fig. 11. BMP-induced EGFP expression is independent from nodal signalling. Brightfield and fluorescent lateral views of embryos at 24 hpf from epifluorescent microscope, left to right.

Chordin is a major Bmp2/4 antagonist, expressed in Zebrafish by shield stage. Both BMP and TGF-b belong to TGF-b superfamily and have a similar transduction pathway. However, they require specific receptors and receptor-activated smads. BMP and TGFb exert opposite role in neural induction (negative and positive effects, respectively). To evaluate the specificity of our transgenic line for TGFb-smad2/3, reporter expression has been evaluated in embryos missing the activity of chordin. Despite the obvious morphological changes due to axis specification disruption, we did not observe changes on fluorescence level in the nervous system of mutants (Fig. 10C-C'''). This seems to demonstrate an independent action of smad2/3-mediated signalling on neural induction (Jia et al., 2009). Furthermore, it is known that smad2/3 act on neural induction during gastrulation, at least in part, through chordin, but nodal signalling represent a subgroup of TGFb family. Nevertheless, other ligands, such as activin, can activate smad3 and, consequently, reporter expression.

These transgenic lines have been created using elements recognized by smad3 transcription factor. To test their specific responsiveness, 1-2 cell-stage embryos of the 12xSBE lines have been injected with morpholinos for smad2/3a/3b/4 and their fluorescence has been checked at 24

hpf (Fig. 12 and S1). The morpholinos for smad2/3a/3b have been already tested and validated by Jia S. et al. (2008) and are able to induce different degree of neural degeneration and growth retardation; morphant embryos failed to form floor plate, had eyes malformation and bent nothocord (Jia et al., 2008) When injected in the 12xSBE lines, MO-smad2 was partially affecting the reporter activity in the neural tube. On the other hand, fluorescence was drastically reduced with MO-smad3b and completely abolished with MO-smad3a, evidencing a strong specificity of the 12xSBE transgenic lines for smad3 activity (Fig. 12 and S1).

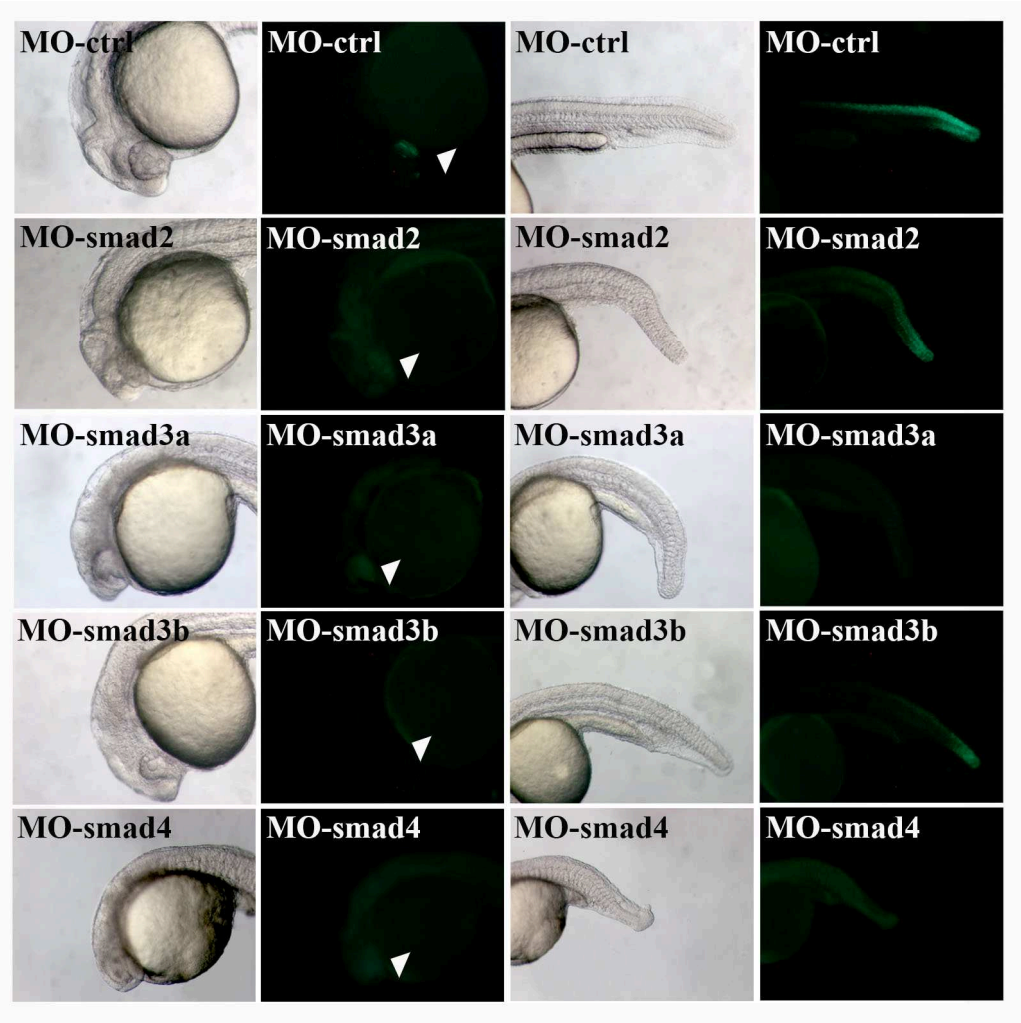

Fig. 12. Different responsiveness of tg(12xSBE:EGFP)^{ia16} line to smad2, smad3a, smad3b and smad4 morpholinos. Brightfield and fluorescent lateral images of smad2-, smad3a-, smad3b- and smad4-morphants at 24 hpf at the epifluorescent microscope, left to right. smad2, 3a and 3b morphants show a similar phenotype: anterior truncation, a curved shortened body axis, absence of floorplate and an enlarged intermediate cell mass. smad4 morphants have a worst phenotype: similar characteristics of the other morphants accompanied to a shortened dorsalyzed body due to BMP inhibition. Reporter expression

is completely inhibited in smad4 and 3a morphants and strongly reduced in smad3b morphants. smad2 morphants lack GFP expression in the cardiac mesoderm and telencephalon like the other morphants (white arrow head) and display a mild reduction in the neural tube.

Both zebrafish smad3 isoforms, 3a and 3b, are expressed in the tail region (Pogoda and Meyer, 2002) (Hsu et al., 2011) and the major efficacy of MO-smad3a might be due to either a higher activity of morpholino for smad3a or a higher expression/function of this gene. The higher reduction of mCherry transgene likely depends on intrinsic properties of this fluorescent molecule (Fig. S1). Whilst its fluorescence is as strong as EGFP, it needs more time to reach similar expression levels. Therefore, when smad-mediated transcription of mCherry is blocked, a longer time is needed to observe a level of mCherry compared with EGFP. In all smad3a, smad3b and smad2 morphants groups no fluorescence has been detected in the cardiac mesoderm. In fact these genes are known to play an important role in the mesoderm specification and outflow tract formation (Jia et al., 2008) (Zhou et al., 2011). Smad4 is a transcription factor, common to TGF-b and BMP signalling, that is necessary for the activation of the r-smad-mediated signalling. For smad4, four morpholinos have been designed and tested for their ability to abolish GFP expression both in our TGF b-responsive. MO3-smad4, specific for a splicing-donor site, was the most efficient in this effect and was used for injection (Fig. 13).

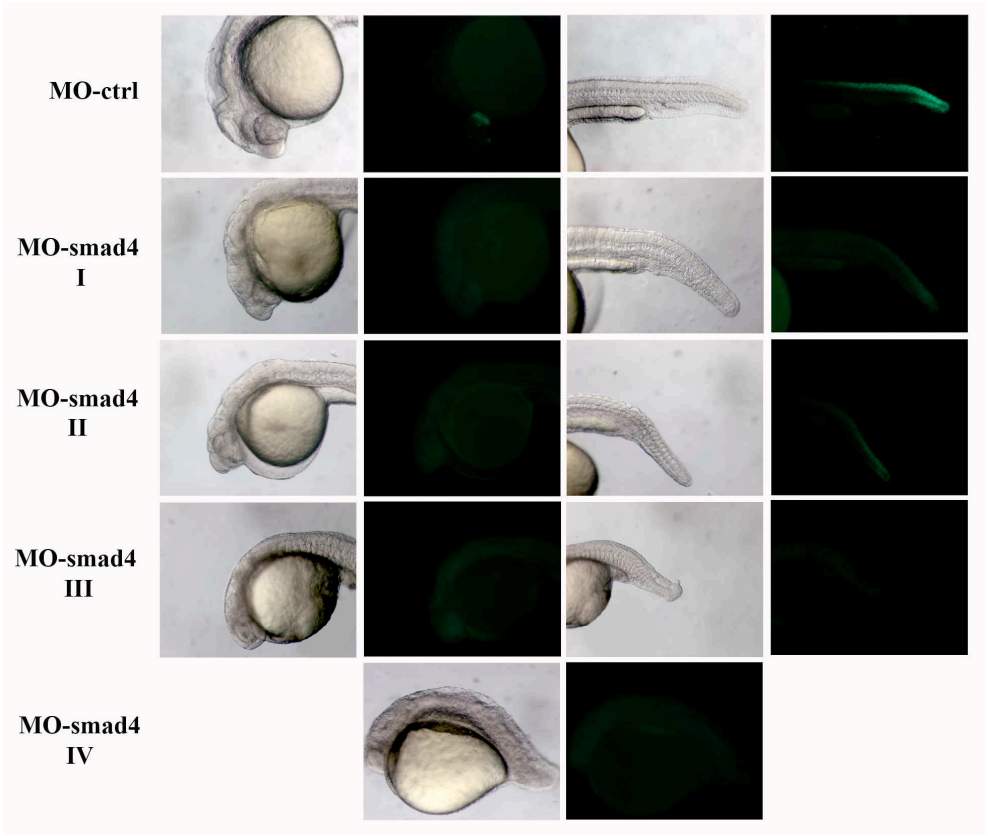

Fig. 13. Different responsiveness of tg(12xSBE:EGFP)^{ia16} line to the 4 morpholinos drawn for smad4. Brightfield and fluorescent lateral images of smad4 (I), smad4(II)-, smad4(III) and smad4(IV)-morphants at 24 hpf at the epifluorescent microscope, left to right. All morphants show anterior truncation, a curved body axis and a dorsalyzed body due to BMP inhibition, but only MO-smad4(III) and MO-smad4(IV) morpholinos completely inhibit reporter expression. Furthermore, MO-smad4(III) and MO-smad4(IV) morpholinos cause a worst phenotype with more marked body defects.

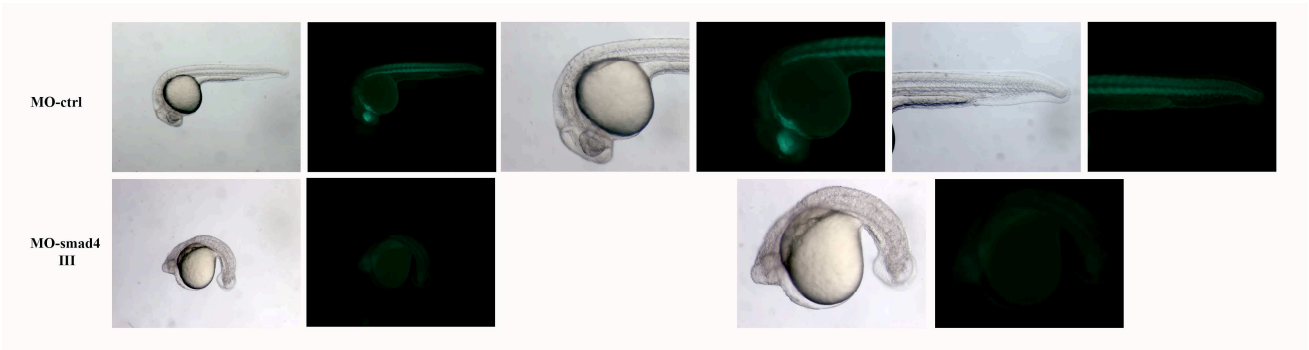

Fig. 14. smad4-knock-down inhibits GFP expression in tg(BMPRE:EGFP)^{ia18} embryos. Brightfield and fluorescent lateral images of smad4 (III) morphant at 24 hpf at the epifluorescent microscope, left to right. All morphants show anterior truncation, a curved body axis and a dorsalyzed body due to BMP inhibition. Morpholino completely blocks reporter expression.

Smad4 morphants show the most severe growth retardation, eye malformation and nothocord defects when compared with smad2/3a/3b-morphants. 24 hpf smad4 morphant embryos are also dorsalized, as a consequence of BMP inhibition. As expected, smad4 morphants failed to activate the reporter (Fig. 11 and 12). Same result has been observed with the tg(BMPRE:EGFP)^{ia18} line (Fig. 14). This confirms both the specificity of our BMPRE line and the efficacy of the selected smad4 morpholino.

To further demonstrate the specificity of our 12xSBE lines, we induced the overexpression of either smad7 or smad3b in 24hpf embryos (Fig. 15). Smad7 is an inhibitory smad able to block smad3-mediated TGFb signalling by inhibiting phosphorylation of type I receptor, recruiting smurf1 and 2 and leading to proteasomal degradation of ligand-receptor complex (Yan et al., 2009). To induce an increase of smad7, the tg(12xSBE:nlsmCherry)^{ia15} line has been crossed with a transgenic line expressing the smad7-YFP fusion coding sequence under the control of hsp70 regulatory region. Heat-shocked larvae analysed at the confocal microscope reveal a strong activation of YFP and a concomitant dramatic reduction of mCherry in the entire embryos (Fig. 15A-A'').

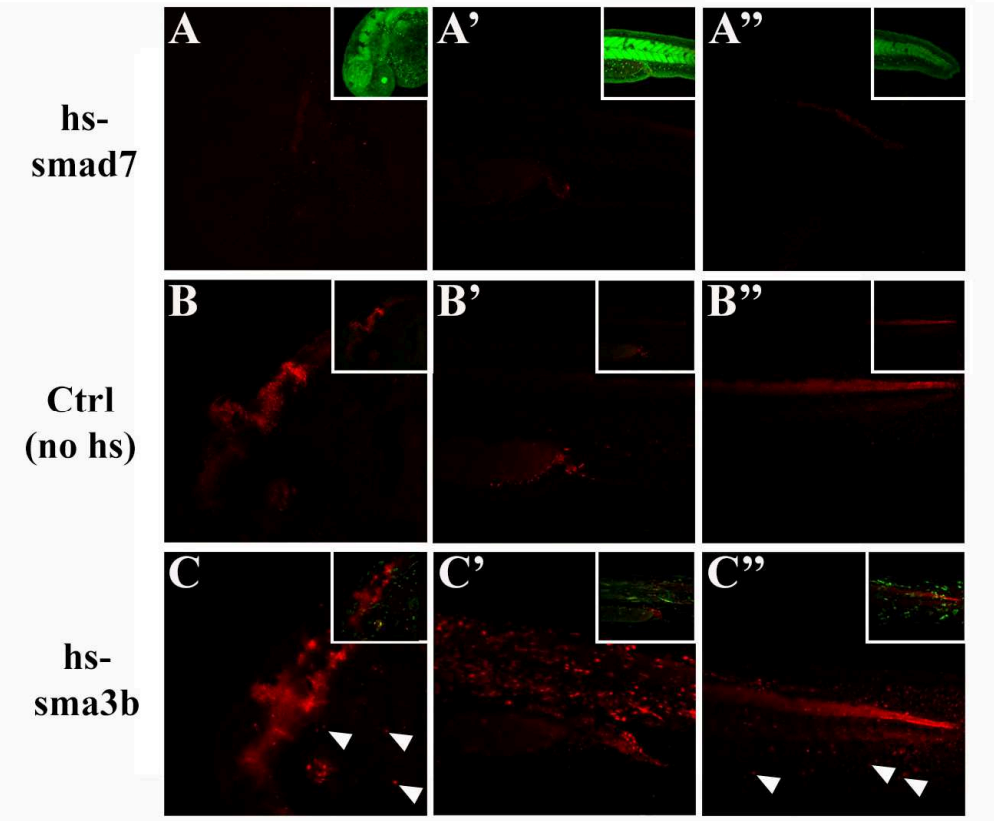

Fig. 15. Tg(12xSBE:nls-mCherry)^{ia15} line is responsive to smad7 and smad3b overexpression. A-A'', confocal lateral images of 48 hpf double transgenic larvae, tg(12xSBE:nls-mCherry)^{ia15}/hs-smad7/YFP. Heat-shock causes an overexpression of the reporter gene and an ubiquitous production of YFP. **B-B''**, confocal lateral images of 48 hpf not heat-shocked double transgenic larvae, tg(12xSBE:nls-mCherry)^{ia15}/hs-smad7/YFP and tg(12xSBE:nls-mCherry)^{ia15}/hs-smad3b/YFP. Only not heat-shock tg(12xSBE:nls-mCherry)^{ia15}/hs-smad7/YFP is shown as control. **C-C'',** confocal lateral images of 48 hpf heat-shocked double transgenic larvae, tg(12xSBE:nls-mCherry)^{ia15}/hs-smad3b/YFP. The heat-shock leads to a smad3b overexpression confirmed by mosaic production of YFP. An ectopic expression of the mCherry protein is the interesting effect of the heat shock, well visible in the muscles of the trunk, **C'**. White arrow heads show ectopic expression also in the head and tail, **C,C''**. Each picture shows mCherry fluorescence following the heat-shock and it is accompanied by a small figure representing merge of YFP (green) and mCherry (red) (upon, surrounded by white square).

To stimulate an increase of smad3b expression, 1-2 cell stage embryos of the tg(12xSBE:nlsmCherry)^{ia15} line have been injected with a plasmid containing the smad3b-YFP fusion coding sequence under the control of hsp70 regulatory region. Embryos at 24 hpf stage have been heat-shocked three times every 12 hours at 30°C for 30 min and analysed by confocal microscopy. As shown in the picture, only heat-shocked embryos show expression of the YFP.

Due to the fact that a plasmid has been injected, the expression is mosaic. Notably, 12xSBE reporter expression levels are significantly increased and accompanied by an ectopic activity (i.e., muscle in the trunk) meaning that smad3 driven by hsp70 promoter is able by itself to activate the reporter (Fig. 15C-C").
In conclusion, pharmacological, mutants, morpholinos and molecular analyses show that the zebrafish 12xSBE lines are *bona fide* TGFb/smad3 responsive, *in vivo*.

2. Fluorescence expression pattern in Wnt, BMP and Shh reporter lines

For all reporter lines, fluorescence expression has been observed from 1 to 4 dpf at the epifluorescent and confocal microscopes.
In the 7xTCF-Xla.Siam lines, reporter expression is active during formation and maintenance of sensory organs, such as the lateral line, olfactory bulbs, taste buds, otic vescicles as well as in cardiovascular tissues, including heart valves and endothelial cells of the brain, liver and gills (Moro et al., 2012) (Fig. 16a).
In the BMPRE lines the main reporter expression areas are vasculature and heart, muscle, maxillary and mandibular processes, pharyngeal arches, dorsal retina, otic vesicle, cloaca. (Fig.16b).
For 12xGli lines reporter expression is restricted to the ventral side of the central nervous system, median musculature and craniofacial tissues (Fig. 16c).
For both BMP and Shh reporter lines, fluorescence expression seems to be similar to that of similar reporter lines, produced with the same transcription factors-responsive sequences and already published (Laux et al., 2011) (Schwend et al., 2010).

2.a Fluorescence expression pattern in TGFb/smad3 reporter line

We then decided to analyze the spatio-temporal fluorecescent activity of 12xSBE lines. While a wide GFP expression is visible early after fertilization in the offspring of female Tg(12xSBE:EGFP)^{ia16} carriers, due to a maternal effect, a more specific and zygotic fluorescence appears at late somitogenesis (15 hpf) in the tail (both mesoderm and neural tube) and cardiac mesoderm region (Fig. 17). At 26 hpf fluorescence is also visible in telencephalic region. At 48 hpf reporter expression gradually extends to the entire neural tube, maintaining a gradient decreasing from the tail (Fig. 17).
Tg(12xSBE:EGFP)^{ia16} and tg(12xSBE:nlsmCherry)^{ia15} lines show a similar fluorescence expression pattern (Fig. S2). Differences have been seen in time expression due to the specific

intrinsic properties of each reporter gene.

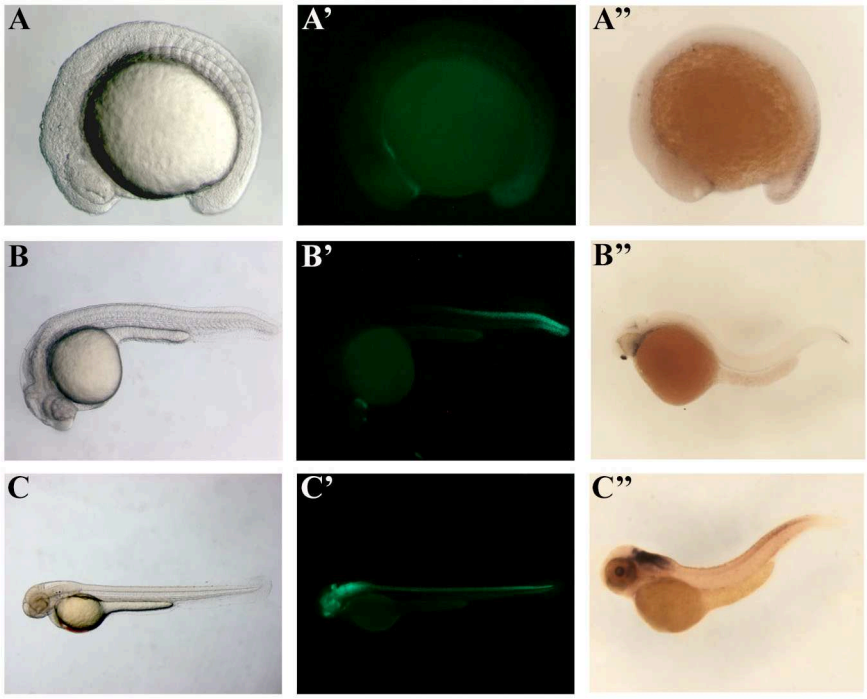

Fig. 17. Fluorescence expression in early development of tg(12xSBE:EGFP)^{ia16} line. Brightfield and fluorescent lateral views of tg(12xSBE:EGFP)^{ia16} embryos at 15, 26 and 48 hpf, left to right. For each stage, it is reported mRNA *in situ* hybridization for GFP. **A-A'',** images of 15 hpf embryo of tg(12xSBE:EGFP)^{ia16} line. **B-B''**, pictures of 26 hpf embryo of tg(12xSBE:EGFP)^{ia16} line. **C-C'',** pictures of 48 hpf larva of tg(12xSBE:EGFP)^{ia16} line. GFP expression appears in late somitogenesis in the tail and cardiac mesoderm region. **A**t 26 hpf GFP is also visible in the telencephalic region and clearly expressed in the embryo neural tube and tail mesoderm. At 48 hpf reporter expression is extended to the entire neural tube, maintaining a decreasing gradient from the tail and in some areas of the brain.

A more detailed observation of the tg(12xSBE:EGFP)^{ia16} line at the confocal microscope gives a better understanding of cellular types activating TGFb signalling.

In the anterior, the reporter is activated in the hindbrain, diencephalon and telencephalon as evidenced in Fig. 19 and Vibe-Z analysis (Ronneberger et al., 2012).

In the neural tube, fluorescent cells occupy ventricular and transition zones, where neuronal precursors proliferate and neuroblasts start their differentiation, respectively (Fig. 18E-F).

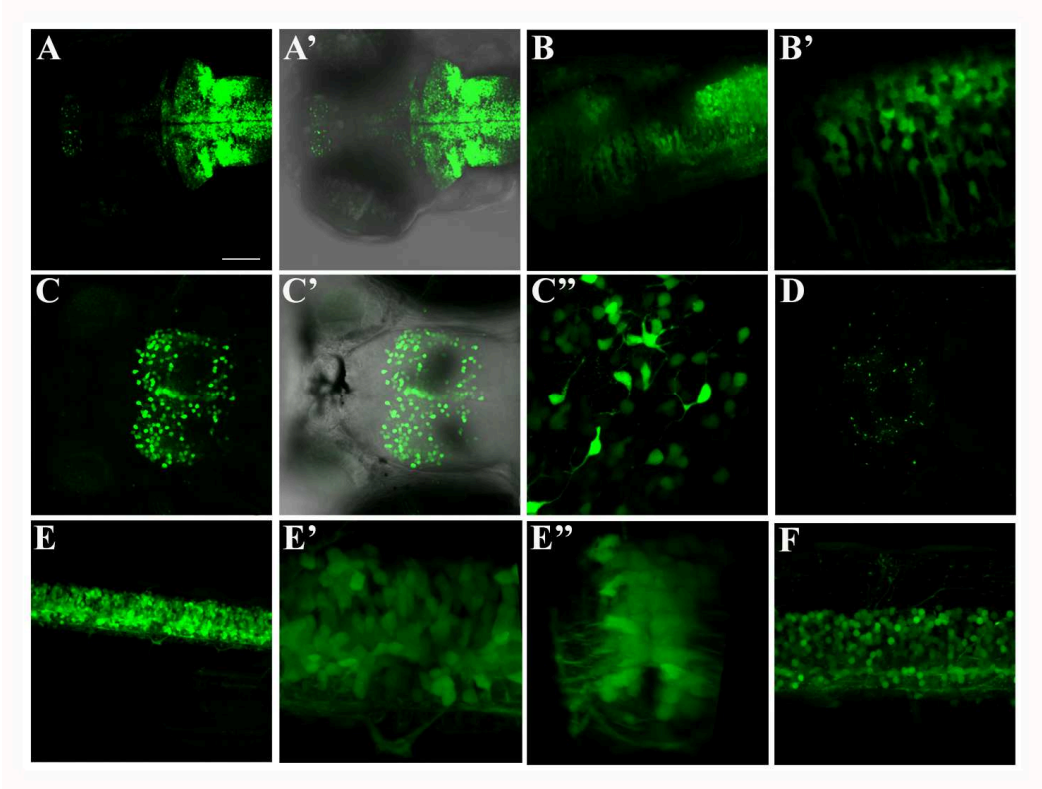

Fig. 18. Reporter expression during early larval development: central nervous system. Confocal images of brain and neural tube of tg(12xSBE:EGFP) larvae at different stage of development. **A-A',D,** error bar of 100 µm; **B,C-C', E,** error bar of 50 µm; **B', C'', E'-F,** error bar of 20 µm. **A-A'**, dorsal view of the brain of a 4 dpf larva. GFP is expressed in the hindbrain, diencephalon and telencephalon. **B-B',** zoom lateral views of hindbrain in a larva at 3 dpf. GFP is expressed in radial glia. **C-C''**, magnified dorsal views of GFP-expressing cells in the telencephalic region of 10 dpf larva magnification of the hindbrain. **D,** zoomed dorsal view of a 15 dpf larva telencephalon. **E,** lateral view of the neural tube in a 72 hpf larva and, **E'-E''** lateral and sagittal magnified views of a 3d-reconstruction of the neural tube at the same stage. Reporter expression is mainly localized around the ventricular zone. **F,** zoomed lateral view of a 6 dpf larva neural tube.

Outside of the central nervous system (CNS), fluorescence is distinguishable in the retina, lens and olfactory epithelium (Fig. 19D-E). Reporter-expressing cells are found in cardiac mesoderm at 24 hpf, where they give rise to the outflow tract (Zhou et al., 2011) (Fig. 20A-B'). In the heart region, the reporter is still expressed at 3-4 dpf in the outflow tract and some cells distributed in the dorsal aorta (Fig. 19C-C'). Few fluorescent cells are also distinguishable in the jaws at 4 dpf (Fig. 19F-F'), while a weak GFP expression is visible in pectoral fins and cloaca. These areas are even more appreciable in tg(12xSBE:nlsmCherry)^{ia15}. In the tail and cardiac region, the reporter

expression is also found in mesoderm cells. In fact, smad3 signalling is known to be involved in mesoderm specification via Nodal signalling (Jia et al., 2008).

At about one month post-fertilization, fluorescence decreases in the entire central nervous system, where it is still expressed at low level in ventral part of the neural tube, particularly in the telencephalic region. Notably, at this stage, some muscle fibers of the median musculature start expressing the reporter gene (Fig. 19H). In facts, the role of TGFb signalling in the control of muscle development is well-known (Ge et al., 2012) (Hsu et al., 2011).

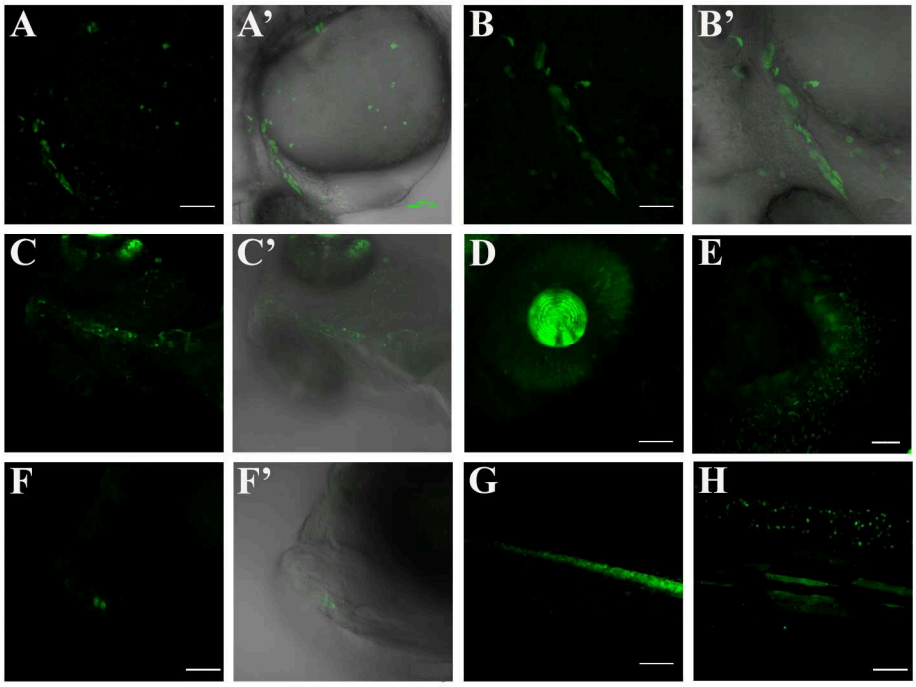

Fig. 19. Confocal images of GFP-positive regions external to CNS during the first month of development. A-A', confocal lateral view of 26 hpf embryo. Reporter gene is activated in the cardiac mesoderm and around the outflow tract. Spared cells are also visible in the yolk ball. **B-B',** zoomed heart region of a 26 hpf embryo. **C-C'**, ventral view of heart and dorsal aorta of a 4 dpf larva. GFP expression in this area is no longer visible beyond this stage. **D**, zoomed view of the eye of a 48 hpf larva. GFP-positive cells are visible both in retina and lens. **E**, zoomed view of an olfactory pit of a 6 dpf larva; **F-F'**, magnified image of jaw of 5 dfp larva. Few cells are visible in this area during the early larval development; **G**, lateral image of a 26 hpf embryo trunk. GFP expression is present in the neural tube with a decreasing gradient from the tail and cloaca. **H**, zoomed lateral view of the trunk region of a 40 dpf larva. Reporter expression is still present in the neural tube. Some fibers of the median musculature seem to activate smad3-mediated signalling during this developmental stage.

In adult fishes, EGFP expression is localized along the spinal cord and into the lens, whilst in

tg(12xSBE:nlsmCherry)[ia15] fluorescence is detectable in ventricular zone of brain and telencephalic region (Fig. 20).

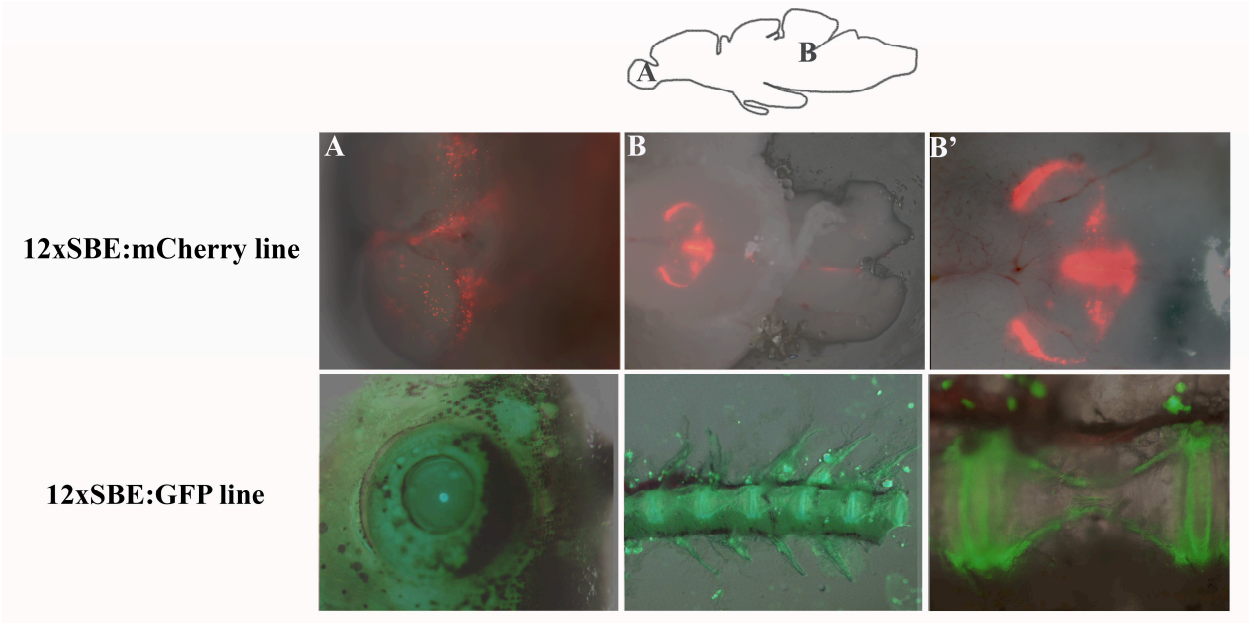

Fig. 20. Images of reporter expression in adult fishes of 12xSBE lines. . Brightfield and fluorescent views of tg(12xSBE:EGFP)[ia16] and tg(12xSBE:nls-mCherry)[ia17] adult fishes. Both reporter lines retain reporter expression, but in different districts: brain (telencephalon and ventricular zone) expresses the reporter gene in tg(12xSBE:nls-mCherry)[ia17] (on the left), whilst tg(12xSBE:EGFP)[ia16] expresses GFP along the spinal cord and in the lens (on the right).

3. Smad3-mediated neurogenesis in Zebrafish1: *in vivo* study through a smad3-responsive transgenic line

3.a TGFb/smad3 signalling is activated in glia and neuronal precursors

Smad3 activation is known to have a neurotrophic effects on DOPAminergic neurons (Krieglstein et al., 2002) (Tapia-Gonzalez et al., 2011), motor neurons (Ho et al., 2000), interneurons (Garcia-Campmany and Marti, 2007) and also GFAP-expressing cells (Tapia-Gonzalez et al., 2011). In these cell types, it seems to be involved in axons growth (motor neurons), differentiation process (interneurons), dislocation of differentiating neurons in the neural tube and radial glia differentiation (Stipursky and Gomes, 2007).

Thus, supported by the pattern expression of 12xSBE lines, we focused our attention trying to understand the nature of cells in which the reporter is active. For this purpose,

tg(12xSBE:nlsmCherry)^{ia15} line has been crossed with some transgenic lines expressing GFP under the control of different promoters specific for neural progenitors (Ngn1), precursors (NeuroD and GFAP) and committed neural cells (Mnx1 and Nkx2.2a) (Fig. 21 and S31, S4 and S5).

The reporter expression of each double transgenic has been followed during the first week of development at the confocal microscope. At a first glance, the higher colocalization has been seen with neuronal and glial precursor markers, GFAP and NeuroD. This was quantified in the tail region by using Volocity Software and representing it as Manders'coefficient referred as the percentage of mCherry (TGFb) intensity fluorescence colocalizing with GFP (neuronal and glial markers) (Fig. 21A''', B''', C''', D''' and E'''). For both these markers, the highest value has been obtained at 2 and 3 dpf.

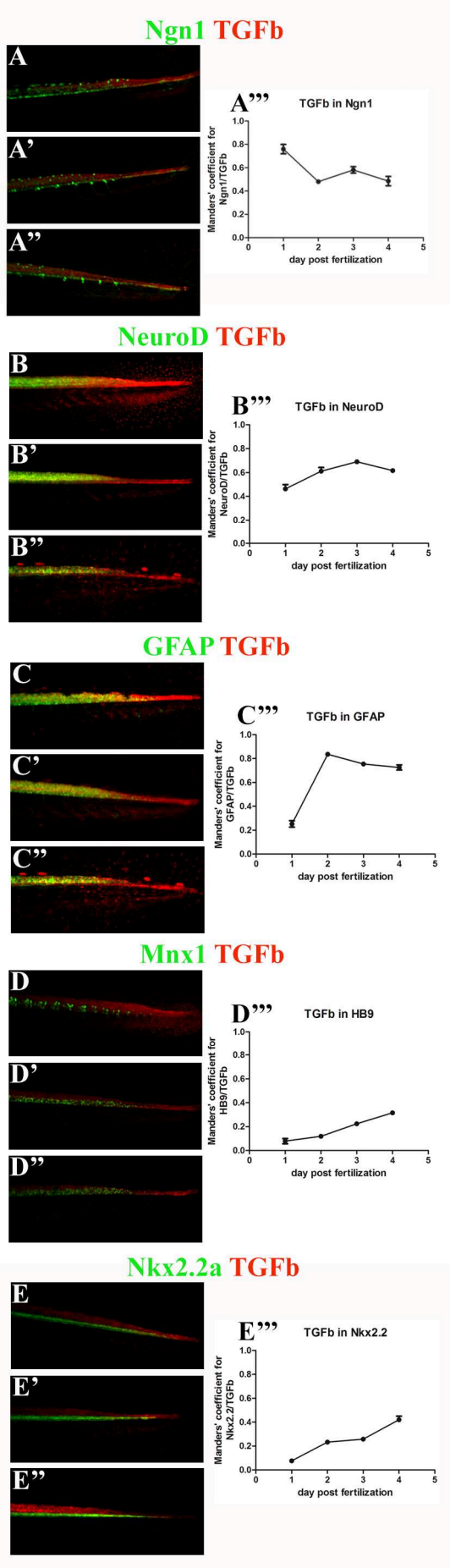

Fig. 21. Reporter expression correlates to neuronal and glial differentiating cells. Confocal lateral view of tail of double transgenic larvae at 2, 3 and 4 dpf obtained mating tg(12xSBE:nls-mCherry)^{ia15} line with some transgenics expressing GFP in different neuronal and glial cells: tg(Ngn1:GFP)^{sb1}, tg(-2.4kb neurod:EGFP), tg(gfap:GFP)^{mi2001}, tg(Mnx1:GFP)^{ml2} and tg(Nkx2.2a:mGFP)^{vu17}. On the right, the last column reports graphs of colocalization measured in tail of each double transgenic larvae at 1, 2, 3 and 4 dpf. Colocalization has been expressed as Manders' coefficient referred to mCherry (percentage of mCherry fluorescence colocalizing with GFP) and has been calculated in six larvae. The average value has been reported on the graph for each time-point. **A-A'',** confocal lateral images of tails of double transgenic larvae tg(Ngn1:GFP)^{sb1} /tg(12xSBE:nls-mCherry)^{ia15} at 2, 3 and 4 dpf with the corresponding colocalization graph. **B-B'-B''**, confocal lateral images of tails of double transgenic larvae tg(-2.4kb neurod:EGFP)/tg(12xSBE:nls-mCherry)^{ia15} at 2, 3 and 4 dpf with the corresponding colocalization graph. **C-C'-C'',** confocal lateral images of tails of double transgenic larvae tg(gfap:GFP)^{mi2001}/tg(12xSBE:nls-mCherry)^{ia15} at 2, 3 and 4 dpf with the corresponding colocalization graph. **D-D'-D'',** confocal lateral images of tails of double transgenic larvae tg(Mnx1:GFP)^{ml2}/tg(12xSBE:nls-mCherry)^{ia15} at 2, 3 and 4 dpf with the corresponding colocalization graph. **E-E'-E'',** confocal lateral images of tails of double transgenic larvae tg(Nkx2.2a:mGFP)^{vu17}/tg(12xSBE:nls-mCherry)^{ia15} at 2, 3 and 4 dpf with the corresponding colocalization graph.

To examine the evolution of cells activating TGFb signalling, measures of colocalization have been performed in the tail of 24 hpf double transgenic embryos with the following strategy. Between 15 and 24 hpf stages, somites are formed at a constant rate. Therefore, the tail region has been divided in pairs of somites and colocalization (expressed as Manders'coefficient referred to TGFb/mCherry fluorescence) has been evaluated in four regions starting from the edge of the tail toward the trunk (Fig. 22). The caudal somites are the youngest and the first that activate TGFb signalling in the neural tube. In our graphs, the colocalization of the first pair of somites correspond to the starting point of expression of TGFb signalling (0 hour) and has been plotted on graph in function of the somite/time of TGFb expression. As discernable from the graphs (Fig. 23), at the moment of its activation (time 0 hour) TGFb has its higher colocalization with Ngn1-expressing cells. Ngn1 is a typical marker of proliferating neural progenitors (Korzh et al., 1998). By moving toward the trunk, a reduction of TGFb signalling activation is visible in Ngn1+ cells, whilst it arises in NeuroD expressing cells (Fig. 22A''' and B'''). Notably, NeuroD is a marker of neuronal precursors (Korzh et al., 1998). In Mnx1-expressing cells (differentiating motor neurons), TGFb expression remains low in all four areas examined (Fig. 22D'''). GFAP is a gene associated in radial glia differentiation (Stipursky and Gomes, 2007). By observing results of TGFb colocalization with glial markers, TGFb/GFAP graph shows an evolution similar to that seen in TGFb/NeuroD graph, demonstrating an association of our signal with neuronal and glial precursors (Fig. 22C'''). A low percentage of mCherry expression has been seen in the Nkx2.2a-expressing cells (mature oligodendrocytes and motor neuron precursors) (Fig. 22E''') (Gotoh et al., 2012).

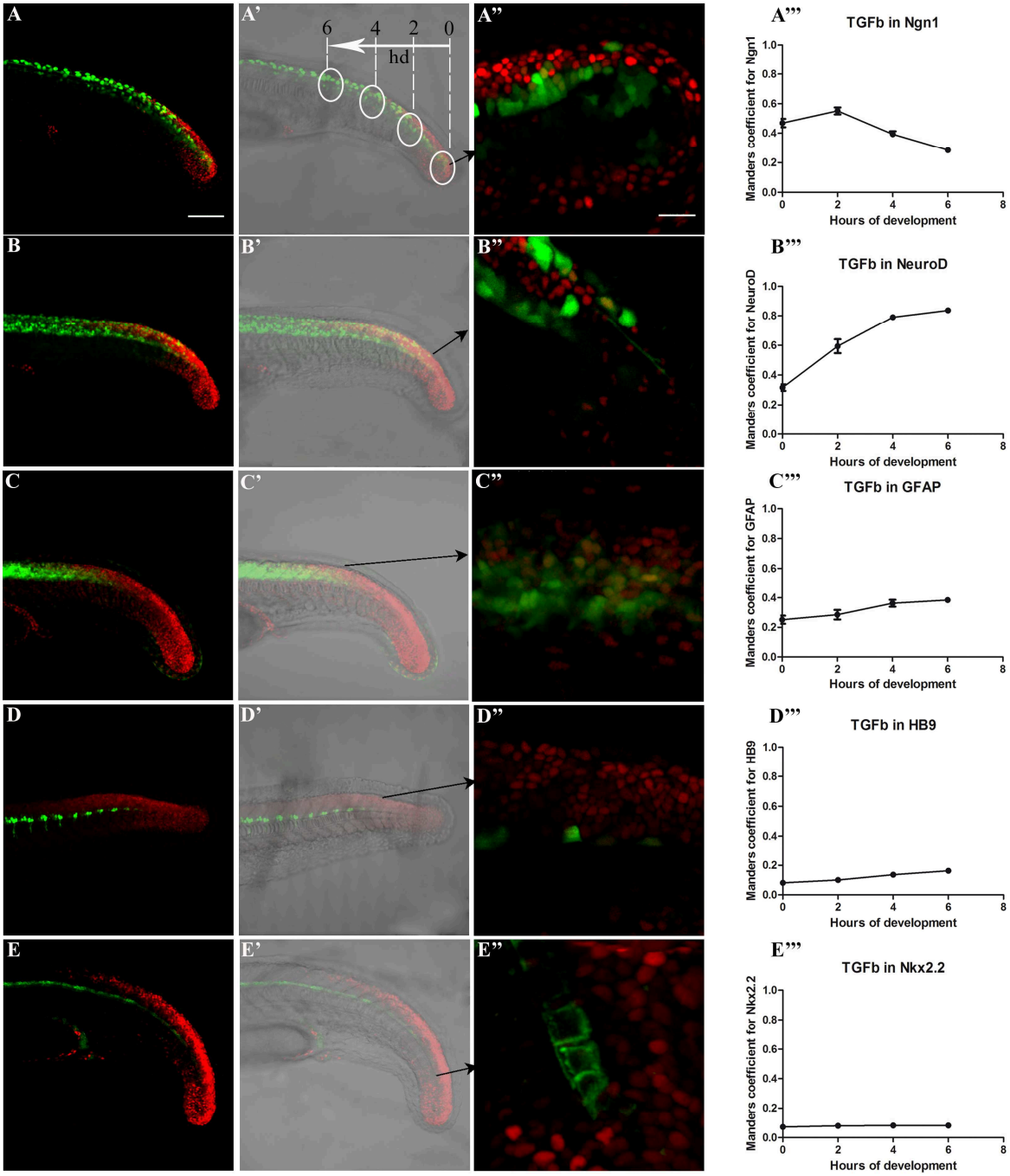

Fig. 22. TGFb signalling appears in progenitor cells and is maintained in precursors. Confocal lateral view of tail of double transgenic embryos obtained crossing tg(12xSBE:nls-mCherry)ia15 to the following transgenics: tg(Ngn1:GFP)^{sb1}, tg(-2.4kb neurod:EGFP), tg(gfap:GFP)^{mi2001}, tg(Mnx1:GFP)^{ml2} and tg(Nkx2.2a:mGFP)^{vu17}. Colocalization measurement has been done in tail of 24 hpf double transgenic embryos with the following strategy. From 15 to 24 hpf, two somites are formed each hour. Therefore, tail region has been divided in pairs of somites and colocalization (Manders'coefficient referred to TGFb-

mCherry fluorescence) has been evaluated in four of them (A', white dotted circles) starting from the edge of the tail toward the trunk, **A'**. For each time point, the average value of Manders' coefficient has been calculated from six double transgenic embryos and plotted on graph in function of the corresponding hour of development (hd), **A''', B''', C''', D''' and E'''**.

3.b EdU assay shows that TGFb is a postmitotic signal

Once established that TGFb signalling is mainly localized in committed neuronal and glial precursors, we wanted to understand the role of this signal in such kind of cells. Functional experiments with neuronal and glial transgenic lines show that smad3 activation is important for neuro- and gliogenesis. To check whether smad3 activation is involved in mitosis, we analysed how a cell proliferation marker, phospho hystone-3 (pH3), changes in MO-smad3a embryos at 24 hpf and larvae treated with LY364947 at 48 hpf (Fig. 23A-D). Results show that reporter signal and pH3 immunofluorescence do not colocalize. Notably, blocking TGFb signalling leads to a significant increase of proliferating cells. To further confirm this, EdU proliferation assay has been performed on 20 hpf embryos, which have been treated with LY364947 at 12 hpf (Fig. 23E-F'). Results show a strong increase of proliferation. Thus, at early stages of development TGFb signal seems to play an important role in regulating the cell cycle. Then, we verified the direct connection of TGF-beta signalling on neural progenitor cell cycle by EdU proliferation assay on tg(12xSBE:EGFP)^{ia16} embryos at 24 hpf (Fig. 23G-H'). Embryos treated with EdU have been fixed and stained after a chase of either 2 or 8 hours. Cells stained after a chase of 2 hours are roughly in S/G2 phase, while cells stained 8 hours after the EdU pulse are in G1 phase. Analysis of colocalization of GFP and EdU show that proliferating cells (2h chase) do not express the reporter, while postmitotic cells (8h chase) do it. In other words, at 24 hpf, the majority of cells with activated smad3 do not proliferate but have just undergone mitosis, letting us conclude that TGFb is a postmitotic signalling during central nervous system development.

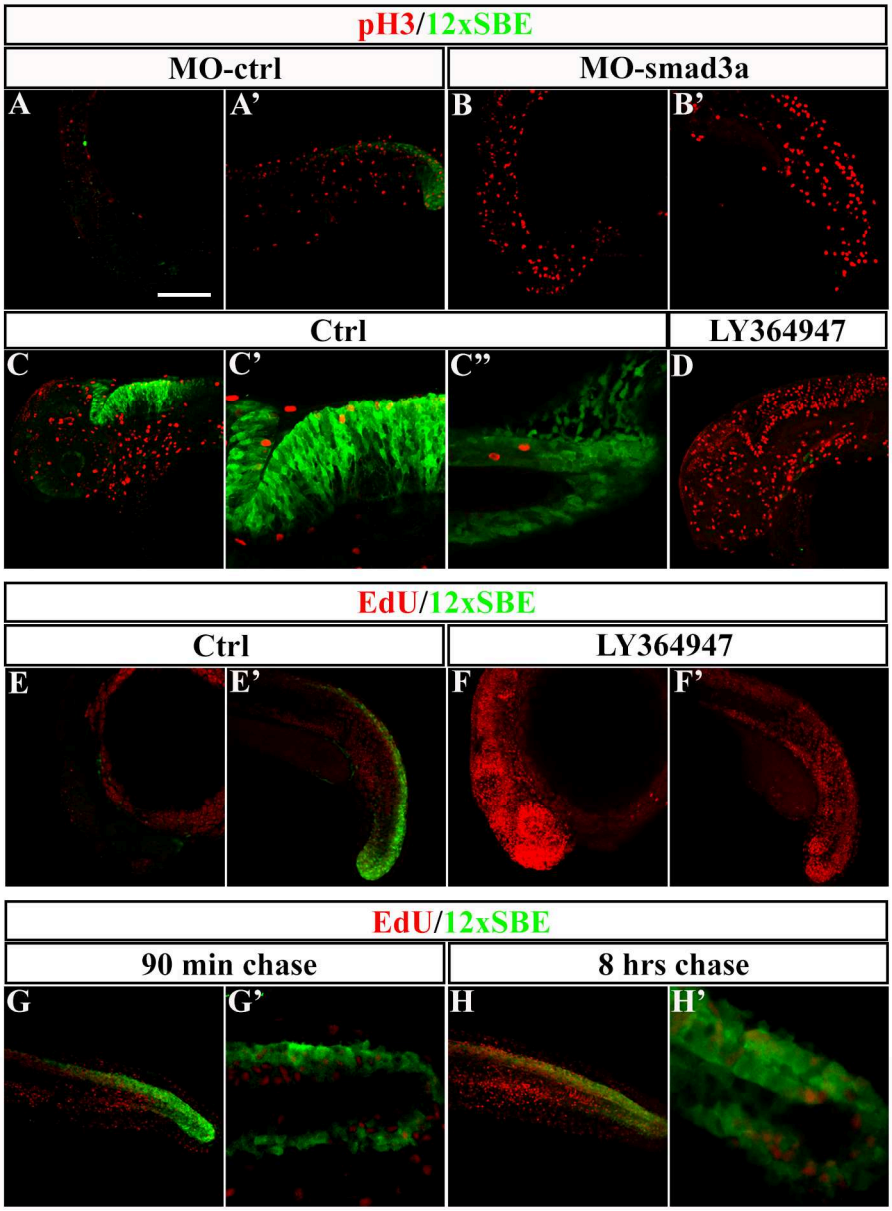

Fig. 23. Smad3/TGFb signalling is active in post-mitotic cells. A-B',E-F',G,H, error bar of 100 µm; **C'-C''**, error bar of 50 µm; **G',H',** error bar of 20 µm. **A-B'**, confocal lateral views of fluorescent immunohistochemistry for GFP (green) and phospho-hystone3 (red) on tg(12xSBE:EGFP)^{ia16} embryos injected at 1-2 cell stage either with the control, **A-A'**, or smad3a-morpholino, **B-B'**. **C-D**, confocal lateral images of fluorescent immunohistochemistry for GFP (green) and phosphor-hystone3 (red) on 2 dpf larva of tg(12xSBE:EGFP)^{ia16} line treated with either DMSO (**C-C''**) or LY364947 (**D**). **C'-C''**, confocal zoomed views of hindbrain and tail of the fluorescent immunohistochemistry for GFP and phospho-hystone3 on DMSO-treated larva of 12xSBE line. **E-F',** confocal lateral images of EdU assay on 20 hpf embryos treated with either DMSO (**E-E'**) or LY364947 (**F-F'**) at 12 hpf. **G-H'**, confocal lateral images of pulse and chase EdU assay on 24 hpf embryos of tg(12xSBE:EGFP)^{ia16} line. Embryos have been fixed after a chase of either 2 (**G-G'**) or 8 (**H-H'**) hours (hrs) and stained for EdU (red) and GFP (green). EdU+ cells fixed after 2 h are roughly in S/G2 phase, while EdU+cells fixed after 8 h of chase are post-mitotic

cells.

3.c *In vivo* blocking smad3-mediated TGFb signalling impairs neuronal and glial differentiation and increases the pool of progenitor cells

To confirm the hypothesis that TGFb signalling blocks proliferation of some progenitor cells allowing their differentiation, smad3a and smad3b morpholinos have been injected in 1-2 cell stage embryos of the transgenic lines, tg(Ngn1:GFP)^{sb1}, tg(-2.4kb neurod:EGFP), tg(gfap:GFP)^{mi2001}, tg(Mnx1:GFP)^{ml2} and tg(Nkx2.2a:mGFP)^{vu17} (Fig. 24). At 24 hpf both smad3a and smad3b morphant embryos show a decrease of GFP expression in motor neurons (hlbx9), with defects in axon development and soma position in the neural tube (Fig. 24D-D''). A similar decrease is also seen in oligodendrocytes in smad3a and b morphant embryos as revealed with GFP driven by the Nkx2.2a regulatory region (Fig. 24E-E''). The reduction of these cells in embryos treated with morpholinos against either smad3a or b is accompanied by a loss of their precursors as revealed by NeuroD and GFAP transgenics as well as an increase of neural progenitors revealed in Ngn1:GFP line (Fig. 24A-C'''). To complete the study of smad3 effect in functions in neural development, we have also co-injected smad3a and b morpholinos (data not shown). The results show that blocking both smad3 isoforms causes an aggravation of the embryo phenotype. However, the effects on the observed neural markers seem to be similar to those observe using each morpholino separetely. Therefore, smad3a and b seem to play both a necessary and additive genetic effect in the developing neural tube.

Moreover, to further confirm the idea that TGFb signalling is a postmitotic signal able to stop progenitors proliferation and allow differentiation, a chemical approach has been followed by treating the same fish lines with the Alk5-inhibitor LY364947 either from 2 hpf to 24 hpf (Fig. 24) or 24 hpf to 72 hpf (Fig. 25). As shown in Fig. 24 and 25, results of chemical treatments essentially recapitulate what already observed and reported with smad3 morpholinos: an increase of progenitors (Ngn1) together with a concomitant decrease of neuronal precursors and number of differentiated cells. In conclusion, both the chemical and genetic approaches have given same results on the role of TGFb in controlling the progenitor/precursor switch.

To complete study of smad3 function, we have checked by immunohistochemistry markers linked to EMT (E-cadherin, cdh1, and N-cadherin, cdh2) in embryos and larvae analysed at 24 hpf and at 48 hpf, respectively, and previously injected with MO-smad3a or treated with LY364947 (Fig. 26). Both chemical and genetic approaches used to block TGFb signalling led us to similar conclusions: while in physiological conditions smad3-responsive cells express N-

cadherin, Smad3/TGFb inhibition reduces both reporter fluorescence and N-cadherin (Fig. 26A-D') activating a concomitant increase of E-cadherin (Fig. 26E-H').

Therefore, we can say that the TGFb inhibition by blocking EMT determines a misplacement of mature neural cells such as motor neurons.

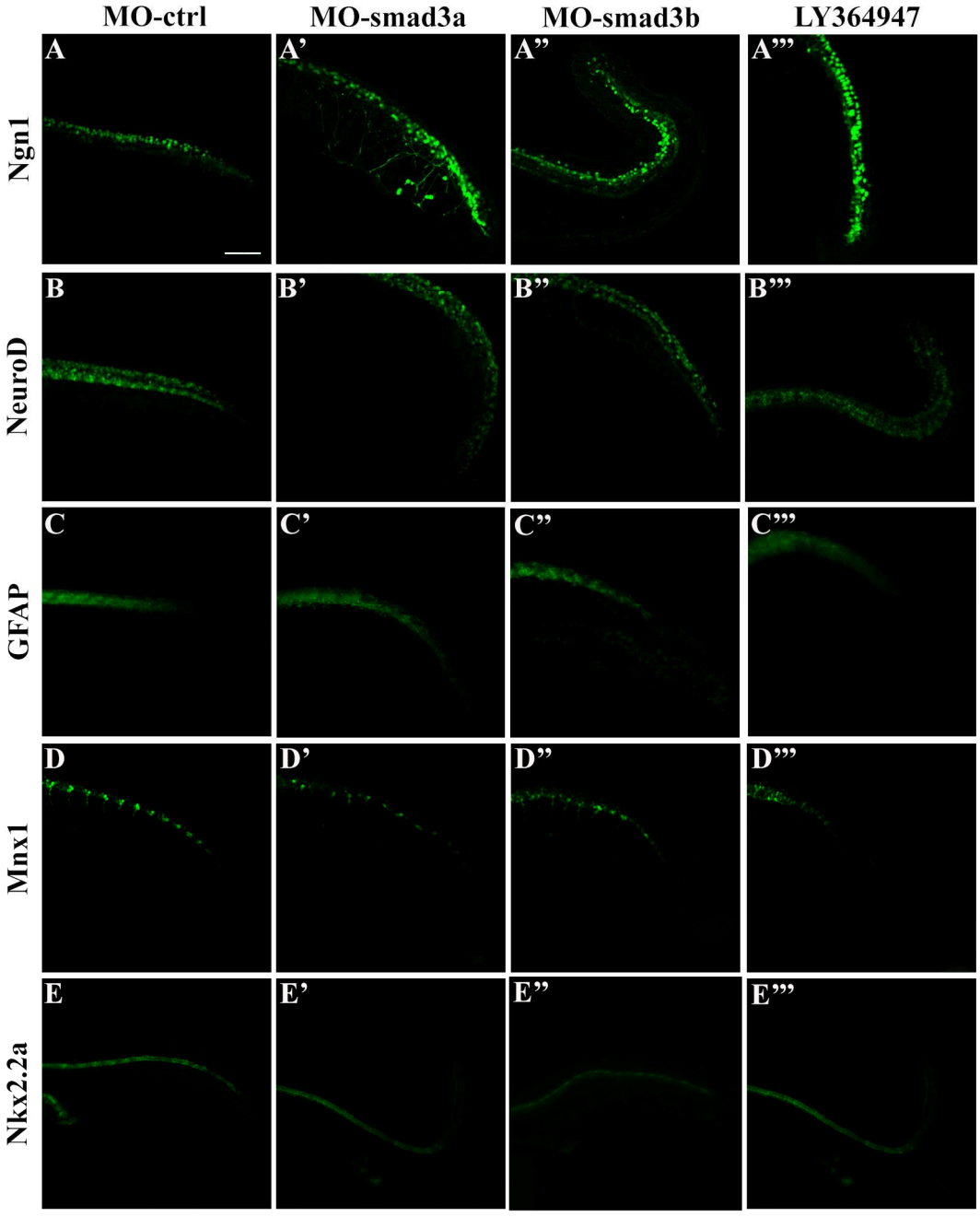

Fig. 24. ***In vivo*** **blocking of smad3/TGFb signalling impairs neuronal and glial differentiation during early embryonic development.** Confocal Z-stack images of tail of 24 hpf transgenic embryos expressing GFP under control of either a glial or neuronal promoter: Ngn1, NeuroD, GFAP, Mnx1 and NKx2.2a. All these transgenic lines have been injected with morpholinos for smad3a and smad3b at 1-2

cell stage or treated at 2hpf with Alk5-inhibitor LY364947. Morpholinos and drug treatment give similar results: increase of proliferative cells (Ngn1), decrease of differentiating cells (NeuroD and GFAP) and reduction of late differentiating motor neurons and oligodendrocytes (Mnx1 and Nkx2.2a). Morpholinos and drug have been picked up, transgenics on the left. Ngn1 is tg(Ngn1:GFP)^{sb1}. NeuroD is tg(-2.4kb neurod:EGFP). GFAP is tg(gfap:GFP)^{mi20001}. Mnx1 is tg(Mnx1:GFP)^{ml2}. Nkx2.2a is tg(Nkx2.2a:mGFP)^{vu17}.

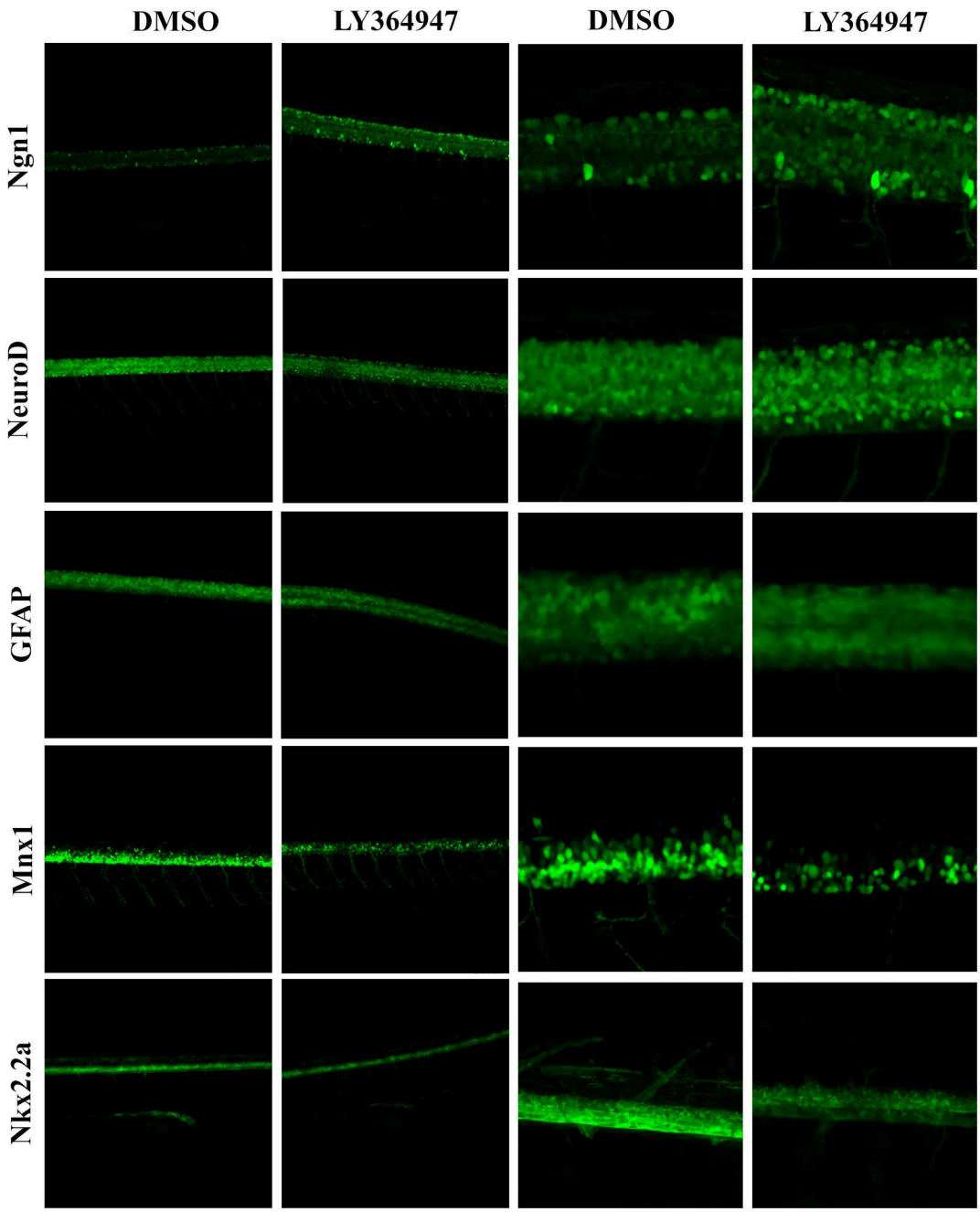

Fig. 25. *In vivo* blocking of smad3/TGFb signalling impairs neuronal and glial differentiation during early larval development. Confocal Z-stack images of trunk of 72 hpf transgenic embryos expressing GFP under control of either a glial or neuronal promoter: Ngn1, NeuroD, GFAP, Mnx1 and

NKx2.2a. All these transgenic lines have been treated at 24 hpf with Alk5-inhibitor LY364947 and confocal observation has been done after two days of treatment. Disturbing Smad3/TGFb signalling at early larval development causes an increase of proliferative cells (Ngn1), decrease of differentiating cells (NeuroD and GFAP) and reduction of late differentiating motor neurons and oligodendrocytes (Mnx1 and Nkx2.2a).

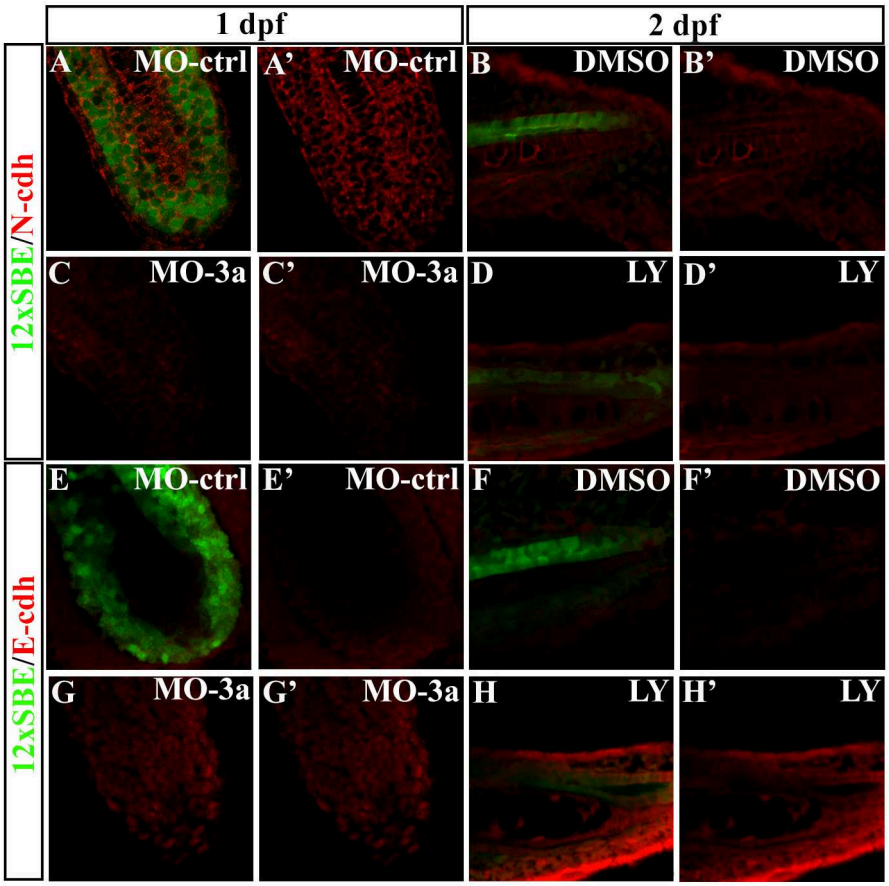

Fig. 26. Smad3/TGFb signalling promotes EMT. A-D', confocal images of fluorescent immunohistochemistry (IHC) for 12xSBE-associated GFP (green), N-cdh (red) and E-cdh (red) on the edge of the tail of control/smad3a 12xSBE morphants at 24 hpf and 12xSBE larvae treated with DMSO/LY364947 and fixed at 2dpf. **A**, IHC for GFP and N-cdh on control morphant tail of tg(12xSBE:EGFP)^{ia16} embryo and, **A',** the same area showing only IHC for N-cdh (red). **B**, IHC for GFP and N-cdh on tg(12xSBE:EGFP)^{ia16} larva (2 dpf) treated with DMSO and, **B',** the same area showing only IHC for N-cdh (red). **C**, IHC for GFP and N-cdh on smad3a morphant of tg(12xSBE:EGFP)^{ia16} embryo and, **C',** the same area showing only IHC for N-cdh (red). **D**, IHC for GFP and E-cdh on tg(12xSBE:EGFP)^{ia16} larva (2 dpf) treated with DMSO and, **D',** the same area showing only IHC for N-cdh (red). **E**, IHC for GFP and E-cdh on control morphant tail of tg(12xSBE:EGFP)^{ia16} embryo and, **E',** the same area showing only IHC for E-cdh (red). **F**, IHC for GFP and E-cdh on tg(12xSBE:EGFP)^{ia16} larva (2 dpf) treated with DMSO and, **F',** the same area showing only IHC for E-cdh (red). **G**, IHC for

GFP and E-cdh on smad3a morphant of tg(12xSBE:EGFP)^{ia16} embryo and, **G',** the same area showing only IHC for E-cdh (red). **H**, IHC for GFP and E-cdh on tg(12xSBE:EGFP)^{ia16} larva (2 dpf) treated with LY364947 and, **H',** the same area showing only IHC for E-cdh (red).

4. Epistasis: how to study *in vivo* chemical signals interactions

4.a Chemical treatment: observation of fluorescence changes at the epifluorescent microscope

The four reporter lines previously described have been used to study *in vivo* the interactions among the corresponding 4 morphogens, involved in various physiological and pathological processes. For this aim, each reporter has been treated with some drugs used to validate the others.

Notch and FGF signalling pathways have been analysed together with these morphogens. Tg(Tp1bglob:eGFP) line and a γ-secretase inhibitor, DAPT, have been used to follow Notch pathway, while a vascular endothelial growth factor receptor (VEGFR) and fibroblast growth factor receptor (FGFR) inhibitor, SU 5402, has been chosen to block FGF signal.

All treatments have been done at 24 hpf, when GFP is widely expressed by all the analysed transgenics. Drugs and dosages are reported in *Material and Methods*.

Considering GFP stability observed during reporters validation, drugs treatment have been conducted for two days.

A photo of an entire larva together with magnified views of anterior and posterior body parts have been taken at the epifluorescent microscope for each drug treatment (Fig. 27, 28, S5, S6, S7 and S8). A general network of putative interactions can be inferred using these preliminary data (Fig. 29).

Some of them confirmed what is known from literature:

- the inhibitory effects of Shh on BMP (Marcelle et al., 1997) (Motoyama and Aoto, 2000)
- the inhibitory effect of Wnt on BMP signal (Nakashima et al., 2005) (Baker et al., 1999) (Marcelle et al., 1997)
- the inhibitory effect of Notch on both Wnt and Shh (Wang et al., 2009) (Deregowski et al., 2006) (Kim et al., 2012) (Roy et al., 2014)

Other treatments have given apparent contrasting results depending on the tissue. For example, the inhibition of FGF signal causes a drastic reduction of GFP in the tg(7xTCF-Xla.Siam:GFP)^{ia4}

larvae, except for the lateral line that appears to be stimulated. It is known that blocking FGF signalling in the pre-somitic mesoderm prevents Wnt activation (Wahl et al., 2007). On the other hand, FGF plays an opposite role during the lateral line formation. The Wnt/β-catenin inhibitor dikkopf1 (dkk1), which is expressed immediately adjacent to the leading zone of Wnt/beta-catenin signalling, is absent upon FGF inhibition. Therefore, there is a negative feedback loop in which FGF signalling inhibits Wnt/beta-catenin through the inhibitor dkk1, thus spatially restricting Wnt/beta-catenin to the leading zone in the migrating primordia (Ma and Raible, 2009). A further example is offered by Shh inhibition that determines a decrease of reporter expression in the tg(7xTCF-Xla.Siam:GFP)^{ia4} larvae and, concomitantly, an expansion of GFP+ cells in the heart region and the increase of reporter expression in the lateral line (Fig. 31). Wnt pathway plays an important role in the development of sensory organs, such as the lateral line. Ken Iwatsuki et al. have demonstrated that blocking Shh up-regulates Wnt signalling in cultured tongue explants and enhances papillae formation (Iwatsuki et al., 2007).

In some cases, inhibition and stimulation of the same chemical signal do not have opposite effect. For example, BIO-induced Wnt stimulation has clearly reduced BMP-associated reporter expression. On the other hand, IWR-1-induced Wnt inhibition did not significantly increase GFP expression in the same reporter line.

In the "Appendix" chapter some confocal views of treated larvae of tg(12xSBE:EGFP)^{ia16}, tg(12xGli-Hsv.Tk:GFP)^{ia11} and tg(7xTCF-Xla.Siam:GFP)^{ia4} lines are displayed and can better shown some of the revealed interactions (Fig. S7, S8 and S9).

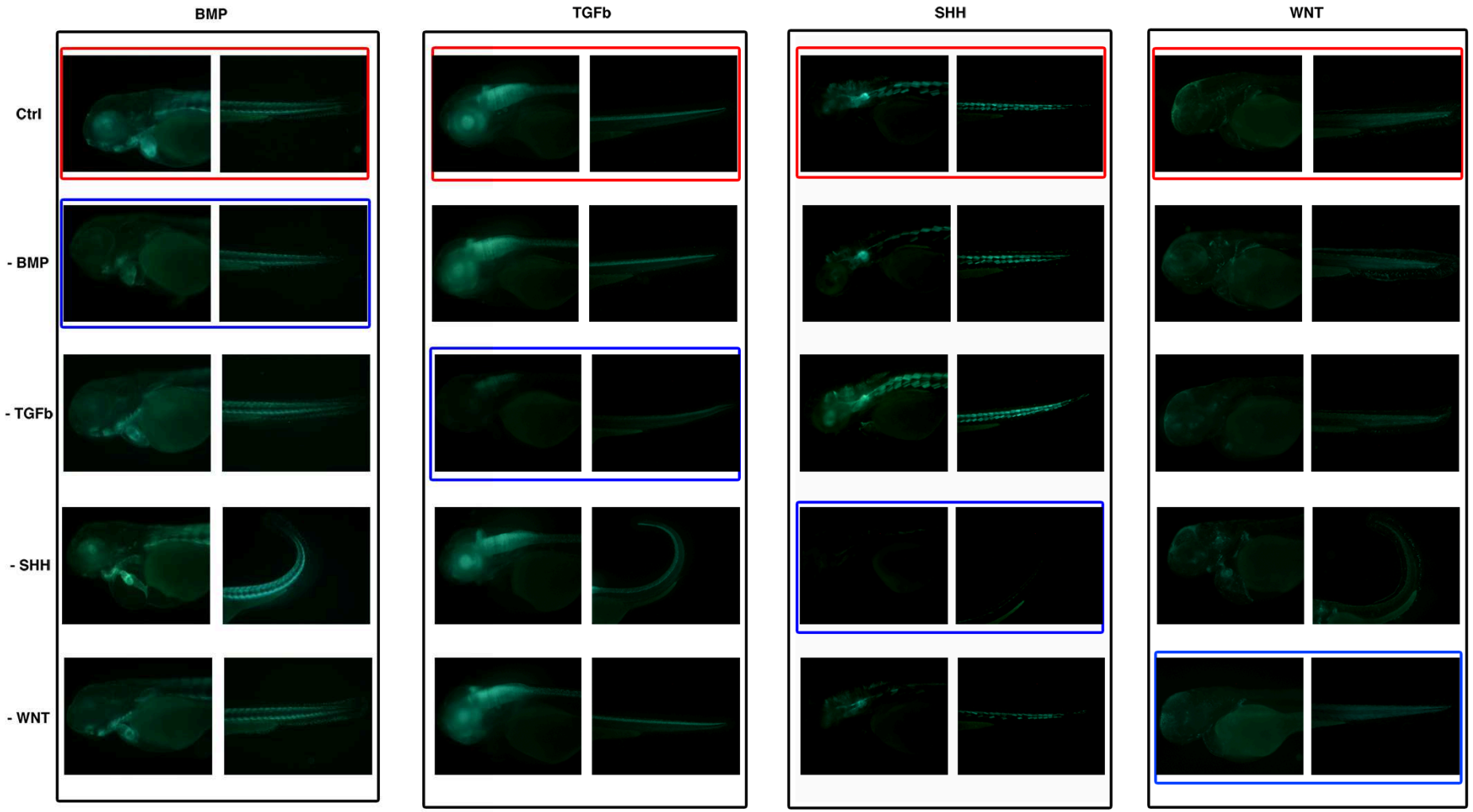
BMP
TGFb
SHH
WNT
Ctrl
- BMP
- TGFb
- SHH
- WNT

Fig. 27. The effects of the inhibitors of the 4 morphogens on tg(12xSBE:EGFP)^{ia16}, Tg(BMPRE:EGFP)^{ia18}, tg(12xGli-Hsv.Tk:GFP)^{ia11} and tg(7xTCF-Xla.Siam:GFP)^{ia4} lines: GFP expression. Fluorescent lateral views of anterior and posterior body parts of tg(12xSBE:EGFP)^{ia16}, tg(BMPRE:EGFP)^{ia18}, tg(12xGli-Hsv.Tk:GFP)^{ia11} and tg(7xTCF-Xla.Siam:GFP)^{ia4} larvae at 3 dpf. Each reporter line has been treated at 24 hpf for 2 days with the inhibitors of the 4 morphogens (BMP, TGFb, Wnt and Shh).

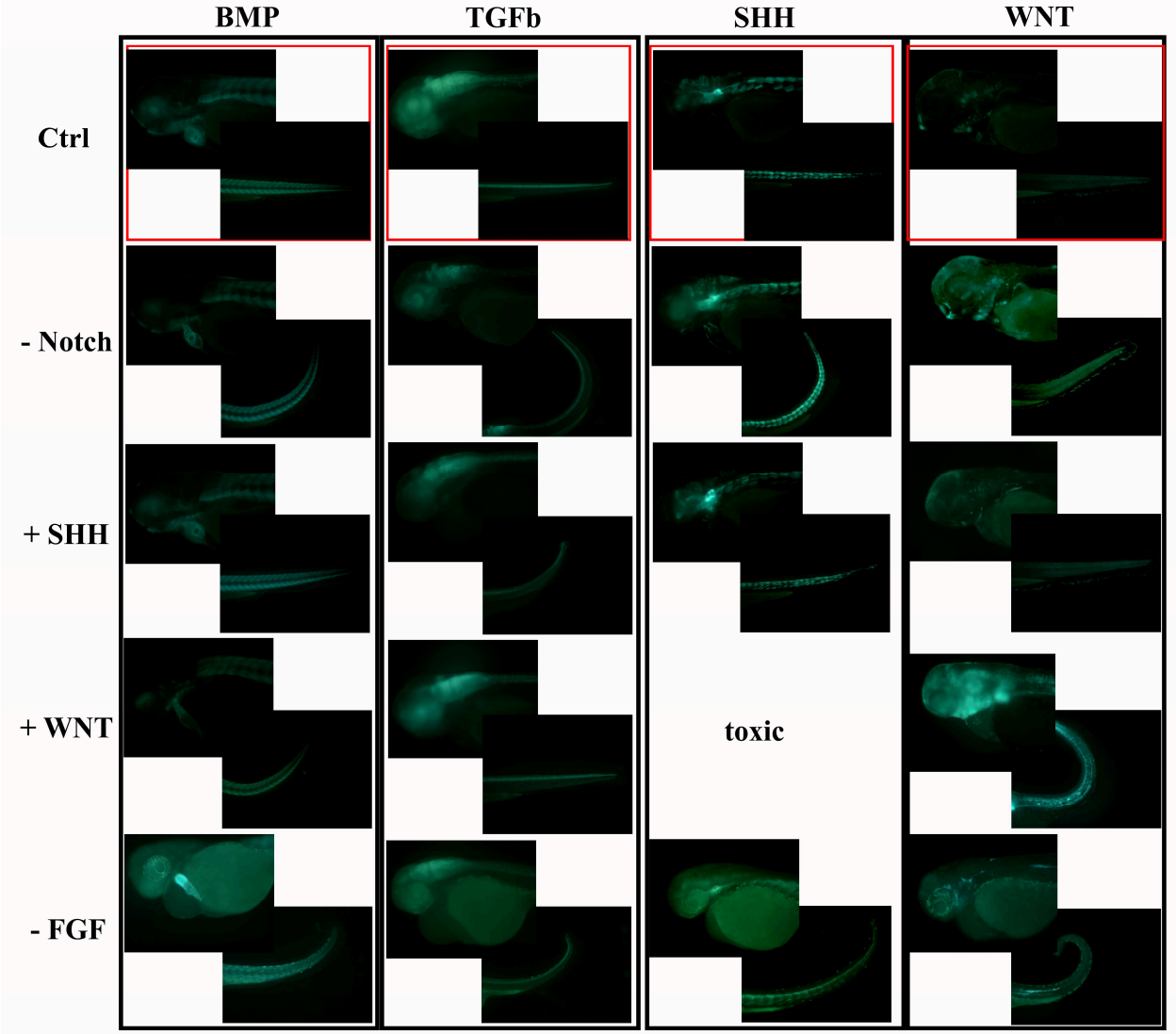

Fig. 28. The effects of the other drugs tested on tg(12xSBE:EGFP)^{ia16}, tg(BMPRE:EGFP)^{ia18}, tg(12xGli-Hsv.Tk:GFP)^{ia11} and tg(7xTCF-Xla.Siam:GFP)^{ia4} lines: GFP expression. Fluorescent lateral views of anterior and posterior body parts of tg(12xSBE:EGFP)^{ia16}, tg(BMPRE:EGFP)^{ia18}, tg(12xGli-Hsv.Tk:GFP)^{ia11} and tg(7xTCF-Xla.Siam:GFP)^{ia4} larvae at 3 dpf. Each reporter line has been treated at 24 hpf for 2 days with Wnt and Shh agonists and the inhibitors of Notch and FGF signalling pathways.

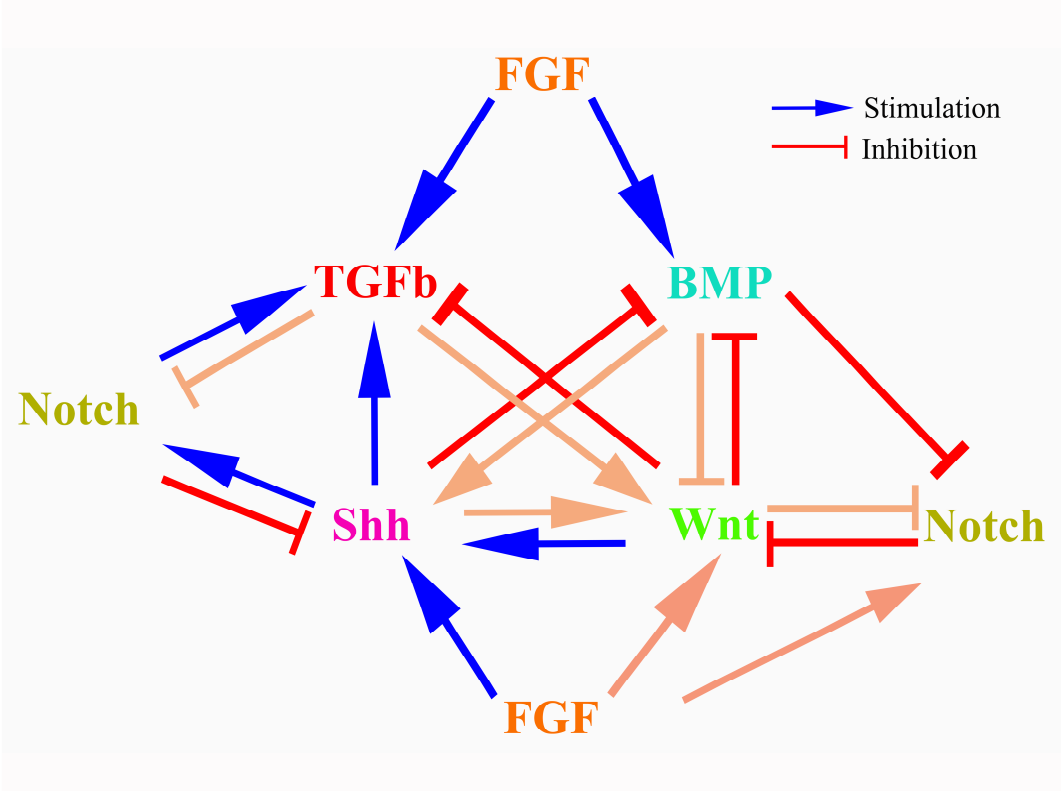

Fig. 29. Epistatic interactions extrapolated from rapid observation of treated larvae of the reporter lines at the epifluorescent microscope: scheme. This diagram represents the epistatic interactions occuring among the 4 morphogens together with Notch and FGF pathways. This interactions has been derived from the fluorescence observation of reporter lines larvae treated with agonists and antagonists of the studied pathways. Purple arrows indicate not clear interactions.

4.b Analysis of GFP transcript levels through mRNA *in situ* hybridization

The previously described observations of GFP expression have been performed on living larvae. This approach makes possible a relatively easy analysis of drugs treatment, but it takes time to visualize any modified reporter expression because of the stability of the fluorescent molecule itself. This can expose the treated larvae to stress conditions that can alter the specific effect of each drug.

In contrast to protein, mRNA is less stable and permits a shorter period of treatment and an easier and clearer evaluation of the results. Therefore, GFP mRNA level has been checked for each treated transgenic larva at 48 hpf through RNA *in situ* hybridization (ISH) (Fig. 30, 31, S12, S13 and S14). Once more, a general scheme of pathways interactions has been inferred from these data (Fig. 32).

BMP
TGFb
SHH
WNT
Ctrl
- BMP
-TGFb
-SHH
-WNT

Fig. 30. The effects of the inhibitors of the 4 morphogens on tg(12xSBE:EGFP)^{ia16}, tg(BMPRE:EGFP)^{ia18}, tg(12xGli-Hsv.Tk:GFP)^{ia11} and tg(7xTCF-Xla.Siam:GFP)^{ia4} lines: ISH for EGFP. Lateral views of anterior and posterior body parts of tg(12xSBE:EGFP)^{ia16}, tg(BMPRE:EGFP)^{ia18}, tg(12xGli-Hsv.Tk:GFP)^{ia11} and tg(7xTCF-Xla.Siam:GFP)^{ia4} larvae at 3 dpf. Each reporter line has been treated at 24 hpf for 1 day with the inhibitors of the 4 morphogens (BMP, TGFb, Wnt and Shh).

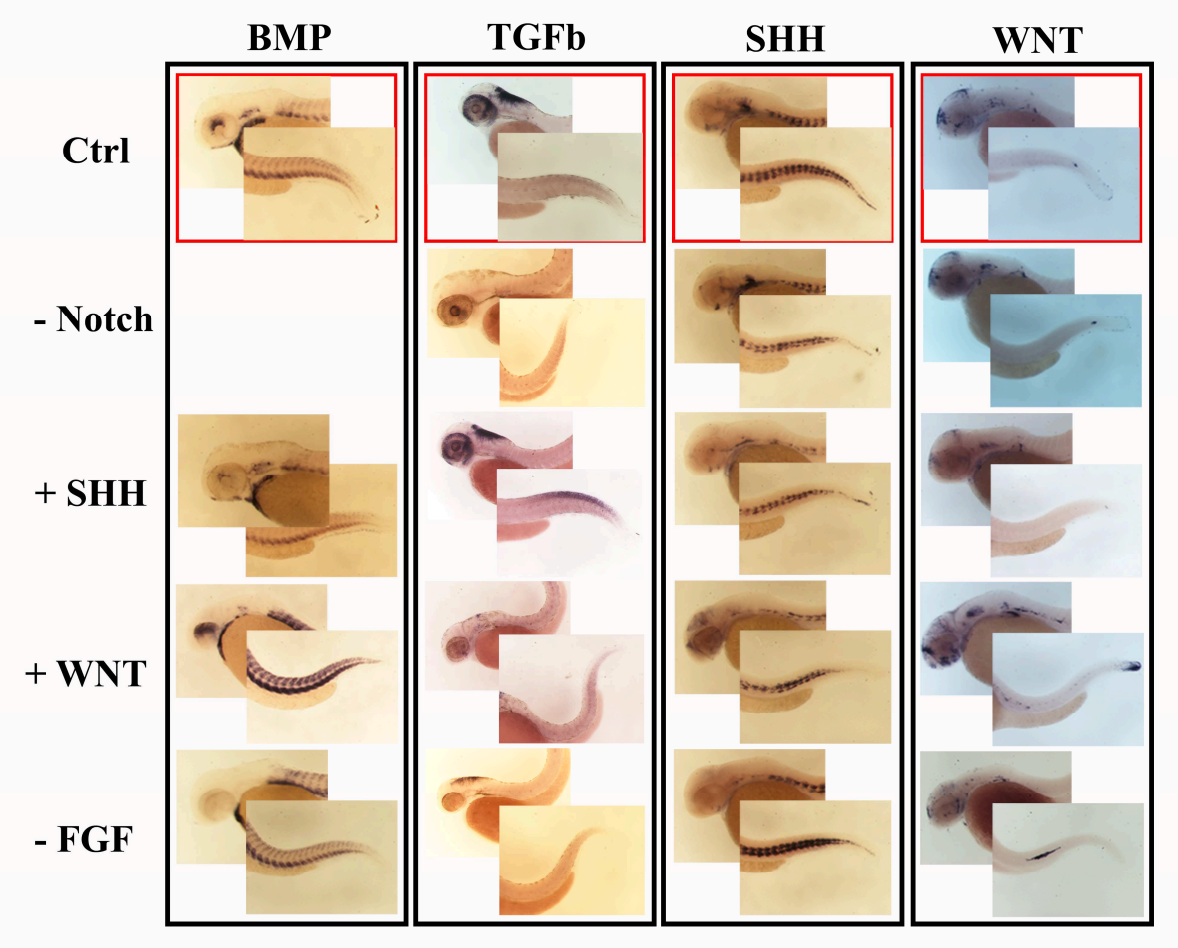

Fig. 31. The effects of the other drugs tested on tg(12xSBE:EGFP)^{ia16}, tg(BMPRE:EGFP)^{ia18}, tg(12xGli-Hsv.Tk:GFP)^{ia11} and tg(7xTCF-Xla.Siam:GFP)^{ia4} lines: : ISH for EGFP. Lateral views of anterior and posterior body parts of tg(12xSBE:EGFP)^{ia16}, tg(BMPRE:EGFP)^{ia18}, tg(12xGli-Hsv.Tk:GFP)^{ia11} and tg(7xTCF-Xla.Siam:GFP)^{ia4} larvae at 3 dpf. Each reporter line has been treated at 24 hpf for 1 day with Wnt and Shh agonists and the inhibitors of Notch and FGF signalling pathways.

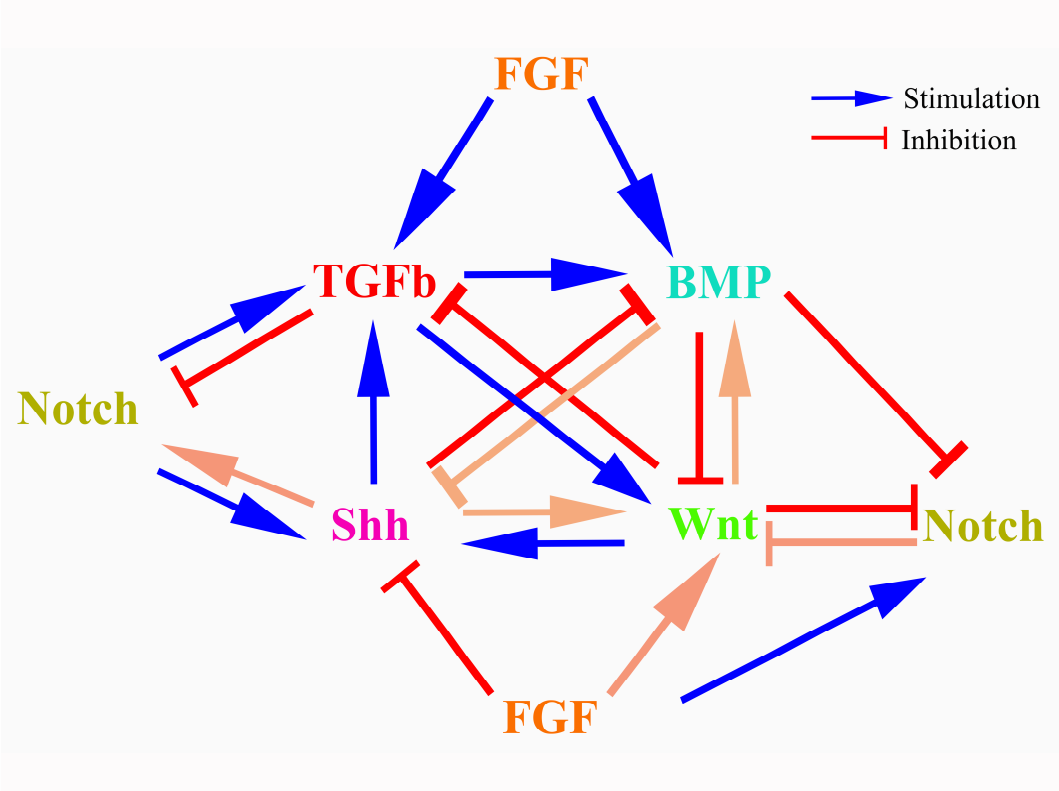

Fig. 32. Epistatic interactions extrapolate from ISH for EGFP on treated larvae of the reporter lines: scheme. This diagram represents the epistatic interactions occuring among the 4 morphogens together with Notch and FGF pathways. This interaction has been derived from the EGFP ISH observation of reporter lines larvae treated with agonists and antagonists of the studied pathways. Purple arrows indicate not clear interactions.

This technique confirms what as seen before at the epifluorescent microscope. For some treatments, it is still hard to define if there is a general either positive or negative interaction. For example, Wnt and TGFb inhibition cause a fluorescence decrease in otic vescicles and eyes in tg(BMPRE:EGFP)^{ia18} larvae, but GFP seems unchanged in the muscles. Wnt signalling controls the formation of the sensory organs, such as eye and inner ear. Together with BMP it forms a dorsal gradient in the eye. BMP does not need Wnt to be induced, but to be maintained in this area (Veien et al., 2008). It is likely that other pathways can counteract the Wnt inhibition in the musculature (i.e., BMP itself,). Notably, TGFb effect on BMP pathway was not so evident at the epifluorescent microscope. mRNA is faster degraded than protein, therefore GFP changes can be easier verified. This aspect let us better understand other interactions, such as TGFb-Notch.

FGF and Shh inhibitions determine a reduction of GFP expression in tg(7xTCF-

Xla.Siam:GFP)^{ia4} larvae, except for the lateral line that is over-activated, as seen at the epifluorescent microscope. Notably, mRNA ISH let us overcome the problem of the background caused by SU5402. This FGF-inhibitor is fluorescent and make the entire larva green-coloured partially hiding the specific GFP fluorescence.

As observed at epifluorescent microscope, in the tg(7xTCF-Xla.Siam:GFP)^{ia4} larvae, Shh inhibition causes an expansion of GFP+ cells in the heart, not more confined to the cardiac valves.

For Shh-responsive line, ISH has revealed a likely increase of GFP transcript after BMP inhibition, in contrast to what has been previously observed at the epifluorescent microscope. Furthermore treatment with DAPT seems to decrease GFP mRNA in the musculature (not observed before) and to block it in the ventral brain in tg(12xGli-Hsv.Tk:GFP)^{ia10} larvae, in contrast to what has been seen at the epifluorescent microscope.

4.c Fluorescence quantification through ImageJ software

The analysis of GFP expression through ISH and fluorescence observation let us propose some likely interactions among chemical signals. Some of these epistasis are not yet well clear, for others (Wnt-BMP, BMP-Shh, FGF-Shh) contrasting results are obtained through the two methods. Therefore, the four morphogen reporter lines have been treated with the same drugs and fluorescence has been quantified in larvae at 3 dpf through ImageJ software. Data have been expressed as integrated fluorescence density of a group of images taken at the epifluorescent microscope for each drug treatment. The mean value has been calculated for each group of images, normalized respect to the control mean value and plotted on graph together with the corresponding standard error (Fig. 33, 34, 35 and 36). These graphs have been used to draw a new epistasis network that has been compared with those previously illustrated (Fig. 37).

Most of the registered interactions have been confirmed. Other data have been useful to understand the opposing results. It is also important to evidence that this method considers the total GFP production. Therefore, different tissue-related responses of a morphogen to a drug cannot be revealed. The effects of FGF and Shh on Wnt efficiently represent this loss of information.

As seen from graphs (Fig. 33, 34, 35 and 36), some differences are not statistically significant and treatments should be repeated to have more trustable results. Both the unexpected and not statistically values plotted on graphs can be a consequence of the missing activity of the drugs. In fact, some drugs, such as IWR-1 and purmorphamine, did not give a statistically significant

change in the fluorescence expression of these reporter line for which are specific (Wnt and Shh reporter lines, respectively).

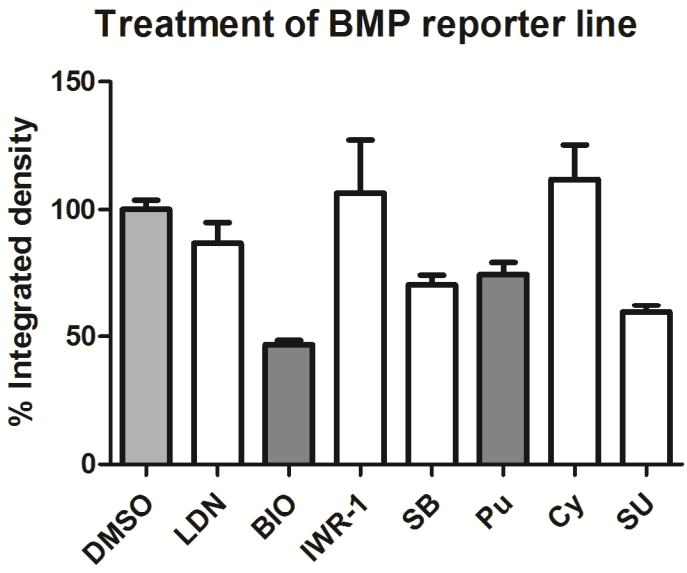

Fig. 33. Fluorescence quantification of tg(BMPRE:EGFP)^{ia18}treated larvae through ImageJ software analysis. Data obtained from fluorescence level measurement have been expressed as percentage of integrated density respect to the control (DMSO treated larvae).

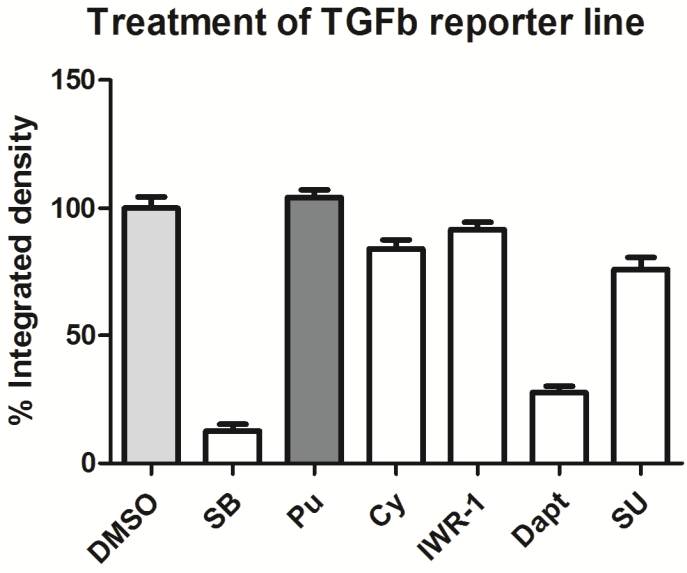

Fig. 34. Fluorescence quantification of tg(12xSBE:EGFP)^{ia16}treated larvae through ImageJ software analysis. Data obtained from fluorescence level measurement have been expressed as percentage of integrated density respect to the control (DMSO treated larvae).

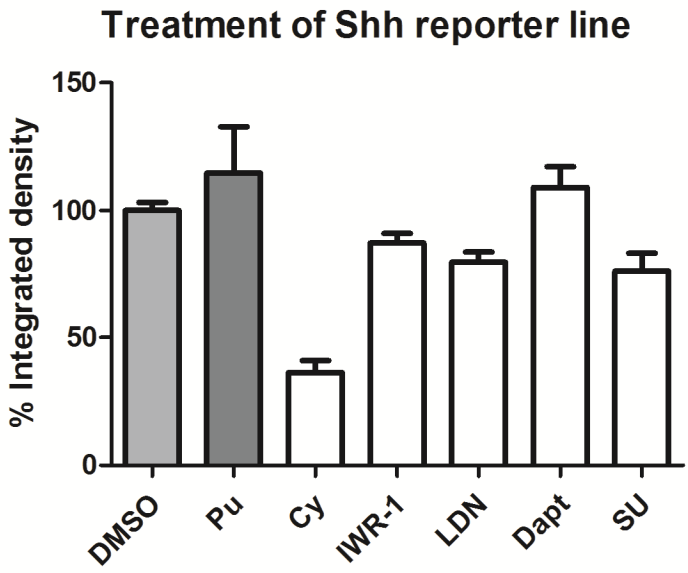

Fig. 35. Fluorescence quantification of tg(12xGli-Hsv.Tk:GFP)^{ia11} treated larvae through ImageJ software analysis. Data obtained from fluorescence level measurement have been expressed as percentage of integrated density respect to the control (DMSO treated larvae).

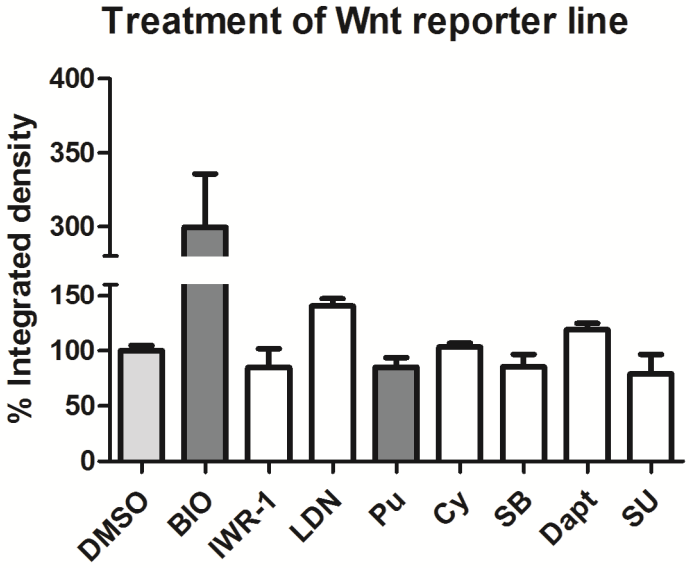

Fig. 36. Fluorescence quantification of tg(7xTCF-Xla.Siam:GFP)^{ia4} treated larvae through ImageJ software analysis. Data obtained from fluorescence level measurement have been expressed as percentage of integrated density respect to the control (DMSO treated larvae).

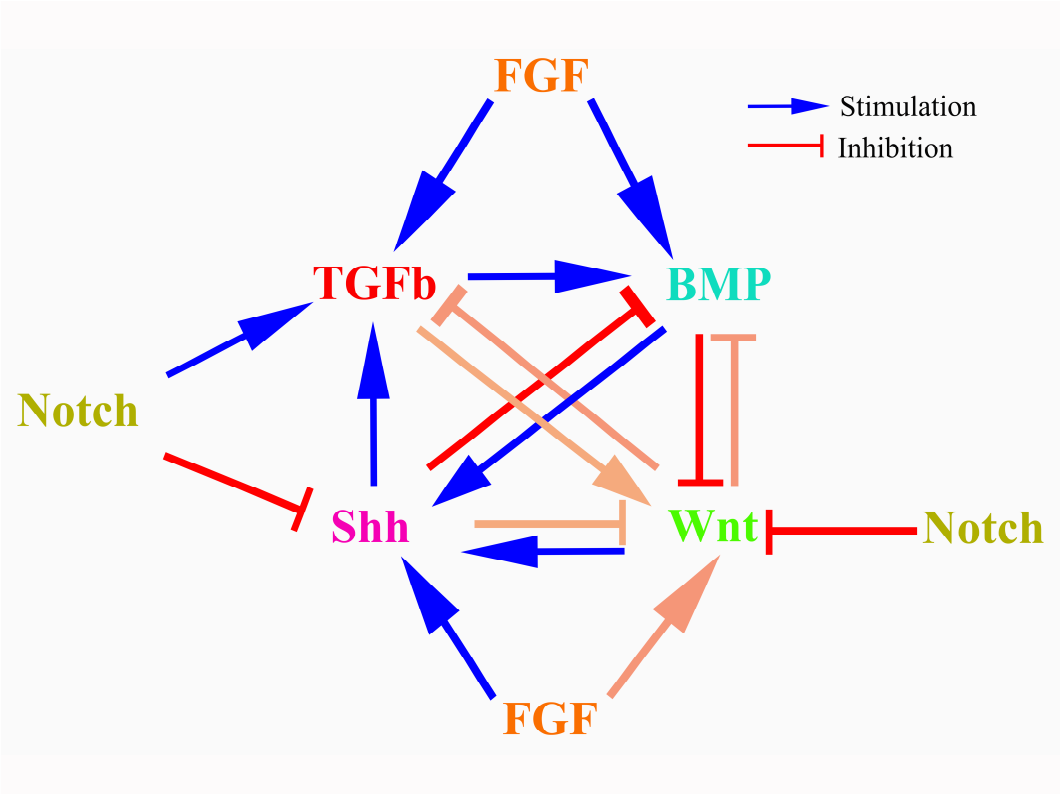

Fig. 37. Epistatic interactions extrapolated from fluorescence quantification on treated larvae of the reporter lines: scheme. This diagram represents the epistatic interactions occuring among the 4 morphogens together with Notch and FGF pathways. These interactions have been derived from fluorescence measurements through ImageJ software. Purple arrows indicate not statisticcaly significant interactions.

4.d Confocal analyses of reporter double transgenics

Epistasis revealed by drug treatments of transgenic lines can be better understood considering the reciprocal expression of each chemical signal inside a larva during its development. Therefore, it has been decided to follow the spatial/temporal interactions of these signals during the first week of development. For this aim, the tg(12xSBE:EGFP)^{ia16} line has been crossed to the other transgenics expressing mCherry protein and larvae have been observed at the confocal microscope. 12xSBE line mainly expresses fluorescence in the CNS, therefore it can represent a simplified model for epistasis study.

As shown previously, the change of a chemical signal can interfere with another one in different way depending on the analysed tissue (i.e. Shh inhibition in tg(7xTCF-Xla.Siam:GFP)^{ia4} larvae). All the registered fluorescence variations in smad3-responsive line were uniform: smad3/TGFb seems to be positively regulated by Shh, FGF and Notch and negatively controlled by Wnt.

Notch reporter line shows a similar expression pattern in the CNS (Fig. 38), where this signalling

is known to maintain the stem cell pool surrounding the ventricular zone (Shimojo et al., 2008) smad3+ cells are also found near the ventricular zone because of the role of TGFb in the neural differentiating process (Fig. 24). It has been also observed that Notch can rule TGFb signals (Fig. 34). There might be a reciprocal interaction between Shh and TGFb morphogens in cooperation with Notch to regulate the development of the nervous system.

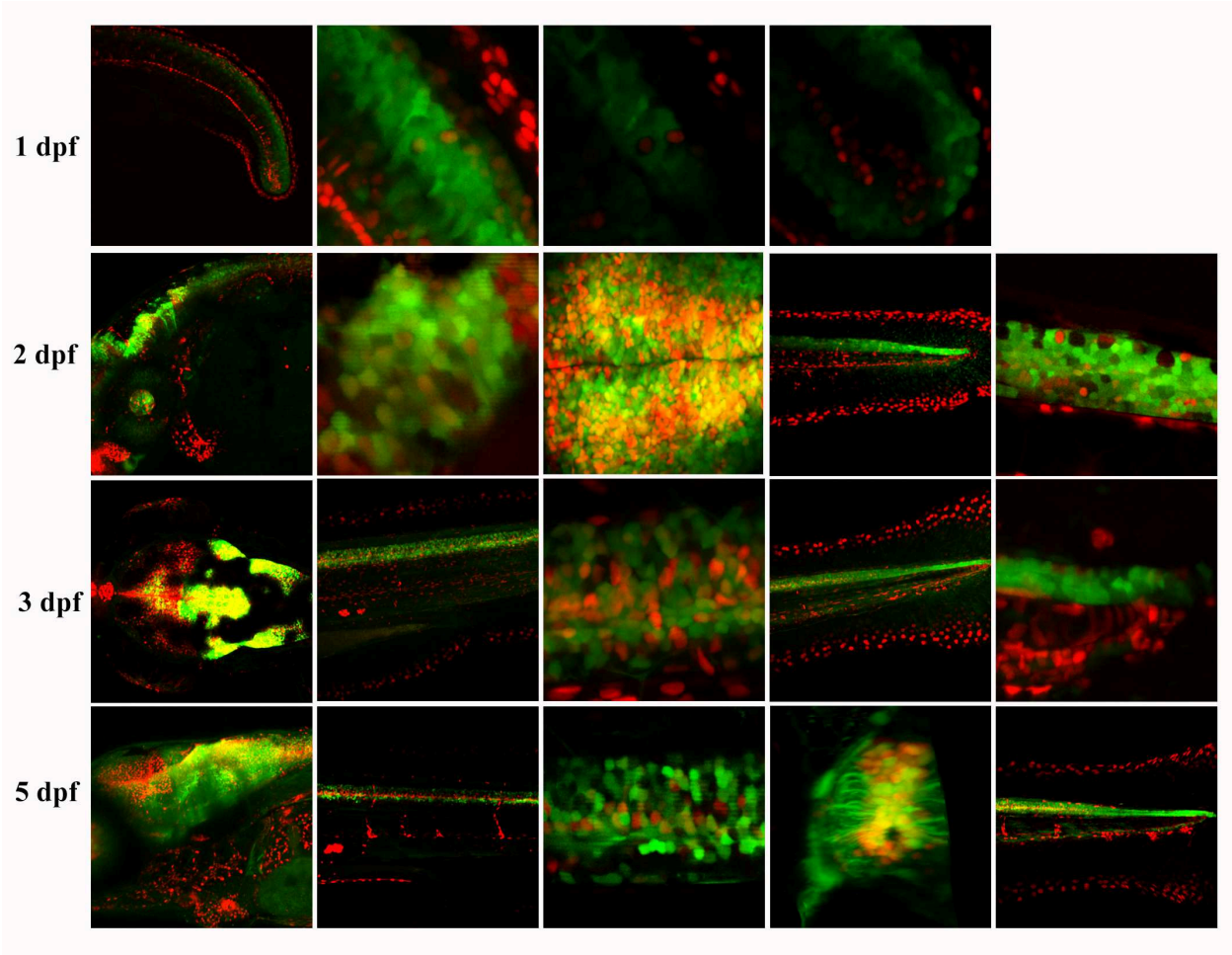

Fig. 38. Notch and TGFb pathways: confocal views. Double transgenic tg(12xSBE:EGFP)^{ia16}/(Tp1bglob:nls-mCherry) larvae observed at the confocal microscope at 1, 2, 3 and 5 dpf. Colocalizing cells are visible in the neural tube as well as in the hindbrain.

In Shh reporter line the fluorescence is expressed in the ventral side of the CNS and in the slow muscle fibers. Shh is known to direct the differentiation of motor neurons, oligodendrocytes and V3 and V3 interneuron populations (Roelink et al., 1995) (Ferent et al., 2013) (Litingtung and Chiang, 2000). TGFb can cooperate with this signal to promote differentiation and this thesis seems to be supported by the presence of some colocalizing cells in the ventral part of CNS (Fig. 39). Nowadays, no interactions have been observed between these pathways in the CNS.

Notably, we envisage that the effects of TGFb inhibition on motorneurons and oligodendrocytes can be at least partially mediated by Shh signalling.

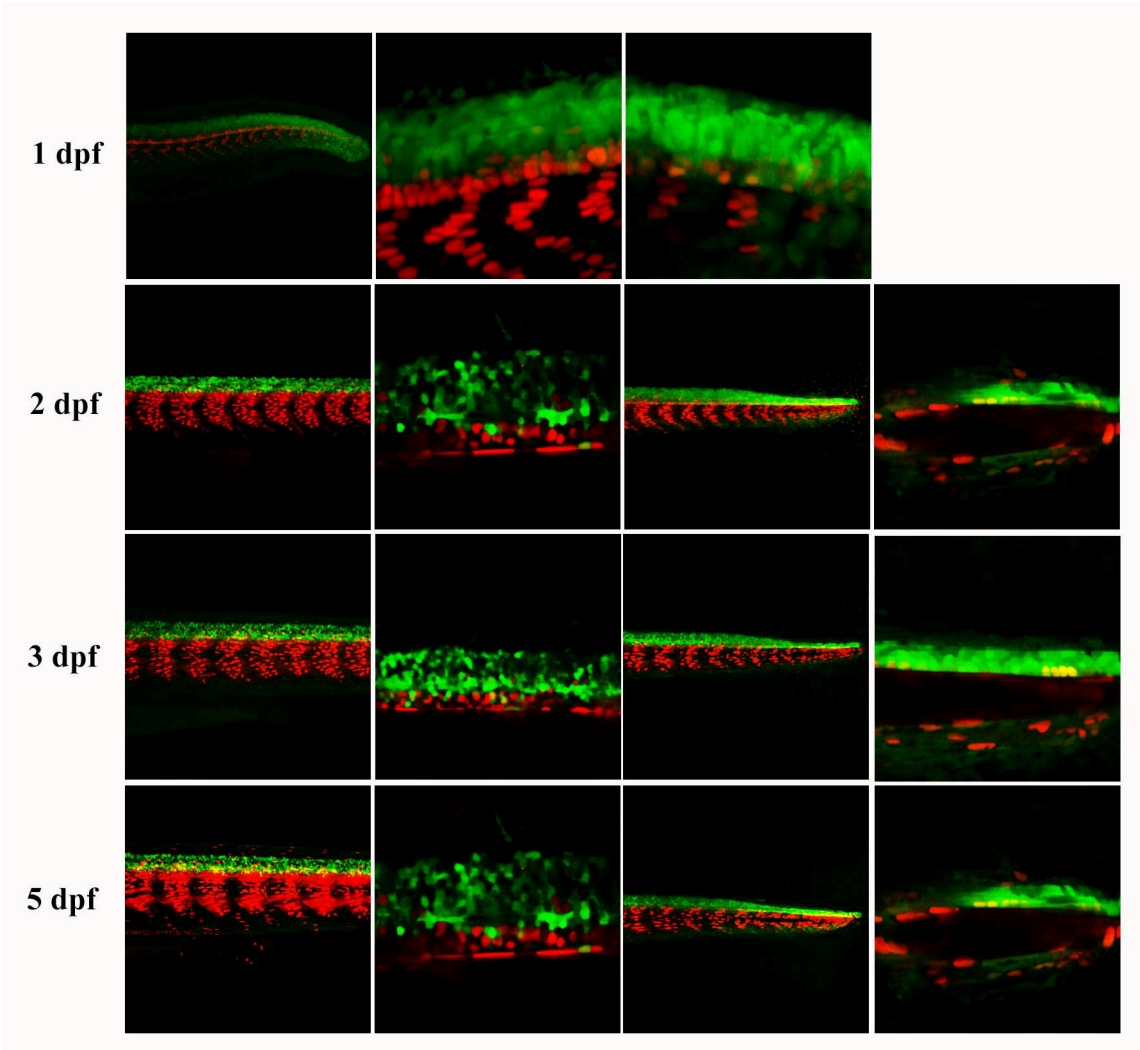

Fig. 39. Shh and TGFb pathways: confocal views. Double transgenic tg(12xSBE:EGFP)^{ia10}/(12xGli-Hsv.Tk:nls-mCherry)^{ia10} larvae observed at the confocal microscope at 1, 2, 3 and 5 dpf. Some colocalizing cells are visible in the ventral neural tube.

Wnt and BMP are respectively involved in neurogenesis and gliogenesis. In CNS they are far from the ventricular zone. TGFb can be negatively controlled by Wnt signalling as confirmed by the absence of colocalizing cells in this area (Fig. 40 and 41).

On the other hand, both BMP and Wnt seem to be coexpressed with TGFb in the mesoderm tail. Fluorescence observation and ISH show a positive regulation of BMP and Wnt reporter by TGFb.

Activin and nodal are known to induce and maintain mesoderm, Wnt and FGF are required for

its maintainance and BMP is responsible for mesoderm patterning, promoting the formation of the ventral mesoderm (Kimelman, 2006) (Heasman, 1997). A common Wnt inhibitor, Dkk-1, is known to be induced for TGFb-mediated Xenopus mesoderm induction. Colocalization of Wnt and BMP+cells with smad3+ cells in the tail mesoderm complies perfectly with this known role of these pathways.

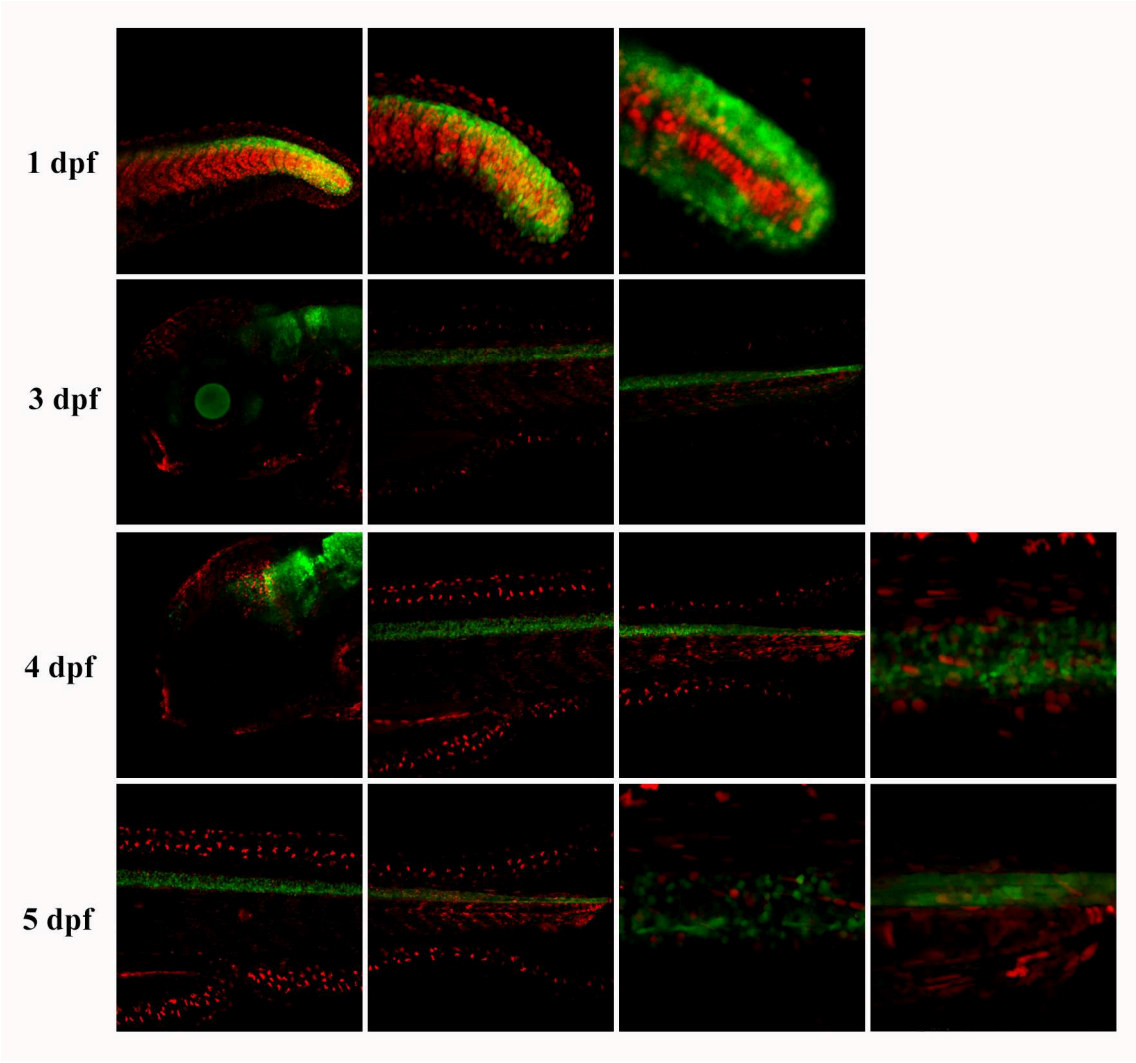

Fig. 40. Wnt and TGFb pathways: confocal views. Double transgenic tg(12xSBE:EGFP)^{ia16}/(7xTCF-Xla.Siam:nls-mCherry)^{ia5} larvae observed at the confocal microscope at 1, 3, 4 and 5 dpf. Colocalizing cells have been observed in tail mesoderm at 24 hpf.

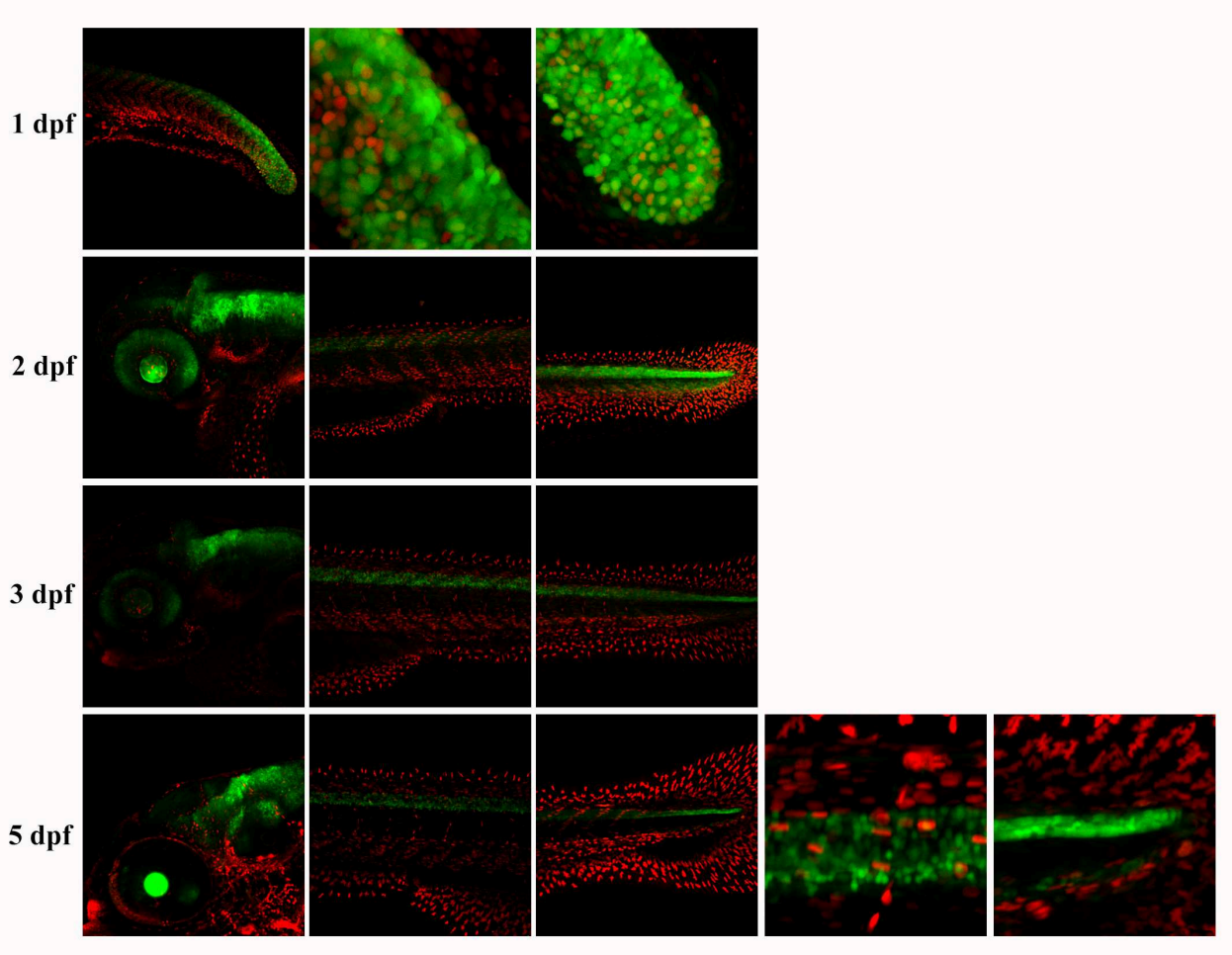

Fig. 41. BMP and TGFb pathways: confocal views. Double transgenic tg(12xSBE:EGFP)^{ia16}/(BMPRE:nls-mCherry)^{ia17} larvae observed at the confocal microscope at 1, 2, 3 and 5 dpf. Some colocalizing cells have been detected in tail mesoderm at 24 hpf.

5. An example of *in vivo* use of the reporter lines for *in vivo* study of pancreas development

The validation of reporter lines and the observation of the fluorescence expression during early larval development at epifluorescent microscope have been an important precondition to all the following *in vivo* study. As our laboratory is focused on pancreas development, we have used the four morphogen reporter lines to see which of them are active in pancreas, at which developmental stage and which cell types require them.

For this aim, we have mated each reporter line expressing either GFP or mCherry with transgenic lines expressing either dsRED or GFP under the control of pancreatic genes, such as nkx2.2a (tg(nkx2.2a:mEGFP)^{vu17}), ins (tg(-1.2ins:HSV.UL23-GFP)^{ia8}and tg(ins:dsRED)^{m1018}), glu (tg(gcga:GFP)^{ia1}), Ptf1a (tg(−5.5Ptf1a:DsRed)^{ia6}) and NeuroD (tg(-2.4kb neurod:EGFP)). These genes are specifically expressed in either exocrine (Ptf1a, (Zecchin et al., 2004)) or endocrine (ins, (Moro et al., 2009)) pancreas, in mature cells (ins in β-cells, glu in α-cells and

Nkx2.2a in the intrapancreatic duct, (Pauls et al., 2007)) or in precursors (NeuroD, (Flasse et al., 2013)).

A fine observation of the previously described double transgenics has been done at the confocal microscope till 30 dpf.

During the early larval development, both Wnt and TGFb reporter lines seem to be not active in pancreas.

On the other hand, Shh signalling seems to be active in early development of the main pancreatic islet till 3 dpf. Some reporter expressing cells colocalize with beta-cells, pointing to a role of Shh in the differentiation of these kind of cells (Fig. 42).

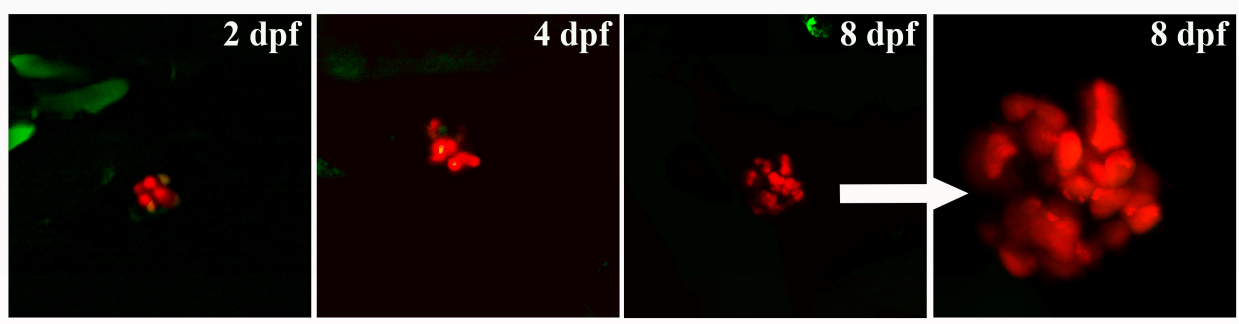

Fig. 42. Shh signalling pathway is active in the main pancreatic islet. Confocal views of double transgenic tg(12xGli-Hsv.Tk:EGFP)^{ia11}/(ins:dsRED)^{m1018} larvae observed at the confocal microscope at 2, 4 and 8 dpf. A partial colocalization has been observed at 2 and 4 dpf, whilst no Shh+ cells could be detected at 8 dpf.

Interesting data have obtained through BMP reporter line observation. Reporter-expressing cells has been individuated both in endocrine (Fig. 43 and 44) and exocrine (Fig. 45) pancreas at roughly 3 dpf. At 4 dpf these cells form vessel-like structures extending throughout the pancreas. These cell types do not colocalize with any of the pancreatic markers described before. A such kind of network seems to characterize the pancreatic vasculature. To confirm this hypothesis, the tg(BMPRE:nls-mCherry)^{ia17} line has been crossed to tg(kdrl:GFP)^{la116} line. Kdrl is specifically expressed in endothelium (Brown et al., 2000). BMP and Kdrl-associated reporters expression perfectly matches in the pancreas (Fig. 46). However, a more general observation of these two reporters has shown us that BMP is not associated to all the vessels irrorating a zebrafish larva. For instance, colocalization has been observed in pancreas and intersegmental vessels, but not in liver.

A more detailed analysis of the role of BMP in angiogenesis has been performed in the pancreas. Although vessels come in contact with the endocrine pancreas at roughly 36 hpf (Fig. S15), no traces of BMP-regulated reporter expression has been detected in this area before 72 hpf. Therefore, it is possible to affirm that BMP is active in pancreatic vessels, but it seems to not be involved in vessel formation.

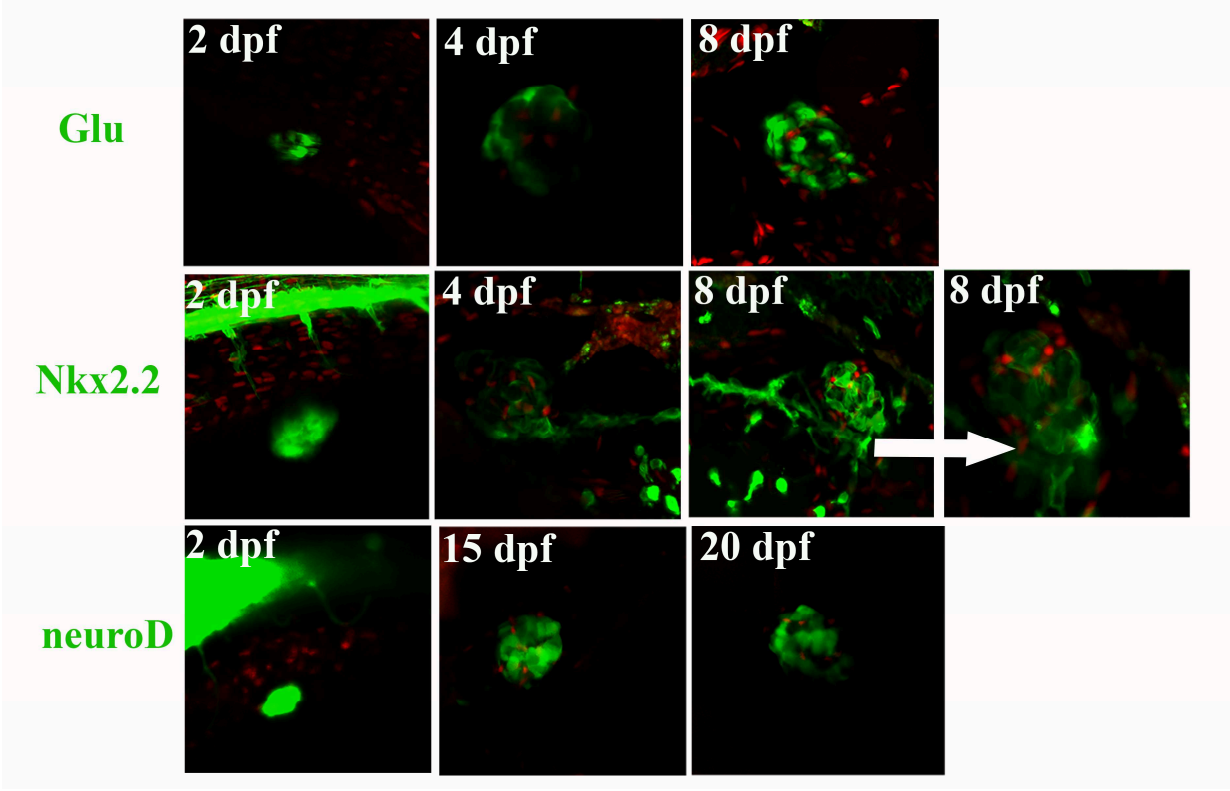

Fig. 43. BMP signalling pathway is active in the pancreatic islet, but it is not expressed by alpha-cells (Glu), pancreatic duct (Nkx2.2a) and endocrine precursor cells (NeuroD). Confocal views of double transgenic larvae obtained maiting tg(BMPRE:nls-mCherry)^{ia17} to tg(gcga:GFP)^{ia1}, tg(nkx2.2a:mEGFP)^{vu17} and tg(-2.4kb neurod:EGFP). No colocalizing cells have been noted during the first month of larval development.

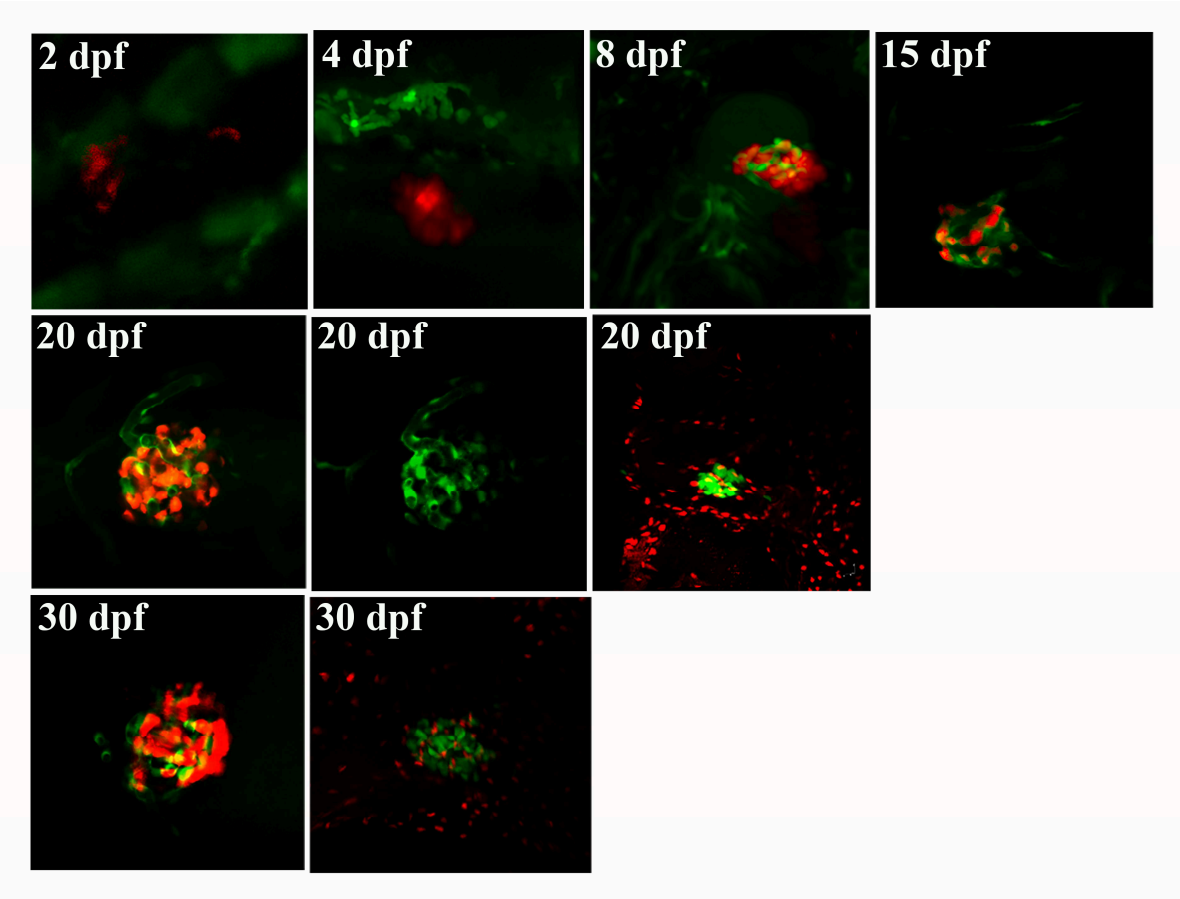

Fig. 44. BMP signalling pathway is active in pancreatic vasculature system irrorating both endocrine and exocrine pancreas. Confocal views of double transgenic tg(BMPRE:EGFP)^{ia18}/(ins:dsRED)^{m1018} and tg(BMPRE:nls-mCherry)^{ia17}/(-1.2ins:HSV.UL23-GFP)^{ia8} larvae observed at the confocal microscope at 2, 4, 8, 15, 20 and 30 dpf. The partial colocalization observed with the tg(ins:dsRED)^{m1018} is a consequence of the dsRED bleed-through into the GFP channel. In fact, no colocalizing cells have been noted using the tg(-1.2ins:HSV.UL23-GFP)^{ia8} and tg(BMPRE:EGFP)^{ia18} lines.

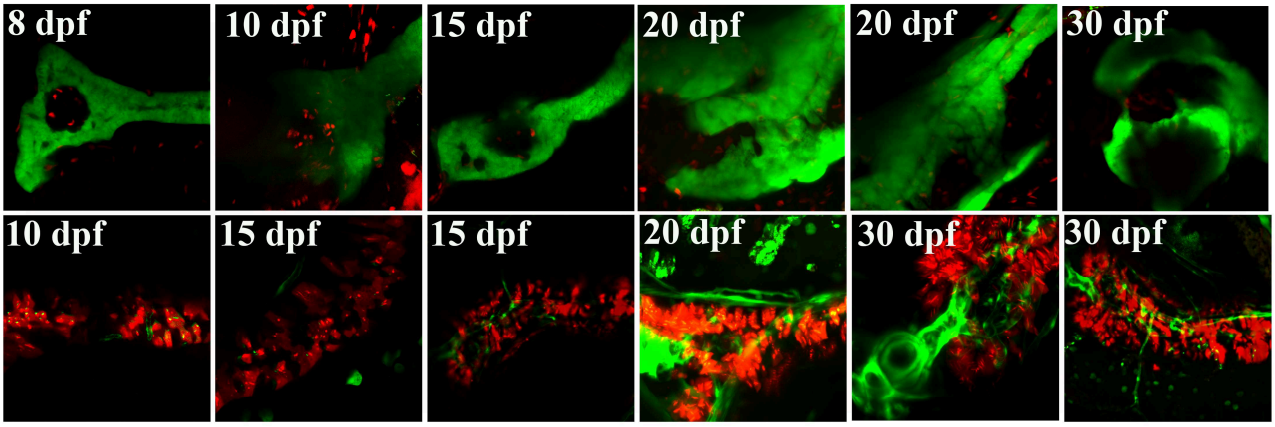

Fig. 45. BMP signalling pathway is active in pancreatic vasculature system irrorating both

endocrine and exocrine pancreas. Confocal views of double transgenic tg(BMPRE:nls-mCherry)^{ia17}/(Ptf1a:GFP) and tg(BMPRE:EGFP)^{ia18}/(−5.5Ptf1a:DsRed)^{ia6} larvae observed at the confocal microscope at 8, 10, 15, 20 and 30 dpf.

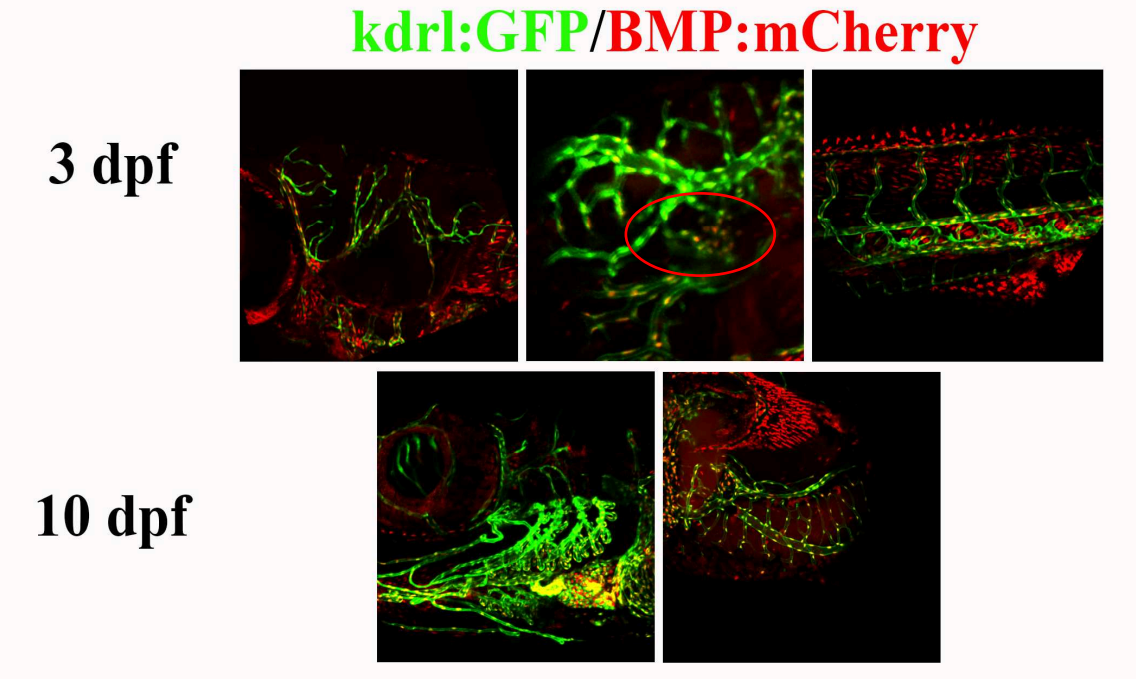

Fig. 46. BMP signalling pathway is active in pancreatic vasculature system irrorating both endocrine and exocrine pancreas. Confocal views of double transgenic tg(BMPRE:nls-mCherry)^{ia17}/(Ptf1a:GFP) and tg(BMPRE:EGFP)^{ia18}/(−5.5Ptf1a:DsRed)^{ia6} larvae observed at the confocal microscope at 8, 10, 15, 20 and 30 dpf.

5.a BMP and angiogenesis during pancreas development

To clarify the role of BMP signalling in the pancreatic vasculature, double transgenic tg(ins:dsRED)/(BMPRE:EGFP)^{ia18} and tg(ins:dsRED)/(kdrl:GFP)^{la116} animals have been treated with LDN193189, an ALK2, ALK3, ALK6 receptor inhibitor, at 1 and 2 dpf.

The effects on β-cells development and pancreatic vasculature formation have been observed at the epifluorescent and confocal microscopes at 3, 5 and 6 dpf.

Observation at the epifluorescent microscope (Fig. 47) demonstrates the efficacy of the BMP inhibition in both double transgenics, as visible from the decrease of BMP-associated fluorescence and the malformed structures such as maxillary and mandibular processes and pharyngeal arches. It is also appreciable a misplacement of the main islet, that it is not properly

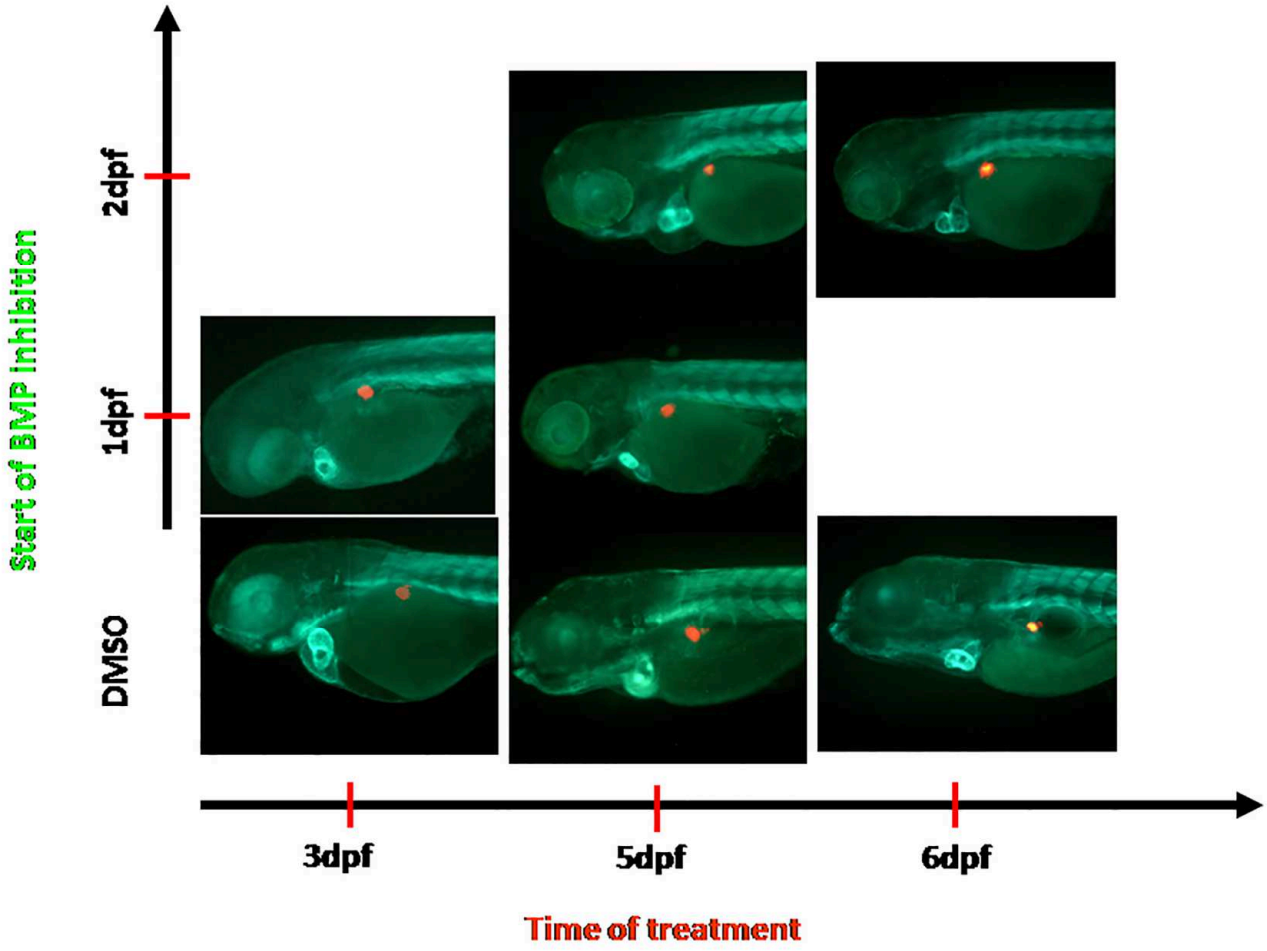

Fig. 47. BMP signalling inhibition at 24 and 48 hpf leads to a failed movement of the pancreatic islet to the later side. Fluorescent lateral views of double trangenic tg(BMPRE:EGFP)^{ia18}/(ins:dsRED)^{m1018} larvae treated at 1 and 2 dpf with an Alk2 and 3 inhibitor and observed at 3 5 and 6 dpf.

A better comprehension of the treatment has been obtained at the confocal microscope. In the double transgenics tg(ins:dsRED)/(BMPER:EGFP)^{ia18}, no BMP-responsive cells was evident during the entire treatment in larvae treated at both 1 and 2 dpf (Fig. 48). No relevant changes of the main islet size are visible. Notably, beta-cells failed to move laterally, confirming what has been noticed at the epifluorescent microscope. Having demonstrated the effect of BMP inhibition on the islet formation, double transgenics tg(ins:dsRED)/(kdrl:GFP)^{la116} animals have been treated with the same dose of BMP inhibitor at the same developmental stages.

In addition to the failed movement of the pancreatic islet in the larva, treatment at 24 hpf causes an altered formation of vessels in this area: the anterior mesenteric artery fails to detach from the

dorsal aorta and kdrl expression is significantly reduced in 24 hpf treated larvae (Fig. 49 and S16). The inhibition at 48 hpf determines an altered development of the vessels, too (Fig. 49 and S16). The anterior mesenteric artery delays to form (visible at 5 dpf instead of 4 dpf) and it does not properly place, and abnormal branching is visible at the pancreatic islet level. Nevertheless, any relevant decrease of kdrl-associated fluorescence has been observed.

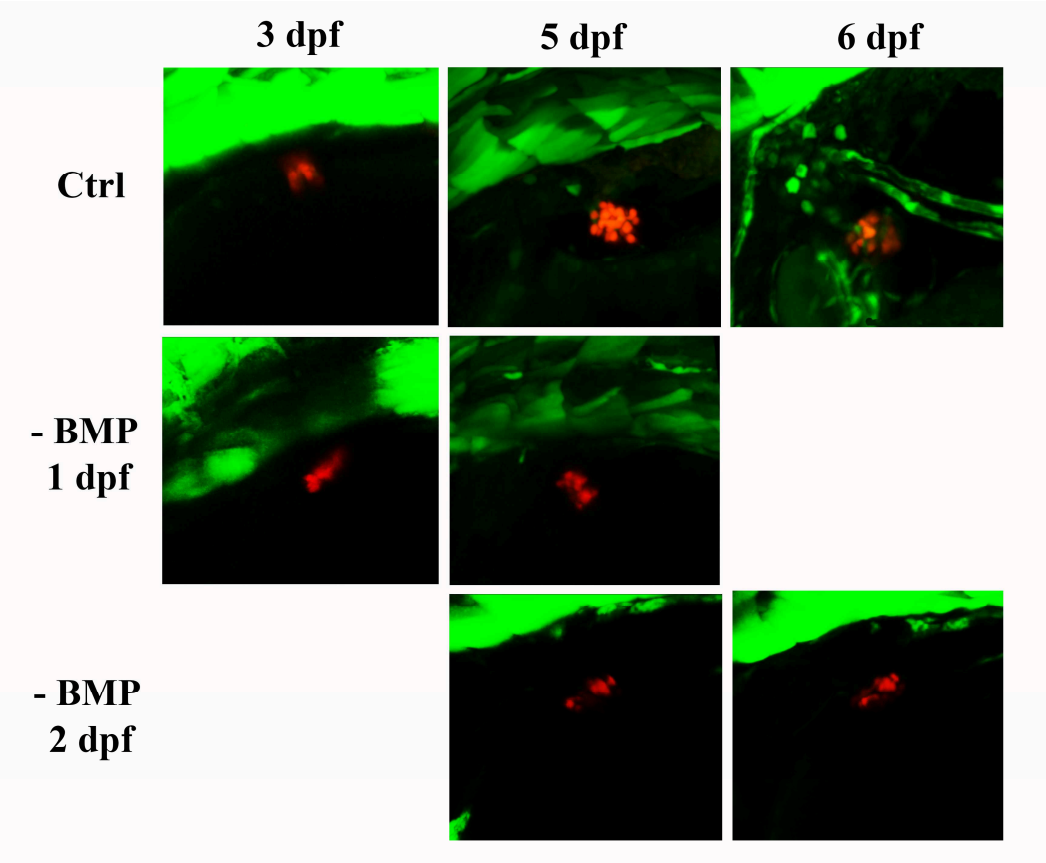

Fig. 48. BMP signalling inhibition at 24 and 48 hpf leads to a failed movement of the pancreatic islet to the later side. Confocal views of the pancreatic islet in the double trangenic tg(BMPRE:EGFP)^{ia18}/(ins:dsRED)^{m1018} larvae treated at 1 and 2 dpf with an Alk2 and 3 inhibitor and observed at 3, 5 and 6 dpf.

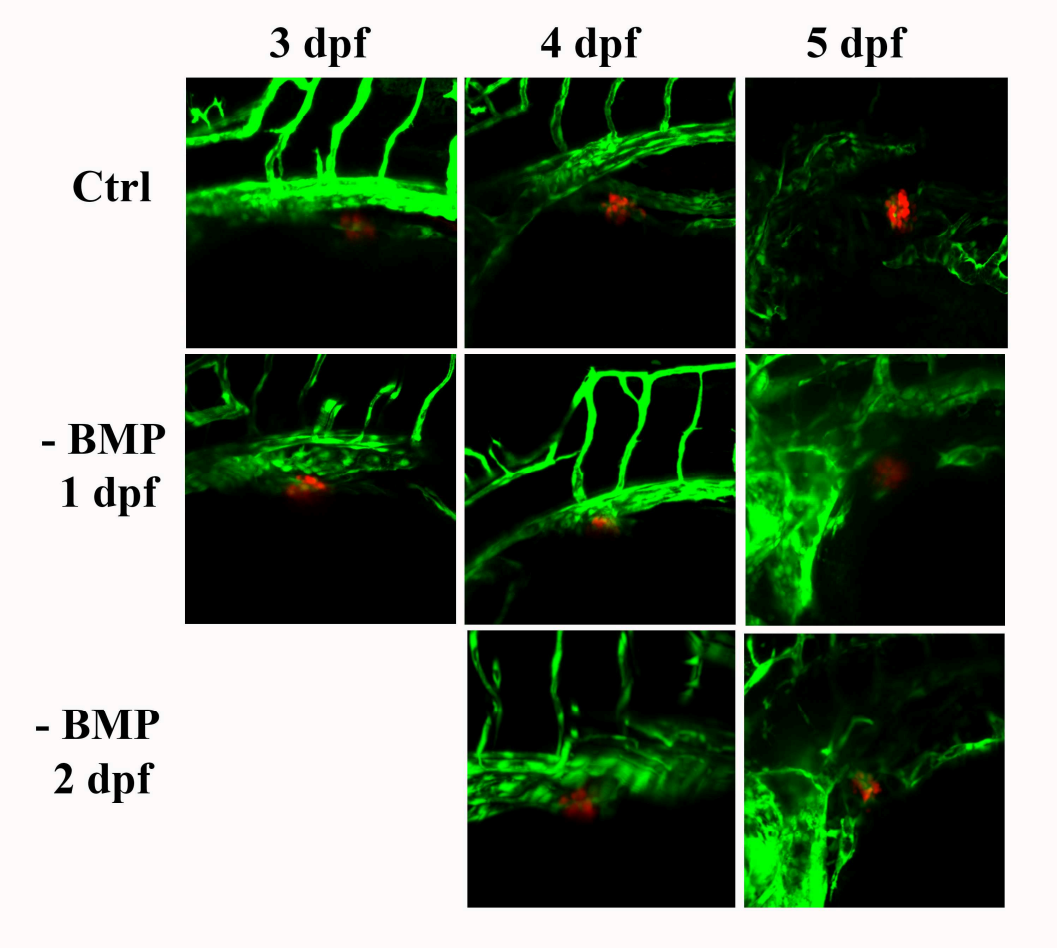

Fig. 49. BMP signalling inhibition at 24 and 48 hpf causes an anomalous angiogenesis. Confocal views of the pancreatic islet in the double transgenic tg(BMPRE:EGFP)^{ia18}/(ins:dsRED)^{m1018} larvae treated at 1 and 2 dpf with an Alk2 and 3 inhibitor and observed at 3, 4 and 5 dpf. BMP inhibition at both 1 and 2 dpf causes vessel misplacement in the pancreas area and a missed positioning of the islet in the left side of the larva. Furthermore, treatment at 1 dpf decreases significantly kdrl-associated GFP expression in the islet region.

DISCUSSION

1. Validation of reporter lines

Our lab has developed the expertise to create transgenic lines to follow *in vivo* signalling pathways (Moro et al., 2013). Both physiological and pathological mechanisms are ruled by chemical signals that are involved in the control of cell proliferation and differentiation.

Taking advantage of relatively easy genetic manipulation of Zebrafish model, a series of transgenic lines have been produced to report some signalling such as BMP, TGFb, Shh and Wnt.

Treatments with specific inhibitors and agonists have shown their specific responsiveness. GFP expression is reduced within 24 hpf and almost completely abolished after 2 days of treatment, whilst the corresponding mRNA has shown a shorter half-life (6-8 hours) (Fig. 7a, 7b, 7c, 7d, 8a and 8b). These aspects have to be considered when performing experiments with these reporters. In fact, the chemical stream represents one of the major disadvantages of all reporter transgenic lines. This phenomenon is caused by reporter protein stability. As a consequence, dividing cells transmit reporter protein to their daughter cells. These are fluorescent without activating that chemical signal, responsible for the reporter expression in the original cell. All the conclusions extrapolated with these models should keep count of it and be confirmed by assays that evaluate reporter mRNA (i.e, mRNA ISH, real time PCR) and/or target genes expression of the analysed pathway.

The tg(7xTCF-Xla.Siam:GFP)^{ia4} line has been previously validated, characterized and published by our lab (Moro et al., 2012).

BMP and Shh reporter lines are chemically responsive to specific drugs and have a similar expression pattern of those created with the same signalling responsive elements (Laux et al., 2011) (Schwend et al., 2010).

Therefore, beyond the chemical treatment with specific inhibitors and the observation at both epifluorescent and confocal microscope during early larval development, no further analyses have been performed on them. The few genetic analyses performed on tg(BMPRE:EGFP)^{ia18} line have been useful to confirm their efficacy and specificity for smad3/TGFb signalling.

The first part of this thesis project concerns the study of the unpublished 12xSBE line.

1.a 12xSBE line: a smad3/TGFb responsive line

In this work we have developed a zebrafish transgenic line, namely 12xSBE line, responsive to smad3/TGFb signaling. Through pharmacological, genetic and molecular characterization we have shown that this transgenic line faithfully reproduces smad3 activation and it can be used to follow *in vivo* TGFb signaling, both temporally and spatially at a single cell resolution.

Treatment with chemical Alk4- and Alk5-inhibitors (SB-431542 and LY-364947) has proved that blocking type-I receptors, specifically involved in TGFb signaling activation, inhibits reporter expression: the transcription of the reporter gene is abolished within 8 hours of treatment with SB-431542 (Fig. 7d-E), whilst fluorescence level is reduced after 1 days of treatment (data not shown) and completely blocked after 2 days (Fig. 7d-A-D'). Moreover, through fluorescent immunohystochemistry we have demonstrated that reporter expression is consecutive to nuclear localization of phosphorylated smad3 (Fig. S18).

Genetic and molecular approaches gave us more specific details regarding reporter expression in the transgenic line. GFP expression of tg(12xSBE:EGFP)^{ia16} line has been observed in two different genetic background: one-eyed-pinhead (*oep*) and chordin (*dino*) mutants. One-eyed-pinhead (*oep*) is an EGF-CFC protein that functions as cofactor necessary for nodal/TGFb signalling. In the transgenic line, GFP expression was absent in the cardiac mesoderm of *oep* mutants (Fig. 9B-B'''). No significant changes have been observed in the neural tube, where smad3 activity seemed to be independent from nodal ligands. Although Aquilina-Beck et al. have demonstrated that nodal signalling is involved in anterior neural tube closure and neuroectoderm specification (Aquilina-Beck et al., 2007) and it acts through smad2/3 (Jia et al., 2009), it is in facts dispensable for neural induction (Jia et al., 2009).

The mutation of this cofactor did not affect reporter expression in tg(BMPRE:EGFP)^{ia18} line. Nodal signalling can interact with BMP signalling during the embryonic development, but its impairment do not block BMP-mediated GFP expression (Fig. 11). Therefore, we can affirm that BMPRE line responds to BMP signals and *oep* mutant line correctly represent an altered TGFb signal.

As BMP and TGFb show a similar transduction pathway distinguished for different types of receptors, r-smads and their relative target sequence in the genome, we have tested effects of BMP activation on smad3-mediated reporter expression by analysing mutants of chordin, a bmp2/4 antagonist. Albeit it has been demonstrated that smad2/3 upregulate bmp inhibitors, such as chordin, and BMP inhibition is important for neural induction (Jia et al., 2009) (Cruz et al., 2010), levels of GFP expression in the neural tube of *dino* mutants compared with that of sibs

confirming the specificity of 12xSBE transgenic line for TGFb-associated r-smads (Fig. 9C-C'''). Morpholino-mediated knock-down of r-smads and co-smad has confirmed the specificity of both tg(12xSBE:EGFP)^{ia16} and tg(12xSBE:nlsmCherry)^{ia15} lines for smad3/4.

Smad4 is needed for both BMP and TGFb signalling activation (Aristidis Moustakas et al., 2001). The absence of reporter expression in both 12xSBE and BMPRE lines has given us an important proof that TGFb superfamily signalling activates both reporter lines. Notably, this common effect confirms the efficacy of the chosen smad4 morpholino.

Concerning r-smads morphants, the transgenic lines seemed to be sensitive to both zebrafish isoforms of smad3: smad3a and smad3b. When embryos were injected with smad3a morpholino, they failed to express both EGFP and mCherry (Fig. 12 and S2). On the other hand, knock-down of smad3b strongly inhibited reporter expression, which was limited to the very end of the tail. We envisage two possible explanations for these results: a) higher efficacy of smad3a morpholino respect to the smad3b one; b) different levels of genetic additivity for the two loci allowing smad3a to partially compensate for smad3b absence in the neural tube, but not *viceversa*.

Albeit the transgenic lines have been designed with smad3-responsive sequence (Dennler et al., 1998), the injection of smad2 morpholino inhibited reporter expression in the cardiac mesoderm and partially interfered with fluorescence in the tail region (Fig. 12 and S2). This might be a consequence of smad2/3 interaction. In fact, smad2 can heteromerize to smad3, translocate to the nucleus and together cooperate to activate the expression of smad3 target genes (Lan, 2011) (Miguez et al., 2013). In contrast to what has been seen for smad2 and 3 in the chicken neural tube (Lan, 2011) (Miguez et al., 2013), knock-down of smad2 determines a reduction of CAGA12 box-depending reporter expression. However, the different techniques used to inhibit and study smad2 in zebrafish (this work) and chicken (Miguez et al., 2013) such as morpholino/short-hairpin RNA, microinjection of eggs/electroporation of neural tube, stable line/transient expression, can explain the differences. Alternatively, smad2-3a-3b and 4 interact in different ways in neural tube formation of the two animals. In any way, the zebrafish 12xSBE line will be a useful tool, together with a still missing smad2 reporter line (possibly based on activin response elements, ARE) (Chen et al., 1996), to dissect the functional interactions between the TGFb specific transcriptional effectors *in vivo*.

Characterization of tg(12xSBE:nlsmCherry)^{ia15} line has been completed overexpressing smad7 and smad3b. Overexpression of smad7 caused a drastic reduction of reporter expression in all domains of activity (Fig. 15A-A''). On the other hand, overexpression of smad3b by plasmid

injection has led to a mosaic expression of smad3b and, consequently, of the reporter (Fig. 15C-C''). Notably, it was evident an ectopic activation of mCherry in smad3-competent cells (i.e. the muscle) supporting the idea that muscle cells do not possess epigenetic mechanisms to inactivate this pathway.

Furthermore, the reporter expression correlates to the zones of release of tgfb2 (Chen and Kimelman, 2003) and tgfb3 (Thisse and Thisse, 2004): notochord, pectoral fins and lens. These data underline the dependence of the reporter from tgfb ligands.

2. Smad3-mediated neurogenesis in Zebrafish1: *in vivo* study through a smad3-responsive transgenic line

Confocal observation of the transgenic line showed that in the neural tube the reporter is active in cells surrounding the ventricular zone (Fig. 19E''). This area is known to be a region in which genetic signals lead neural progenitor cells to exit cell cycle and start differentiation (Schmidt et al., 2013). To understand the role of smad3 activation in this area, the tg(12xSBE:nlsmCherry)^{ia15} line has been crossed to some transgenic lines expressing GFP in different neuronal and glial cells: tg(Ngn1:GFP)^{sb1}, tg(-2.4kb neurod:EGFP), tg(gfap:GFP)^{mi2001}, tg(mnx1:GFP)^{ml2} and tg(Nkx2.2a:mGFP)^{vu17}. The quantitative analysis of colocalization has shown that reporter expression was mainly activated in differentiating neurons (NeuroD+ cells) and glia (GFAP+ cells) (Fig. 22). Colocalization of smad3-responsive cells with NeuroD+ and GFAP+ cells rose up between 1 and 2 dpf (Fig. 21B''' and C'''), during axon growth and the secondary neurogenesis. A significant degree of colocalization has been measured with Ngn1+ cells. From these observations we have concluded that TGFb signalling could be active in ex-progenitor cells, which exit the cell cycle and start differentiating. Therefore, late progenitors, such as Ngn1+ cells, expressed both the differentiation marker (GFP) and the reporter (mCherry). On the other hand, differentiated cells seemed to be smad3/TGFb negative. Nevertheless, for motor neurons (Mnx1+ cells) and oligodendrocytes (Nkx2.2a+ cells), a significant increase of Manders' coefficient has been observed between 3 and 4 dpf, possibly for a mCherry retention trail in differentiated cells. This theory has been confirmed analyzing TGFb evolution in the tail of double transgenic embryos at 24 hpf by using somites as timeline (Fig. 22). At the onset of TGFb signalling (t=0), progenitor cells (Ngn1+ cells) expressed TGFb signal (Fig. 22A'''). This colocalization has been observed and maintained with differentiating neuronal (NeuroD+ cells) and glial (GFAP+ cells) cells (Fig. 22B''' and C'''). Motor neurons (Mnx1) and

oligodendrocytes (Nkx2.2a) did not show significant colocalization at any of the time-points analysed (Fig. 22D''' and E''').

The hypothesis of TGFb involvement in differentiating process might comply with its role in the control of epithelial-to-mesenchymal transition (EMT) (Song, 2007). The smad3 control of proliferation is crucial during early-postnatal differentiation of cerebellar neurons into postmitotic neurons, activating cyclin-dependent kinase inhibitors p21, p27 and markers of neuronal differentiation (Uwe and Thomas, 2013). A clear inhibitory function of smad3 on neural progenitors proliferation was shown in chicken developing spinal cord, where smad3 also promotes differentiation of selected neurons and glia (Garcia-Campmany and Marti, 2007). Both immunohistochemistry for phospho-hystone3 on smad3a morphant embryos at 24 hpf (Fig. 23A-B') and LY364947-treated larvae at 48 hpf (Fig. 23C-D') and EdU proliferation assay on embryos treated with Alk5 inhibitor, LY364947, (Fig. 23E-F') showed a massive increase of proliferating cells in many tissue compartments, included NS. All these experiments have confirmed that smad3/TGFb regulates negatively cell cycle and is inactive in proliferating cells. Colocalization studies have indicated that smad3-responsive cells mainly correlate to differentiating cells rather than proliferating and mature cells in NS. Pulse and chase EdU proliferation assay has confirmed that on 24hpf tg(12xSBE:EGFP)^{ia16} embryos GFP-expressing cells are mainly post-mitotic (Fig. 23G-H'). We can conclude that smad3 acts on cell cycle by stopping cell proliferation and it is expressed postmitotically at 24 hpf.

After having demonstrated that smad3 is expressed in NS by differentiating cells, we have carried out some functional *in vivo* studies blocking TGFb activity in embryos of the transgenic lines used for colocalization measurement: tg(Ngn1:GFP)^{sb1}, tg(-2.4kb neurod:EGFP), tg(gfap:GFP)^{mi2001}, tg(mnx1:GFP)^{ml2} and tg(Nkx2.2a:mGFP)^{vu17}. Both genetic and pharmacological TGFb inhibition has led to similar conclusions (Fig. 24). Smad3/TGFb signalling is important for maintaining a balance between progenitor and mature cells. Turning down this signal has caused an increase of undifferentiating cells (Ngn1+ cells) and a decrease of mature neural and glial cells (Mnx1+ cells and Nkx2.2a+ cells). When the signalling has been blocked immediately after the fertilization, smad3 inhibition manifested its effect mostly on the neural markers of the tail region. This might depend on the role of smad3-mediated signalling in the neuroectoderm posteriorization (Jia et al., 2009). On the other hand, when the smad3 signal has been inhibited after 24hpf, the effects were visible in the entire larva (Fig. 25). This might be a consequence of the smad3 role in the secondary neurogenesis (from 2dpf) and in axogenesis process (from 14 to 24 hpf) (Chapouton et al., 2010). Concerning motor neurons, TGFb

inhibition affected their number as well as the somata positioning in the neural tube and their proper axons formation. Results presented here have shown that TGFb signalling is important for differentiation and positioning of motor neurons in the neural tube during early development. This might be a direct consequence of an altered smad3-dependent EMT in the progenitors due to the effects of TGFb on extracellular matrix (ECM) and GDNF production (Gomes et al., 2005) (Ho et al., 2000). Another conclusion from our studies is about smad3a and 3b role in the nervous system development: both smad3 isoforms might recognize CAGA box and direct reporter expression in the neural tube. Functional *in vivo* experiments on trasgenics confirmed that the 2 isoforms are equally involved in neurogenesis as the effects on the neural markers seemed to be very similar. Moreover, coinjection of the 2 morpholinos did not cause a further impairment in the neural tube formation, while embryo body appeared to be more severely altered (shortened embryo, smaller malformed head). This let us assert that at least in the neural tube formation smad3a and 3b have similar levels of addictive genetic effects.

Through these assays, we can assert that 12xSBE line is responsive to smad3/TGFb signaling drugs: reporter expression depends on smad3 activation and it is inhibited by smad7 in a cell-autonomous manner. Furthermore, both Zebrafish smad3 isoforms might recognize CAGA box with similar efficacy and equally participate to the differentiation of the neural tube. According to these data, smad3-mediated TGFb signalling seems to have a role in CNS development by controlling mature cells positioning, axons formation and most importantly and primarily, the regulation of the progenitor-precursor switch.

Furthermore, this work wants to represent an alternative approach to study biological mechanisms. The current paradigm of dissecting gene function usually starts with gene identification, the definition of its expression domain, followed by knockdown and description of the phenotypic effects. However, this paradigm falls short if one considers that understanding gene function and phenotypes must necessarily entail the precise identification of the cells in which the gene or pathway are operating, and appreciation of the temporal dynamic of gene activity computed by cells in real tissues. The approach used in this work attempts to surpass this limitation: we started from the strongest expression of a functional reporter to identify the tissues in which a transcription factor (Smad3) is activated by a main developmental signalling pathway pathway (TGFb). Here we analysed the functions of Smad3 in previously underinvestigated tissues and cell types - the periventricular cells of the neural tube - that we reveal as main targets of TGFb ligands emanating from the notochord; in other words, targets of pleiotropic morphogens emanating from a different tissue, endowed of multiple inducing properties.

3. Epistasis: how to study genetic signals interaction *in vivo*

Each of the development stages involves induction, proliferation, locomotion, and cell type or subtype determination, but also prevention of inappropriate cell formation. To reach this goal, a precise mechanism is established, by which each signalling pathway plays its roles exactly and in coordinative manners according to time, space and intensity.

The last part of my project thesis illustrates an innovative approach to this topic. The epistatic relations of the four morphogens (BMP, TGFb, Shh and Wnt) and Notch signalling have been analysed through our reporter lines. Together with these chemical signals FGF pathway has been also partially analysed using a FGF inhibitor, SU5402.

As visible from Fig. 50, molecular networks inside cells are dynamic and complex. A way to understand their logic is to dissect networks in subgroups of interactions, so called motives. This approach let us individuate some feed-forward loops (FFLs), characterized by three transcription factors (x, y and z) and three regulatory interactions: x acts directly on z and indirectly throughout y. FFLs can be divided in two groups: 4 coherent (if x acts in the same way on z, directly and indirectly) and 4 incoherent interactions (if x has opposite results on z acting directly and indirectly) (Macia et al., 2009). FFLs types appear with different frequency in the biological systems. Notably, the most common FFLs are: coherent type I and incoherent type II. As visible in Fig. 50, 5 out of 8 distinguishable FFLs are incoherent: Shh-TGFb-BMP; Notch-Shh-TGFb; FGF-Shh-Wnt; Shh-BMP-Wnt; Wnt-BMP-Shh. 3 out of 8 are coherent: FGF-TGFb-BMP; FGF-Wnt-Shh; BMP-Shh-Wnt. Among the 8 FFLS, 2 are type I coherent interactions. The others appear in biological systems with a low frequency. This let us suppose that some of revealed interactions might not be realistic. These might be results of not specific drug effects (i.e. SU5402 blocks both FGF receptor and VEGF receptor). Furthermore, some epistatic relations might not be the result of a direct interaction between the observed signals, but they might require a "third player". For instance, it has been observed a stimulatory effect of BMP on Shh signalling. Nevertheless, in various tissues and developmental processes, BMP signalling limits Shh activity (Patten and Placzek, 2002) (Piedra and Ros, 2002) (Zhang et al., 2000), rather than stimulates it.

All the incoherent feed-forward loops can be considered as a way of the biological system to maintain a dynamic equilibrium. For example, Notch signalling can directly stimulate TGFb promoting neuronal differentiation. To limit this process, Notch acts on Shh signalling blocking it. Shh is known to be involved in neuronal differentiation. Our data show a positive interaction between Shh and TGFb. Therefore, Notch-mediated Shh inhibition can limit TGFb-induced

neural differentiation.

Another interesting FFL involves FGF, Wnt and Shh: FGF inhibits Wnt signalling through Shh activation, but it also stimulates directly Wnt itself. This might be the mechanism regulating the lateral line formation. FGF signalling inhibits Wnt/beta-catenin through the inhibitor dkk1 and limits Wnt/beta-catenin activity to the leading zone in the migrating primordia (Ma and Raible, 2009). However, Wnt should also be stimulated to promote lateral line formation. FGF-mediated control of this organ development might consist of opposite balanced effects.

Notably, the relative high number of incoherent type FFLs can reflect the contrastasting data found in literature for many of the observed interactions. All these pathways are implicated in various biological processes. They are often expressed in overlapping and/or complementary manners, temporally and spatially (Fig. 38, 39, 40 and 41). Different studies have demonstrated that a pair of signalling pathways can act in a synergistic or antagonistic way, depending on the cellular contest (i.e. the interaction between Wnt and BMP, (Itasaki and Hoppler, 2010). This may be the consequence of multiple players action. Therefore, a better comprehension and analysis of signalling epistasis should consider other chemical signals often involved in the embryogenesis, such as retinoic acid and FGF signals, too. As seen before, this can make hard to extrapolate a general model of signalling interactions.

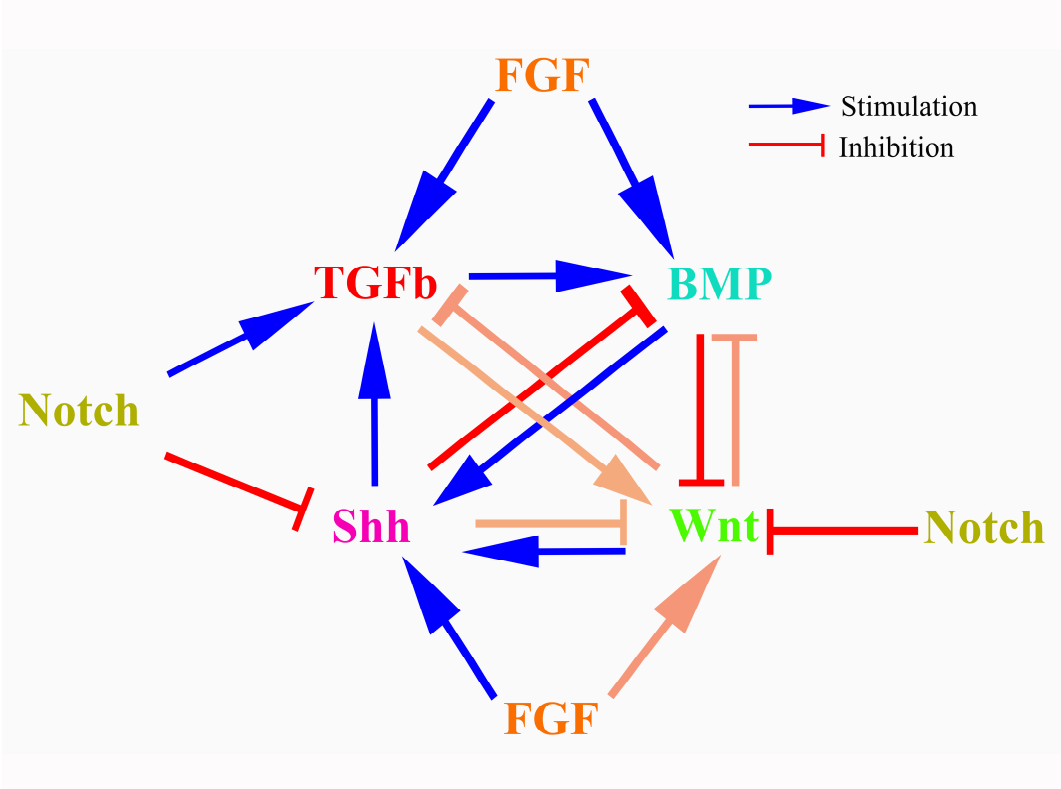

Fig. 50. Epistatic interactions extrapolated from fluorescence quantification on treated larvae of the

reporter lines: scheme. This diagram represents the epistatic interactions occuring among the 4 morphogens BMP, TGFb, Wnt and Shh together with Notch and FGF pathways. These interactions have been derived from fluorescence measurements through ImageJ software. Purple arrows indicate not statisticcaly significant interactions.

Another strategy to study signalling interactions is observed their reciprocal spatio-temporal expression within the embryo. For this aim, 12xSBE:GFP line has been crossed to the other reporter lines expressing mCherry. Shh and Notch signalling can be active with TGFb signalling in the same cells. This justifies the positive effects of both signalling on TGFb pathway. On the other hand, both BMP and Wnt are not co-expressed with TGFb signalling in the neural tube and therefore, Wnt has an inhibitory effect, whilst BMP does not show any epistatic interaction on TGFb. Notably, a significant colocalization has been observed between Wnt/BMP and TGFb signalling in the tail mesoderm. Since GFP is mainly expressed in the nervous system in 12x SBE line, no antagonist effects of BMP and Wnt have been observed. On the other hand, both BMP and Wnt reporter lines are active in mesoderm. TGFb activation in this tissue can result in a stimulatory effect.

The interactions revealed through chemical treatments and reporter lines are confirmed by literature in some cases, as explained in the "Results" chapter. For example, Notch and Wnt signals are closely related in the brain (Hayward et al., 2005). Shh from floor plate and notochord limits Wnt activity to dorsal part of the myotome (Marcelle et al., 1997). On the other hand, no data have been registered regarding the induction of smad3/TGFb by Shh pathway.

Three approaches have been used to observe signalling epistasis: fluorescence observation, GFP mRNA ISH and fluorescence quantification. Looking at both GFP mRNA and protein expression let us identified any tissue-specific interactions (i.e. FGF and Wnt in the lateral line). On the other hand, the fluorescence quantification simplifies the epistatic relations letting us to propose a clearer epistasis model. Even if this last method of data analysis causes a loss of information, it is based on mathematical analysis and, therefore, is the most trustable and objective.

4. An example of use of the reporter lines for *in vivo* study of pancreas development

The use of the four morphogen lines created in our lab has made possible to observe *in vivo* which signalling is active during early larval pancreas development. Most of the information concerning morphogens and pancreas are referred to early development (pre-somitogenesis). Less is known about their action in later stages.

For this reason, our attention has been focused on the first month of larval development: from 2 till 30 dpf.

We do not reveal any smad3/TGFb activation during this lag-time. Even if smad 4 is expressed in murine neonatal and adult pancreatic islets (Hua and Sarvetnick, 2007), the activation of this transcription factor seems to be associated to BMP and not to smad3-medited TGFb signalling. Furthermore, in our lab Schiavone et al. have observed the expression of the smad3-associated reporter in mutated Kras-induced pancreatic tumors (Schiavone, M. et al., 2014). In fact, TGFb is known to have both a tumor-suppresor and oncogenic activity. It promotes apotosis and control inflammatory process, but it also stimulate epithelial-to-mesenchymal transition and neoangiogenesis (EMT) that in turn facilitate the invasiveness of the tumors (de Caestecker et al., 2000).

Although some members of the Wnt pathway have been identified and/or associated to the pancreas development (Papadopoulou and Edlund, 2005) and loss of function of TCF7L2 blocks glucose-stimulated insulin secretion (Liu and Habener, 2010), no Wnt-dependent reporter activation has been registered in the considered lag-time.

Some explanations can be proposed. The tg(7xTCF-Xla.Siam:GFP)^{ia4} line is able to report only a part of the canonical beta-catenin-mediated Wnt signalling. Furthermore, mutational analyses of TCF target enhancers show that TCF sites might be not sufficient for the gene activation *in vivo* (Barolo, 2006). More TCF-binding sites might be needed to reveal the Wnt signalling activation in the pancreas, too.

More interesting results have been obtained with tg(12xGli-Hsv.Tk:GFP)^{ia9} and tg(BMPRE:EGFP)^{ia18} lines. At roughly 2-3 dpf, few Shh+cells have been identified in the pancreatic islet. Notably, this signalling seems to be active in some beta-cells. As said before, Shh promotes migration and differentiation of endocrine precursor cells until early gastrulation contrasting BMP repressive effects. Later, it antagonizes retinoic acid and inhibits endocrine cell differentiation (Tehrani and Lin, 2011). Therefore, it does not surprise to find Shh-induced fluorescence in some beta-cells. However, the study of its role during early organogenesis is still in progress.

4.a BMP and angiogenesis

BMP is known to repress pancreatic cell fate at the expense of the liver cell fate and it also negatively regulates beta-cells differentiation.

BMP-mediated reporter expression appears in pancreas at roughly 3dpf and it is initially confined to few cells in the islet area. Between 5 and 6 dpf GFP starts to be expressed in vessels

that extend from the head to tail of the pancreas. Nevertheless, kdrl-associated GFP is detectable in the pancreatic islet beyond 24 hpf. According to this observation, vasculogenesis in Zebrafish pancreas seems to be BMP-independent. On the other hand, BMP signal seems to correlate to angiogenesis. Furthermore, it is known that BMP signal impairment causes severe vascular defects in mice: missing endothelial differentiation and consequential hemorrhage, and improper vessel formation (Yasunaga et al., 2011). pSmad1/5/8-mediated BMP signal has been found in endothelial cells (Ahnfelt-Ronne et al., 2010) of vessels irrorating pancreas and its inhibition leads to an increase of differentiating endocrine precursors and a misplacement of the nearby omphalomesenteric vein.

Our functional study of vascular system in pancreas does not show any significant alteration of beta-cells formation: double transgenic larvae, tg(kdrl:GFP)^{la116}/(BMPER:nls-mCherry)^{ia17} and tg(BMPRE:GFP)^{ia18}/(ins:dsRED)^{m1018}, have been treated at 24 and 48 hpf for 4 days with a BMP inhibitor, LDN193189, and then observed at the confocal microscope.

Notably, all the previously reported published data have been obtained through an early inhibition of this signal (not beyond early somitogenesis). Other signals can compensate for BMP inhibition and abolish or reduce BMP-mediated effect: retinoic acid positively regulates endocrine specification (Tehrani and Lin, 2011) and Notch and FGF signalling control endocrine progenitor differentiation (Ninov et al., 2012) (Norgaard et al., 2003).

To complete the analysis of BMP influence on endocrine formation, the other cell types forming the pancreatic islets should be analysed: α-γ-δ-ε cells. In fact, it has been demonstrated that injection of BMP4-neutralizing antibodies slightly diminish the number of glucagon cells in adult mice (Hua and Sarvetnick, 2007).

For what concerning the formation of the pancreatic vessel system, blocking BMP at early organogenesis (24 and 48 hpf) causes a defect in vessel branching. Notably, inhibition at 24 hpf leads to a decrease of kdrl-associated GFP. It seems that BMP signalling is important to maintain, but not to induce the formation of endocytes in newly-formed vessels. This is a direct effect of this signalling pathway on this cell type. In fact, mating tg(kdrl:GFP)^{la116} to tg(BMPER:nls-mCherry)^{ia17} lines it has been seen that BMP signalling is specifically active in endothelial cells. A 48 hpf inhibition of BMP signalling do not cause a depletion of endocytes. This seems to confirm the role of the signalling in the newly formed vessels.

Notably, at both 24 and 48 hpf BMP seems to control angiogenesis. Blocking at 24 hpf cause an incomplete separation of the anterior mesenteric artery from the dorsal aorta. This process is later shifted in 48 hpf-treated larvae, even if the previously mentioned artery does not properly place.

In this case, abnormal branching is visible at 4 dpf.

In conclusion, in early larval development BMP signalling seems to direct angiogenesis at least in pancreas. Specifically, it stabilizes the new vessels and it directs their positioning in the organ. The BMP activating source might be the islet itself. In fact, it has been produced and characterized a transgenic mouse that expresses the firefly luciferase gene under the control of Bmp4 promoter. The bioluminescence has been mainly identified in the pancreatic islets (Yasunaga et al., 2011). This may explain why the pancreatic islet fails to move if BMP pathway is inhibited.

5. Conclusion: pros and cons of the use of reporter lines

In this thesis four transgenic reporter lines have been proposed for *in vivo* study of BMP, TGFb, Wnt and Shh signalling pathways.

Their validations demonstrate that they faithfully report the signalling for which they are responsive. The examples of *in vivo* study here described (pancreas, neurogenesis and epistasis) show how this model let us obtain and/or confirm new information concerning different physiological processes in a relatively easy way: the importance of BMP in the pancreatic vasculature development and the role of smad3 in neurogenesis. Notably, a large part of our results have been reached without sacrificing animals that can be an important advantage considering the restrictive laws for the experimental use of animal models.

Furthermore, the *in vivo* study let us observe the organs development also in relation with chemical signals coming from adjacent tissues.

Finally, the embryonic permeability to small molecules let us test some drugs acting on signalling involved in embryonic development and adult tissue homeostasis as well as in several diseases. Through these chemical treatments a scheme of putative epistatic relations has been proposed. Even if these interactions have to be further confirmed, they might represent a good starting-point for detailed analyses of tissue-specific pathways interactions.

Nevertheless, nobody can consider as definitive the data obtained with reporter lines (Barolo, 2006). All the results have to be confirmed through different approaches. Reporter lines are faithfully responsive, but they show only a part of each signalling. This become clearer if you consider the absence of Wnt-associated reporter in the pancreas contrasting to what has been observed in literature (Papadopoulou and Edlund, 2005) (Liu and Habener, 2010).

APPENDIX

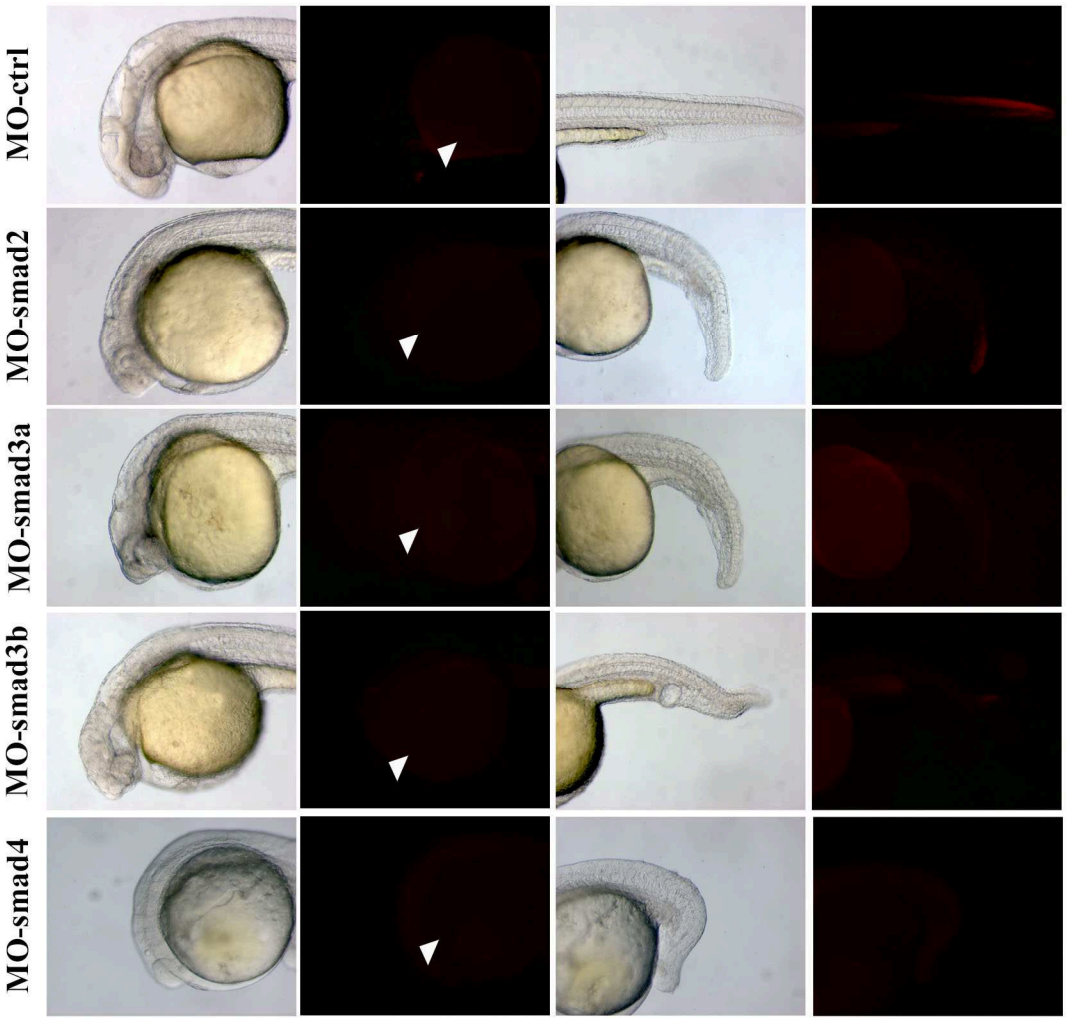

Fig. S1. Different responsiveness of tg(12xSBE:nls-mCherry)i^{a15} line to smad2, smad3a, smad3b and smad4 morpholinos. Brightfield and fluorescent lateral images of smad2-, smad3a-, smad3b- and smad4-morphants at 24 hpf at the epifluorescent microscope, left to right. smad2, 3a and 3b morphants show a similar phenotype: anterior truncation, a curved shortened body axis, absence of floorplate and an enlarged intermediate cell mass. smad4 morphants have a worst phenotype: similar characteristics of the other morphants accompanied to a shortened dorsalyzed body due to BMP inhibition. mCherry expression is completely inhibited in smad4 and 3a morphants and strongly reduced in smad3b morphants. smad2 morphants lack reporter expression in the cardiac mesoderm and telencephalon like the other morphants (white arrow head) and display a mild reduction in the neural tube.

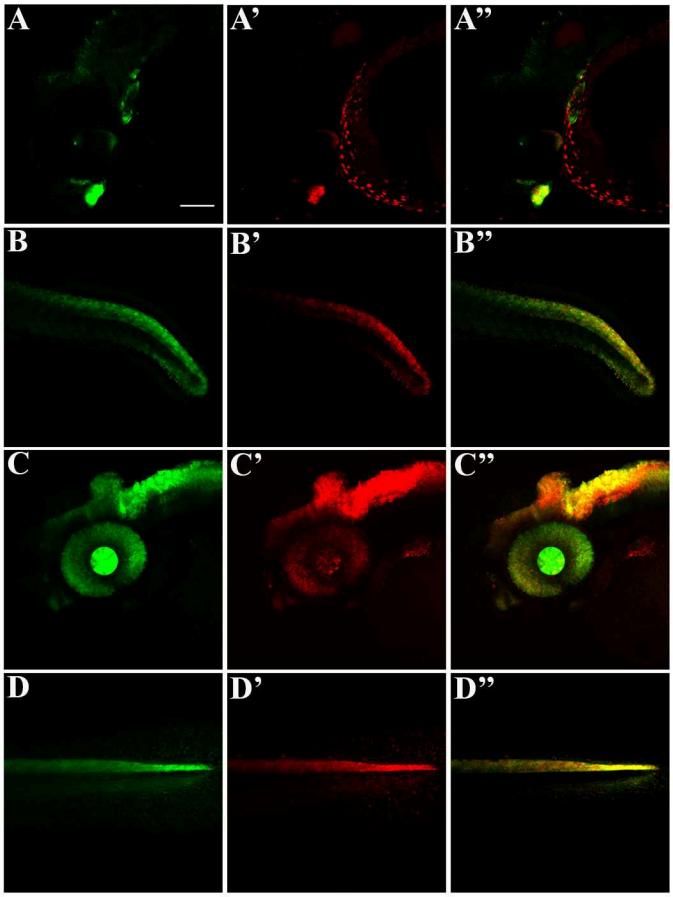

Fig. S2. 12xSBE lines have a similar expression pattern. Confocal lateral images of double transgenic tg(12xSBE:EGFP)^{ia16}/tg(12xSBE:nls-mCherry)^{ia15} 24 hpf embryo and 48 hpf larva, left to right. **A-A'',** anterior part of a 24 hpf double transgenic embryo: **A**, green channel; A', red channel; **A''**, merge; **B-B'',** tail of a 24 hpf double transgenic embryo: **B**, green channel; B', red channel; **B''**, merge; **C-C'',** anterior part of a 48 hpf double transgenic larva: **C**, green channel; **C'**, red channel; **C''**, merge; **D-D'',** tail of a 24 hpf double transgenic embryo: **D**, green channel; D', red channel; **D''**, merge.

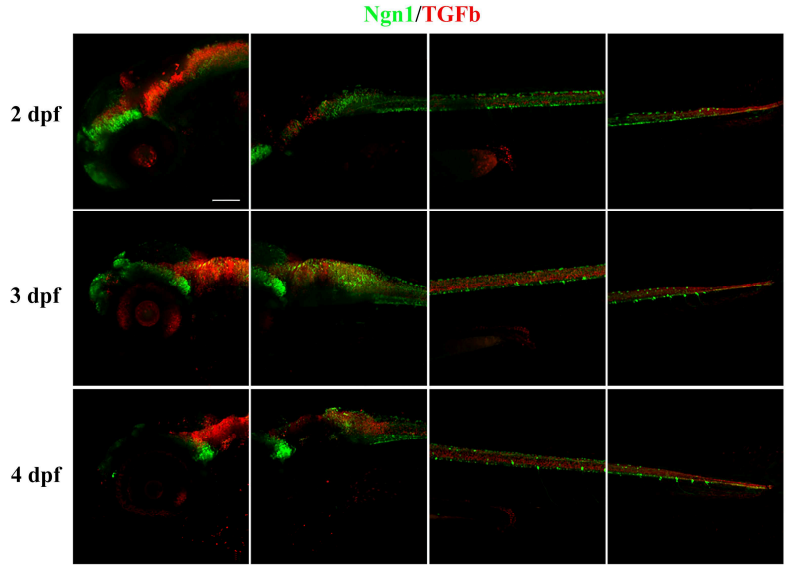

Fig. S3. Confocal lateral images of brain and neural tube in double transgenic larvae tg(Ngn1:GFP)^{sb1}/tg(12xSBE:nls-mCherry). Lateral view of head, hindbrain, trunk and tail in double transgenic larvae tg(Ngn1:GFP)^{sb1}/tg(12xSBE:nls-mCherry) at 2, 3 and 4 dpf.

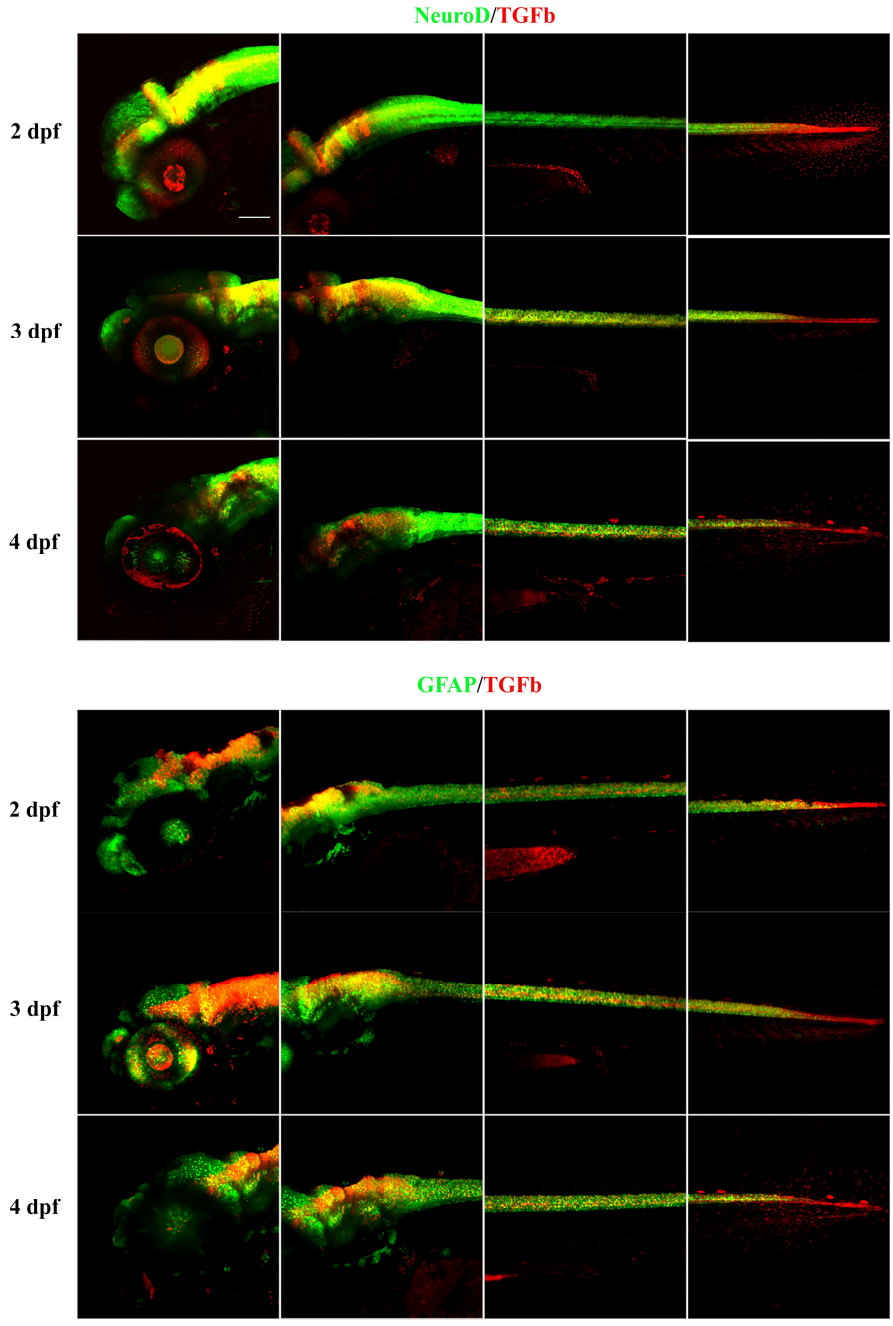

Fig. S4. Confocal lateral images of brain and nerural tube in double transgenic larvae tg(12xSBE:nls-mCherry)/tg(-2.4kb neurod:EGFP) or tg(gfap:GFP)mi20001. Lateral view of head, hindbrain, trunk and tail of double transgenic larvae tg(12xSBE:nls-mCherry)/tg(-2.4kb neurod:EGFP) or tg(gfap:GFP)^{mi20001} at 2, 3 and 4 dpf.

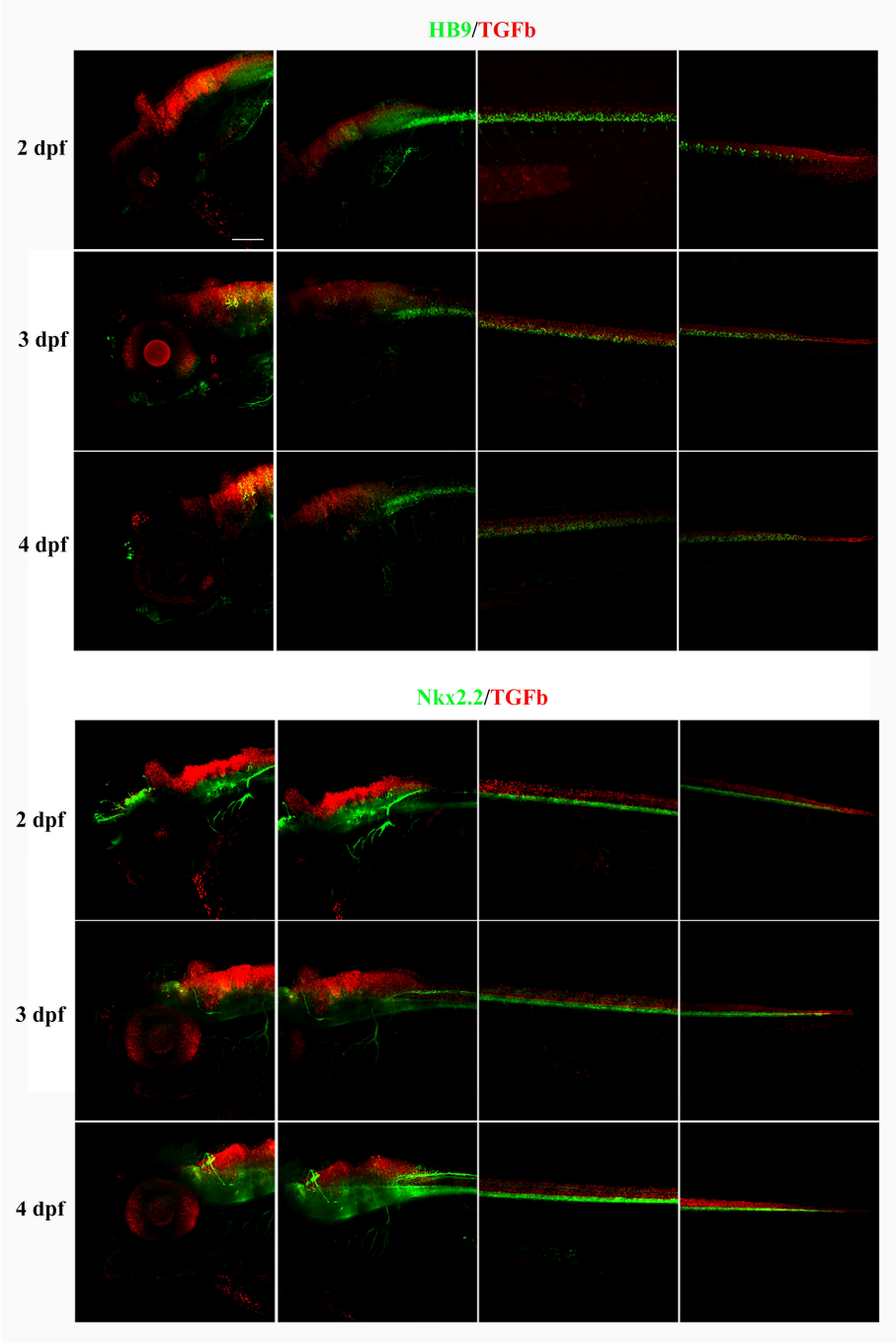

Fig. S5. Confocal lateral images of brain and nerural tube in double transgenic larvae tg(12xSBE:nls-mCherry)/ tg(Mnx1:GFP)^{ml2} and tg(Nkx2.2a:mGFP)^{vu17}. Lateral view of head, hindbrain, trunk and tail of double transgenic larvae tg(12xSBE:nls-mCherry)/tg(Mnx1:GFP)^{ml2} and tg(Nkx2.2a:mGFP)^{vu17} at 2, 3 and 4 dpf.

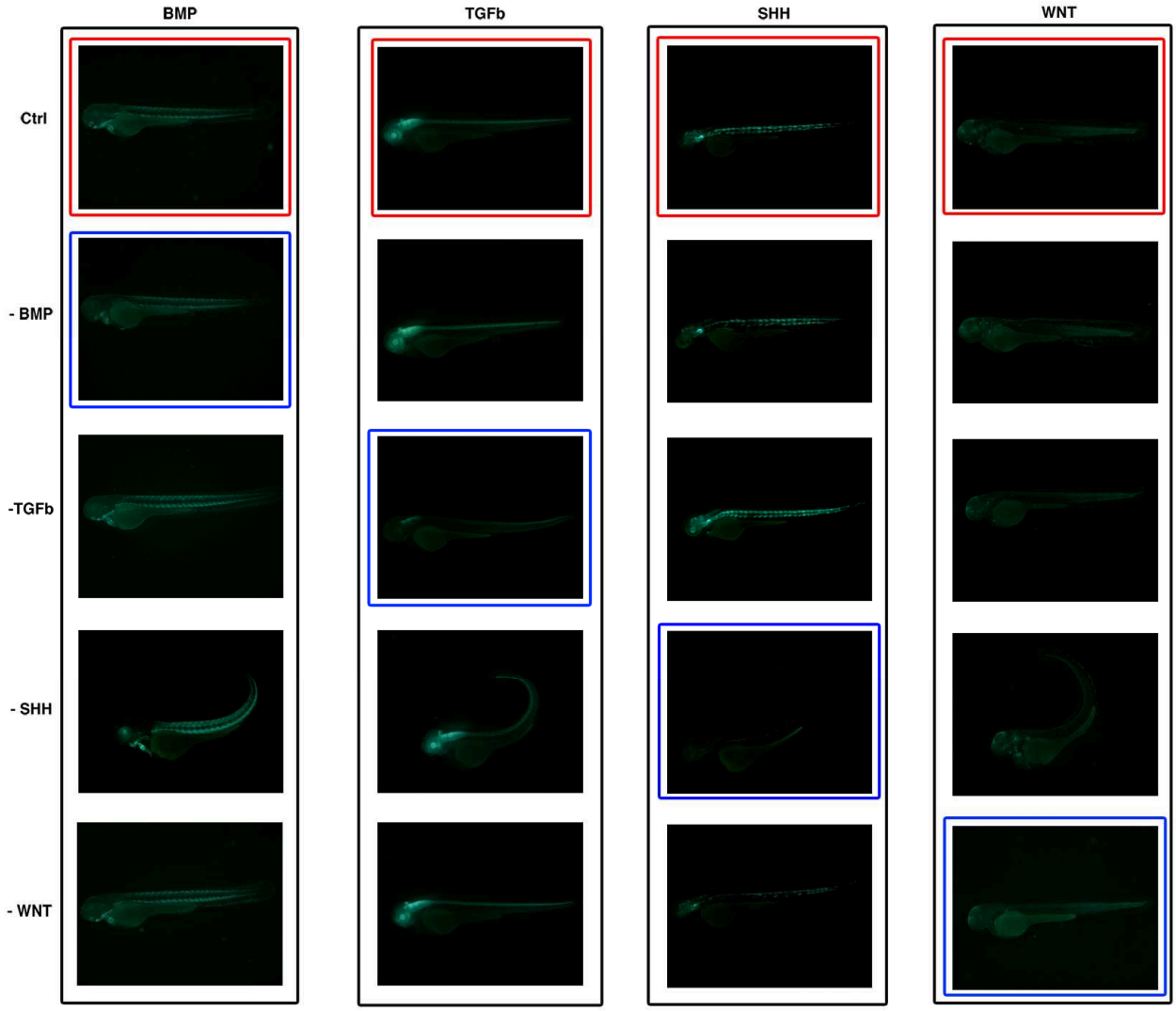

Fig. S6. The effects of the inhibitors of the 4 morphogens on tg(12xSBE:EGFP)^{ia16}, tg(BMPRE:EGFP)^{ia18}, tg(12xGli-Hsv.Tk:GFP)^{ia11} and tg(7xTCF-Xla.Siam:GFP)^{ia4} lines: GFP expression. Fluorescent lateral views of of tg(12xSBE:EGFP)^{ia16}, tg(BMPRE:EGFP)^{ia18}, tg(12xGli-Hsv.Tk:GFP)^{ia11} and tg(7xTCF-Xla.Siam:GFP)^{ia4} larvae at 3 dpf. Each reporter line has been treated at 24 hpf for 2 days with the inhibitors of the 4 morphogens (BMP, TGFb, Wnt and Shh).

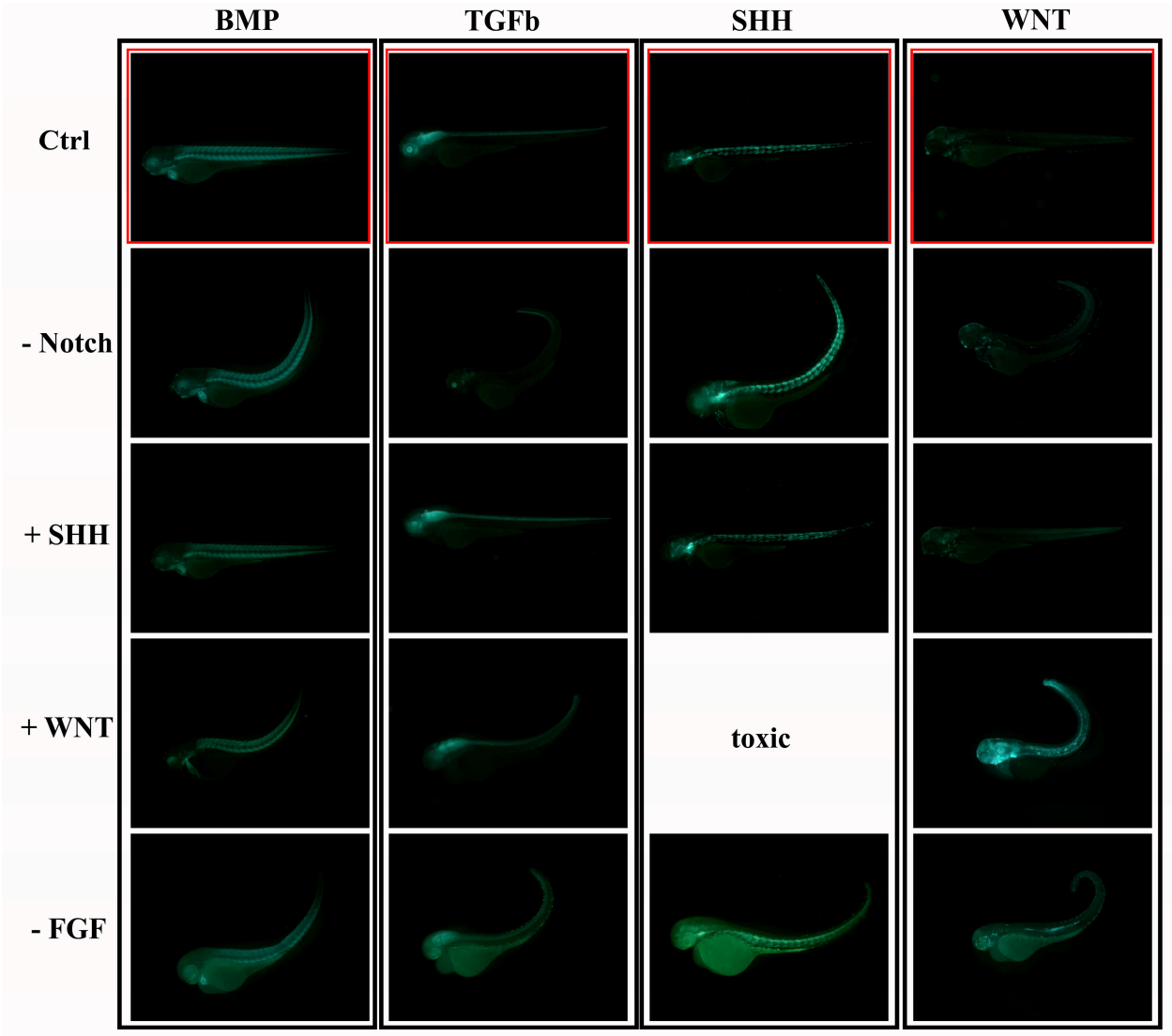

Fig. S7. The effects of the other drugs tested on tg(12xSBE:EGFP)^{ia16}, tg(BMPRE:EGFP)^{ia18}, tg(12xGli-Hsv.Tk:GFP)^{ia11} and tg(7xTCF-Xla.Siam:GFP)^{ia4} lines: GFP expression. Fluorescent lateral views of tg(12xSBE:EGFP)^{ia16}, tg(BMPRE:EGFP)^{ia18}, tg(12xGli-Hsv.Tk:GFP)^{ia11} and tg(7xTCF-Xla.Siam:GFP)^{ia4} larvae at 3 dpf. Each reporter line has been treated at 24 hpf for 2 days with Wnt and Shh agonists and the inhibitors of Notch and FGF signalling pathways.

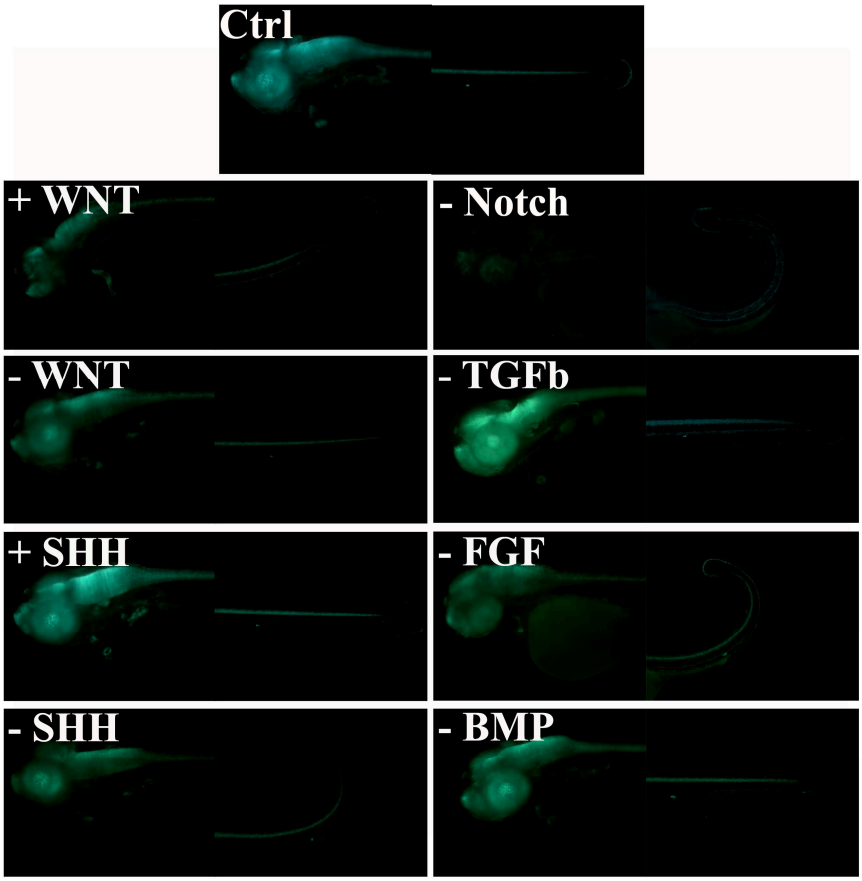

Fig. S8. The effects of the drugs tested on tg(Tp1bglob:eGFP) line: GFP expression. Fluorescent lateral views of anterior and posterior body parts of tg(Tp1bglob:eGFP) larvae at 3 dpf. This reporter line has been treated at 24 hpf for 2 days with drugs that alter Wnt, BMP, TGFb, Shh, FGF and Notch itself pathway.

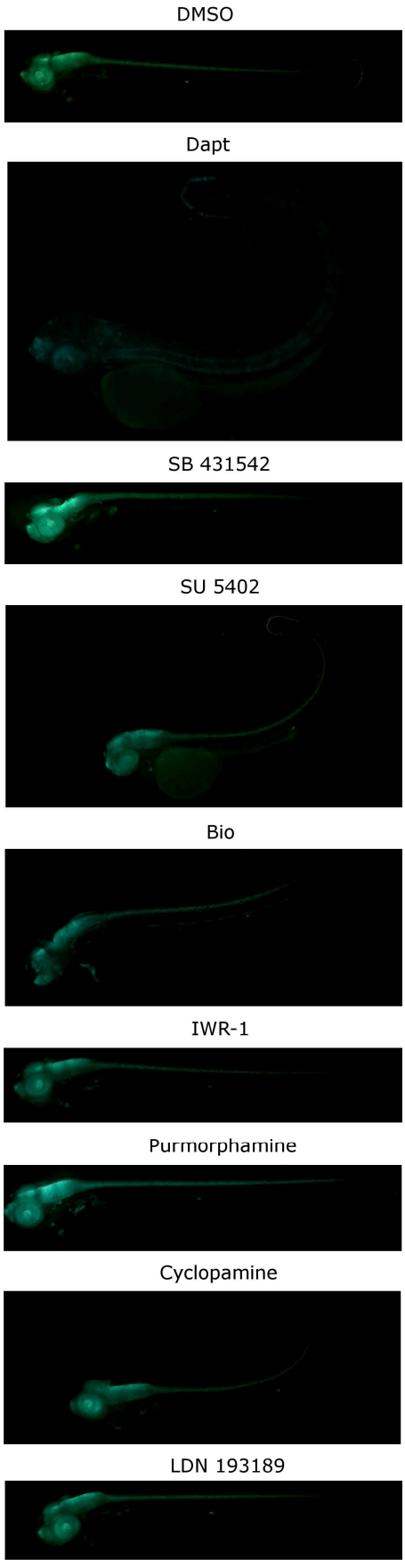

Fig. S9. The effects of the drugs tested on tg(Tp1bglob:eGFP) line: GFP expression. Fluorescent lateral views of tg(Tp1bglob:eGFP) larvae at 3 dpf. This reporter line has been treated at 24 hpf for 2 days with drugs that alter Wnt, BMP, TGFb, Shh, FGF and Notch itself pathways.

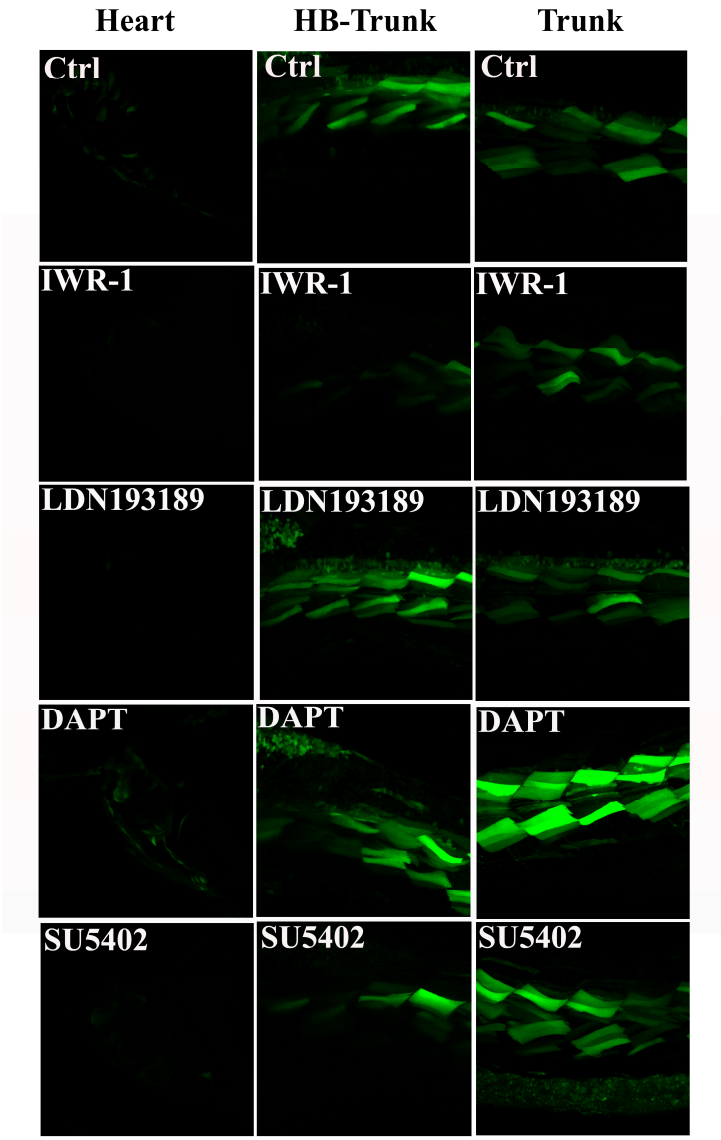

Fig. S10. The effects of some of the drugs used for the epistasis study on tg(12xGli-Hsv.Tk:GFP)^{ia11} line: confocal observation. Confocal views of heart, hindbrain (HB)-trunk and trunk of tg(12xGli-Hsv.Tk:GFP)^{ia11} larvae at 3 dpf.

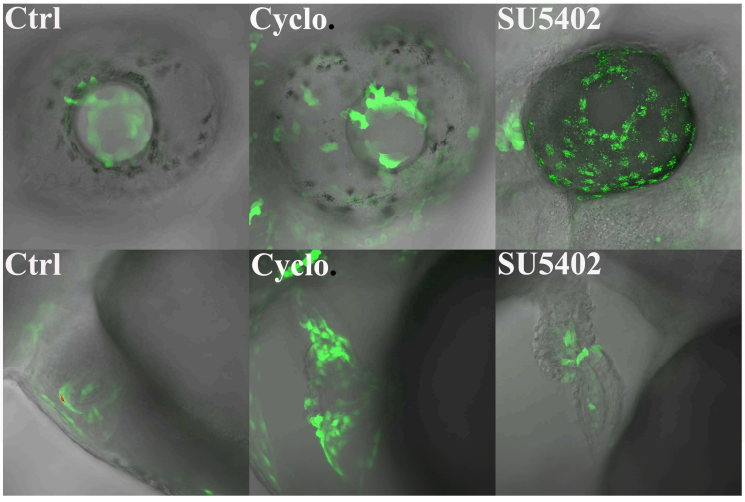

Fig. S11. The effects of FGF and Shh inhibitors on tg(7xTCF-Xla.Siam:GFP)^{ia4} line: confocal observation. Confocal views of heart and eye of tg(7xTCF-Xla.Siam:GFP)^{ia4} larvae at 3 dpf treated with cyclopamine (cyclo.), a Shh inhibitor, and SU5402, a FGF inhibitor.

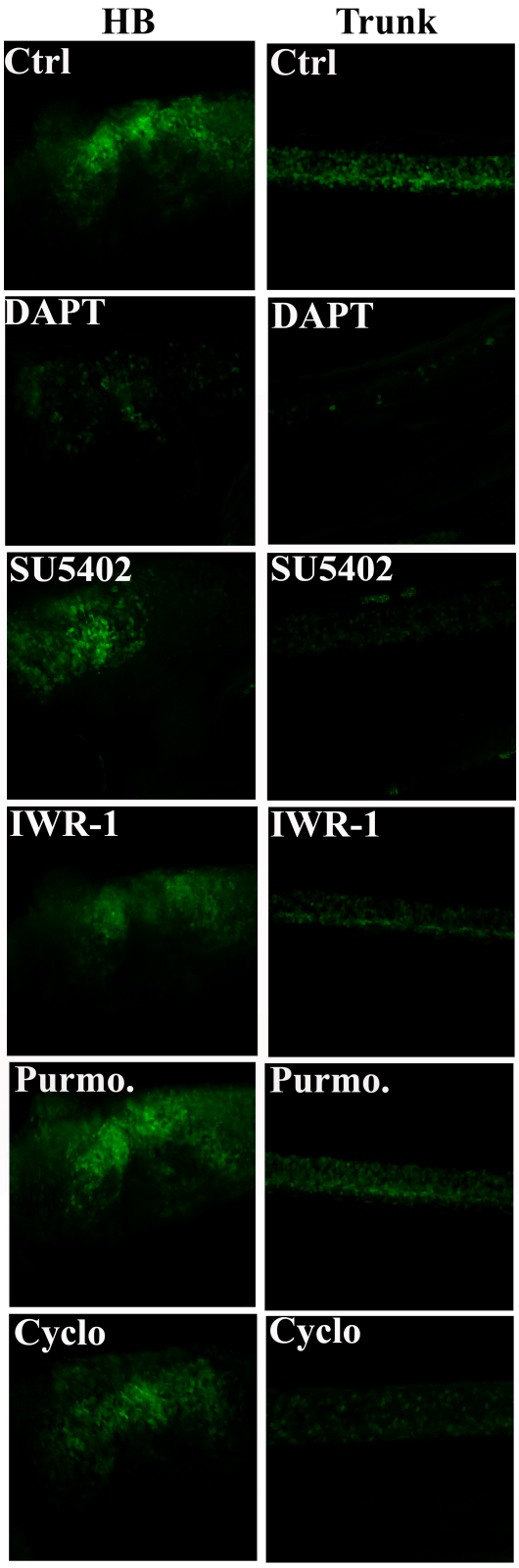

Fig. S12. The effects of some of the drugs used for the epistasis study on tg(12xSBE:EGFP)^{ia16} line: confocal observation. Confocal views of hindbrain (HB) and trunk of tg(12xSBE:EGFP)^{ia16} larvae at 3 dpf.

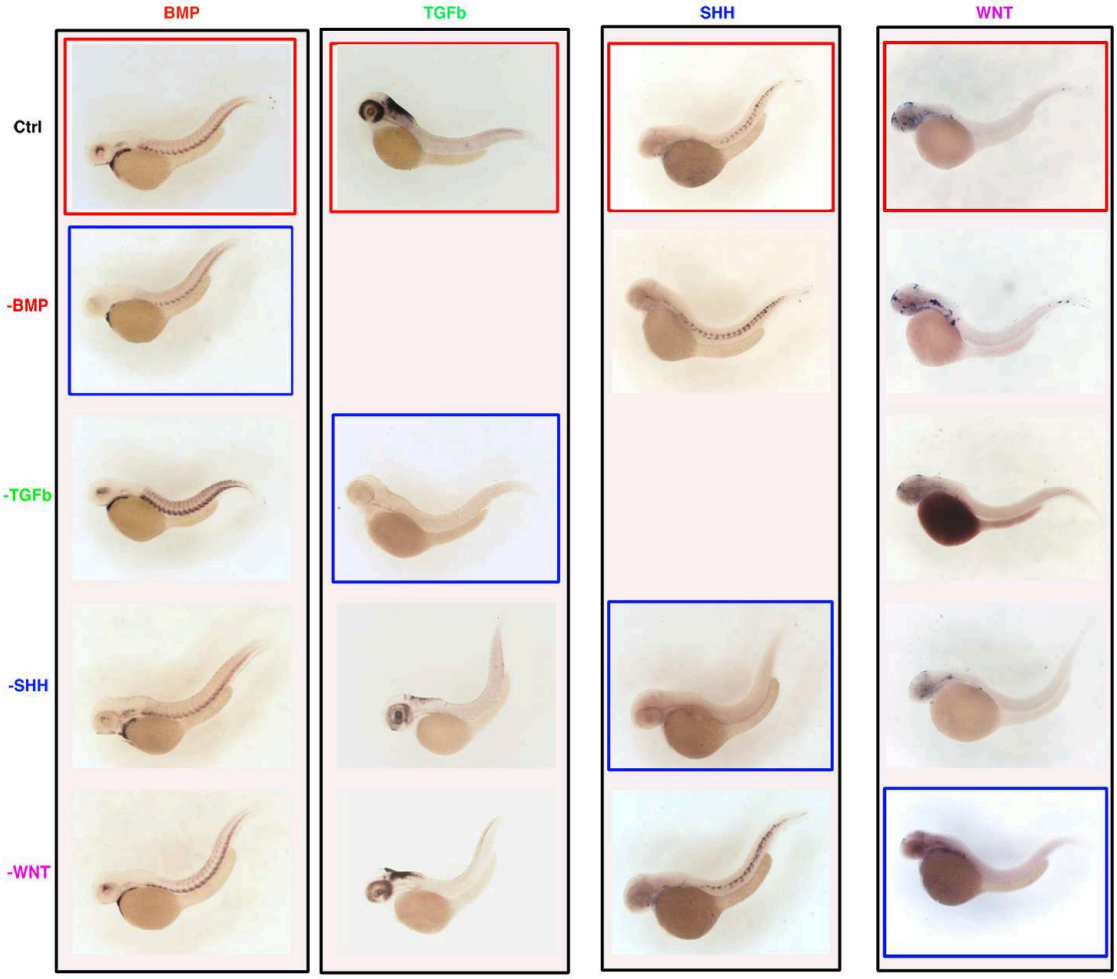

Fig. S13. The effects of the inhibitors of the 4 morphogens on tg(12xSBE:EGFP)^{ia16}, tg(BMPRE:EGFP)^{ia18}, tg(12xGli-Hsv.Tk:GFP)^{ia11} and tg(7xTCF-Xla.Siam:GFP)^{ia4} lines: mRNA ISH for GFP expression. Lateral views of of tg(12xSBE:EGFP)^{ia16}, tg(BMPRE:EGFP)^{ia18}, tg(12xGli-Hsv.Tk:GFP)^{ia11} and tg(7xTCF-Xla.Siam:GFP)^{ia4} larvae at 3 dpf. Each reporter line has been treated at 24 hpf for 2 days with the inhibitors of the 4 morphogens (BMP, TGFb, Wnt and Shh).

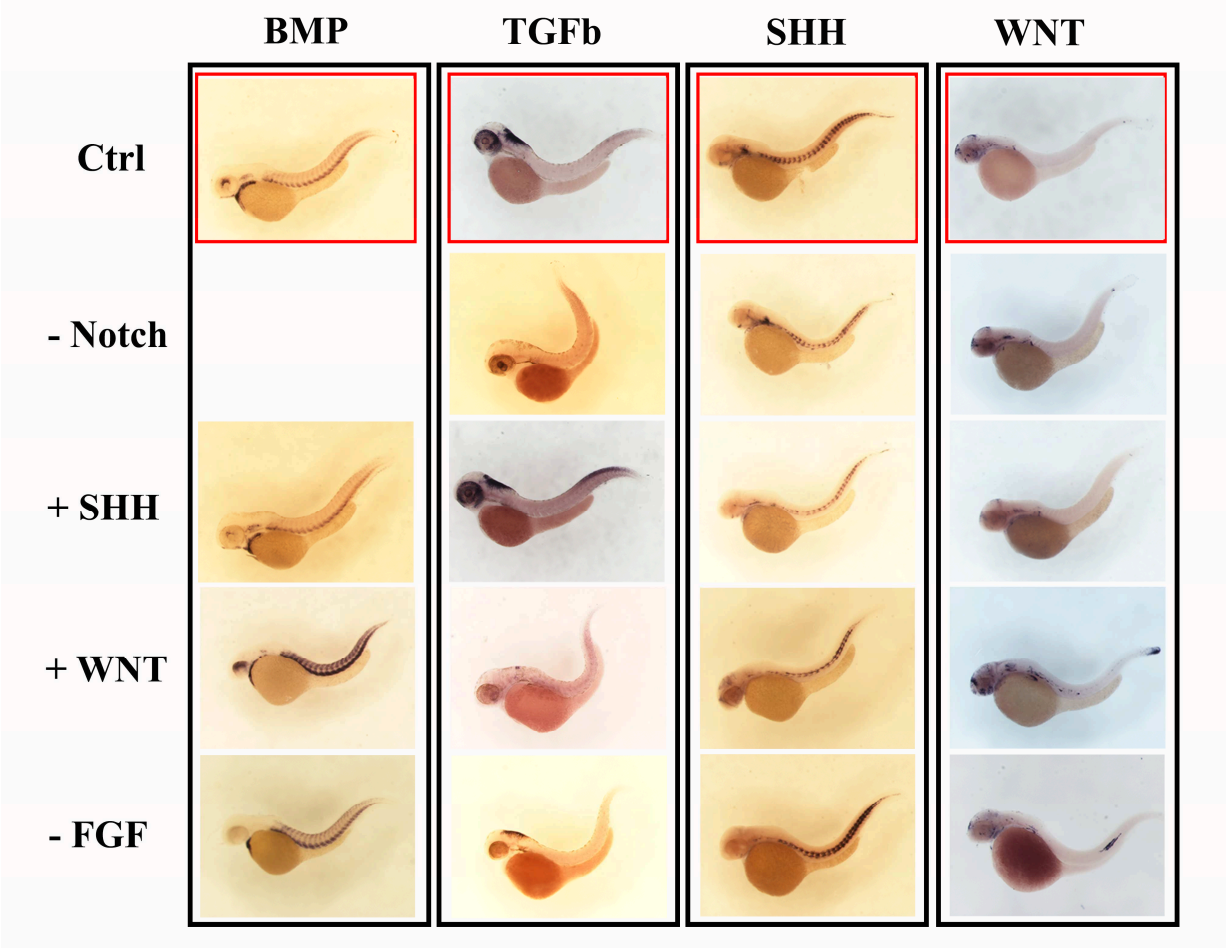

Fig. S14. The effects of the other drugs tested on tg(12xSBE:EGFP)^{ia16}, tg(BMPRE:EGFP)^{ia18}, tg(12xGli-Hsv.Tk:GFP)^{ia11} and tg(7xTCF-Xla.Siam:GFP)^{ia4} lines: mRNA ISH for GFP expression. Lateral views of tg(12xSBE:EGFP)^{ia16}, tg(BMPRE:EGFP)^{ia18}, tg(12xGli-Hsv.Tk:GFP)^{ia11} and tg(7xTCF-Xla.Siam:GFP)^{ia4} larvae at 3 dpf. Each reporter line has been treated at 24 hpf for 2 days with Wnt and Shh agonists and the inhibitors of Notch and FGF signalling pathways.

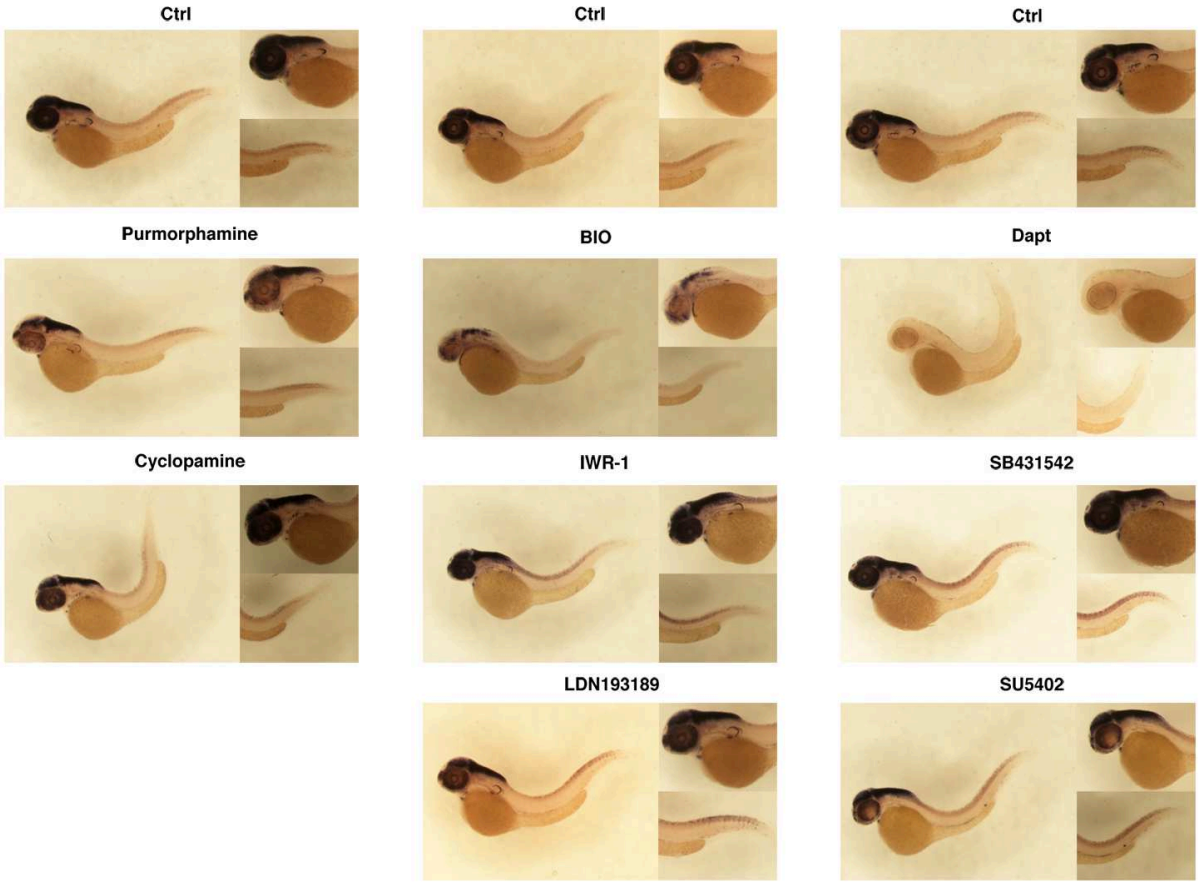

Fig. S15. The effects of the drugs tested on tg(Tp1bglob:eGFP) line: mRNA ISH for GFP expression. Lateral views of Tg(Tp1bglob:eGFP) larvae at 3 dpf with magnified views of anterior and posterior body parts. This reporter line has been treated at 24 hpf for 2 days with drugs that alter Wnt, BMP, TGFb, Shh, FGF and Notch itself pathway.

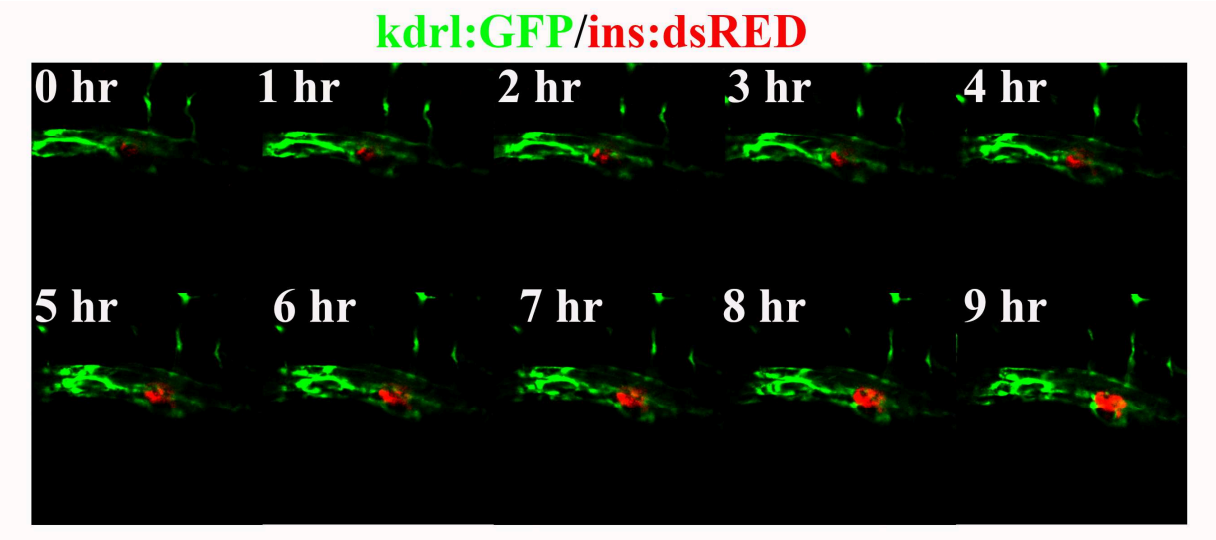

Fig. S16. Vessels make contact to beta-cells between 1 and 2 dpf. Confocal stacks of double transgenic tg(ins:dsRED)^{m1018}/(kdrl:GFP)^{la116} obtained through a time-laps observation between 1 and 2 dpf.

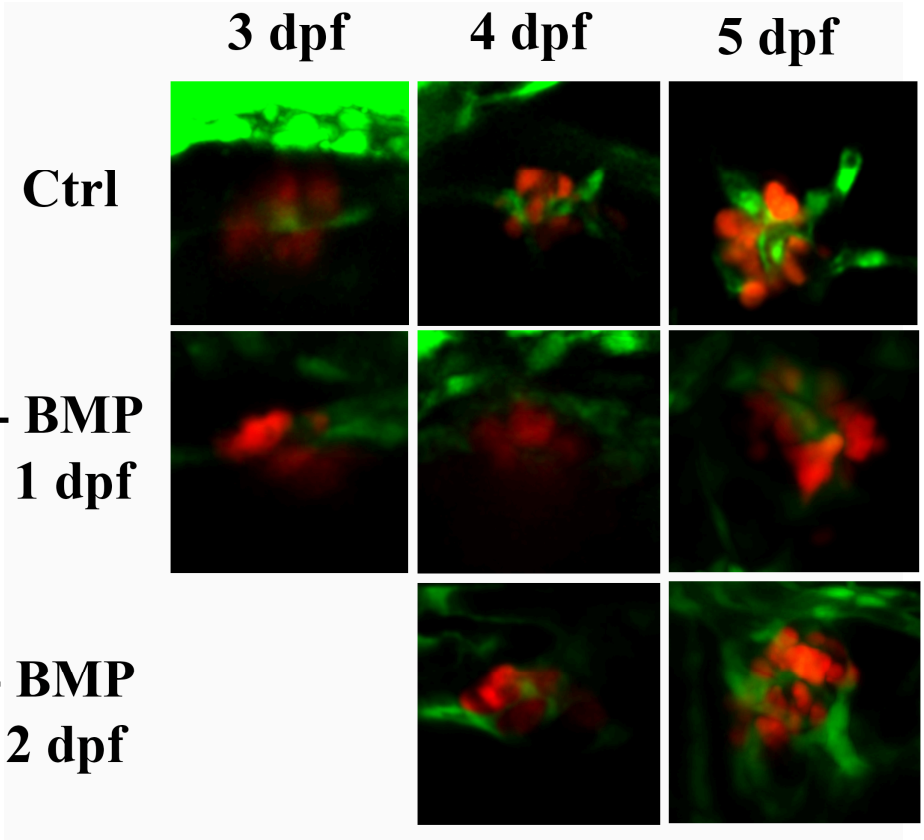

Fig. S17. BMP signalling inhibition at 24 and 48 hpf causes a decrease of GFP-associated endocytes. Confocal magnified views of the pancreatic islet in the double transgenic tg(BMPRE:EGFP)^{ia18}/(ins:dsRED)^{m1018} larvae treated at 1 and 2 dpf with an Alk2 and 3 inhibitor and observed at 3, 4 and 5 dpf. Treatment at 1 dpf decreases significantly kdrl-associated GFP expression in the islet region.

REFERENCES

Ahnfelt-Ronne, J., Ravassard, P., Pardanaud-Glavieux, C., Scharfmann, R. and Serup, P. (2010). Mesenchymal bone morphogenetic protein signaling is required for normal pancreas development. *Diabetes* **59**, 1948-56.

Anthoni, M., Wang, G., Leino, M. S., Lauerma, A. I., Alenius, H. T. and Wolff, H. J. (2007). Smad3 -signalling and Th2 cytokines in normal mouse airways and in a mouse model of asthma. *Int J Biol Sci* **3**, 477-85.

Aquilina-Beck, A., Ilagan, K., Liu, Q. and Liang, J. O. (2007). Nodal signaling is required for closure of the anterior neural tube in zebrafish. *BMC Dev Biol* **7**, 126.

Argenton, F., Zecchin, E. and Bortolussi, M. (1999). Early appearance of pancreatic hormone-expressing cells in the zebrafish embryo. *Mech Dev* **87**, 217-21.

Baker, J. C., Beddington, R. S. and Harland, R. M. (1999). Wnt signaling in Xenopus embryos inhibits bmp4 expression and activates neural development. *Genes Dev* **13**, 3149-59.

Baker, S. J. and McKinnon, P. J. (2004). Tumour-suppressor function in the nervous system. *Nat Rev Cancer* **4**, 184-96.

Barolo, S. (2006). Transgenic Wnt/TCF pathway reporters: all you need is Lef? *Oncogene* **25**, 7505-11.

Barth, K. A. and Wilson, S. W. (1995). Expression of zebrafish nk2.2 is influenced by sonic hedgehog/vertebrate hedgehog-1 and demarcates a zone of neuronal differentiation in the embryonic forebrain. *Development* **121**, 1755-68.

Biemar, F., Argenton, F., Schmidtke, R., Epperlein, S., Peers, B. and Driever, W. (2001). Pancreas development in zebrafish: early dispersed appearance of endocrine hormone expressing cells and their convergence to form the definitive islet. *Dev Biol* **230**, 189-203.

Boyd, N. L., Dhara, S. K., Rekaya, R., Godbey, E. A., Hasneen, K., Rao, R. R., West, F. D., 3rd, Gerwe, B. A. and Stice, S. L. (2007). BMP4 promotes formation of primitive vascular networks in human embryonic stem cell-derived embryoid bodies. *Exp Biol Med (Maywood)* **232**, 833-43.

Brown, L. A., Rodaway, A. R., Schilling, T. F., Jowett, T., Ingham, P. W., Patient, R. K. and Sharrocks, A. D. (2000). Insights into early vasculogenesis revealed by expression of the ETS-domain transcription factor Fli-1 in wild-type and mutant zebrafish embryos. *Mech Dev* **90**, 237-52.

Caneparo, L., Huang, Y. L., Staudt, N., Tada, M., Ahrendt, R., Kazanskaya, O., Niehrs, C. and Houart, C. (2007). Dickkopf-1 regulates gastrulation movements by coordinated modulation of Wnt/beta catenin and Wnt/PCP activities, through interaction with the Dally-like homolog Knypek. *Genes Dev* **21**, 465-80.

Chapouton, P., Godinho, L., H. William Detrich, M. W. and Leonard, I. Z. (2010). Chapter 4 - Neurogenesis. In *Methods in Cell Biology*, vol. Volume 100, pp. 72-126: Academic Press.

Charron, F. and Tessier-Lavigne, M. (2007). The Hedgehog, TGF-beta/BMP and Wnt families of morphogens in axon guidance. *Adv Exp Med Biol* **621**, 116-33.

Chen, Y., Lebrun, J. J. and Vale, W. (1996). Regulation of transforming growth factor beta- and activin-induced transcription by mammalian Mad proteins. *Proc Natl Acad Sci U S A* **93**, 12992-7.

Chung, W. S., Andersson, O., Row, R., Kimelman, D. and Stainier, D. Y. (2009). Suppression of Alk8-mediated Bmp signaling cell-autonomously induces pancreatic beta-cells in zebrafish. *Proc Natl Acad Sci U S A* **107**, 1142-7.

Cruz, C., Maegawa, S., Weinberg, E. S., Wilson, S. W., Dawid, I. B. and Kudoh, T. (2010). Induction and patterning of trunk and tail neural ectoderm by the homeobox gene eve1 in zebrafish embryos. *Proc Natl Acad Sci U S A* **107**, 3564-9.

de Caestecker, M. P., Piek, E. and Roberts, A. B. (2000). Role of transforming growth factor-beta signaling in cancer. *J Natl Cancer Inst* **92**, 1388-402.

Dennler, S., Itoh, S., Vivien, D., ten Dijke, P., Huet, S. and Gauthier, J. M. (1998). Direct binding of Smad3 and Smad4 to critical TGF beta-inducible elements in the promoter of human plasminogen activator inhibitor-type 1 gene. *EMBO J* **17**, 3091-100.

Deregowski, V., Gazzerro, E., Priest, L., Rydziel, S. and Canalis, E. (2006). Notch 1 overexpression inhibits osteoblastogenesis by suppressing Wnt/beta-catenin but not bone morphogenetic protein signaling. *J Biol Chem* **281**, 6203-10.

Dick, A., Mayr, T., Bauer, H., Meier, A. and Hammerschmidt, M. (2000). Cloning and characterization of zebrafish smad2, smad3 and smad4. *Gene* **246**, 69-80.

diIorio, P. J., Moss, J. B., Sbrogna, J. L., Karlstrom, R. O. and Moss, L. G. (2002). Sonic hedgehog is required early in pancreatic islet development. *Dev Biol* **244**, 75-84.

Draper, B. W., Morcos, P. A. and Kimmel, C. B. (2001). Inhibition of zebrafish fgf8 pre-mRNA splicing with morpholino oligos: a quantifiable method for gene knockdown. *Genesis* **30**, 154-6.

Edlund, H. (2002). Pancreatic organogenesis--developmental mechanisms and implications for therapy. *Nat Rev Genet* **3**, 524-32.

Ferent, J., Zimmer, C., Durbec, P., Ruat, M. and Traiffort, E. (2013). Sonic Hedgehog signaling is a positive oligodendrocyte regulator during demyelination. *J Neurosci* **33**, 1759-72.

Field, H. A., Dong, P. D., Beis, D. and Stainier, D. Y. (2003). Formation of the digestive system in zebrafish. II. Pancreas morphogenesis. *Dev Biol* **261**, 197-208.

Fiocchi, C. (2001). TGF-beta/Smad signaling defects in inflammatory bowel disease: mechanisms and possible novel therapies for chronic inflammation. *J Clin Invest* **108**, 523-6.

Flasse, L. C., Pirson, J. L., Stern, D. G., Von Berg, V., Manfroid, I., Peers, B. and Voz, M. L. (2013). Ascl1b and Neurod1, instead of Neurog3, control pancreatic endocrine cell fate in zebrafish. *BMC Biol* **11**, 78.

Fleisch, M. C., Maxwell, C. A. and Barcellos-Hoff, M. H. (2006). The pleiotropic roles of transforming growth factor beta in homeostasis and carcinogenesis of endocrine organs. *Endocr Relat Cancer* **13**, 379-400.

Garcia-Campmany, L. and Marti, E. (2007). The TGFbeta intracellular effector Smad3 regulates neuronal differentiation and cell fate specification in the developing spinal cord. *Development* **134**, 65-75.

Ge, X., Vajjala, A., McFarlane, C., Wahli, W., Sharma, M. and Kambadur, R. (2012). Lack of Smad3 signaling leads to impaired skeletal muscle regeneration. *Am J Physiol Endocrinol Metab* **303**, E90-102.

Gomes, F. C., Sousa Vde, O. and Romao, L. (2005). Emerging roles for TGF-beta1 in nervous system development. *Int J Dev Neurosci* **23**, 413-24.

Gotoh, H., Ono, K., Nomura, T., Takebayashi, H., Harada, H., Nakamura, H. and Ikenaka, K. (2012). Nkx2.2+ progenitors generate somatic motoneurons in the chick spinal cord. *PLoS One* **7**, e51581.

Hashiguchi, M. and Mullins, M. C. (2013). Anteroposterior and dorsoventral patterning are coordinated by an identical patterning clock. *Development* **140**, 1970-80.

Hayward, P., Brennan, K., Sanders, P., Balayo, T., DasGupta, R., Perrimon, N. and Martinez Arias, A. (2005). Notch modulates Wnt signalling by associating with Armadillo/beta-catenin and regulating its transcriptional activity. *Development* **132**, 1819-30.

Heasman, J. (1997). Patterning the Xenopus blastula. *Development* **124**, 4179-91.

Herman, J. M., Fan, K. Y., Wild, A. T., Wood, L. D., Blackford, A. L., Donehower, R. C., Hidalgo, M., Schulick, R. D., Edil, B. H., Choti, M. A. et al. (2013). Correlation of Smad4 status with outcomes in patients receiving erlotinib combined with adjuvant chemoradiation and chemotherapy after resection for pancreatic adenocarcinoma. *Int J Radiat Oncol Biol Phys* **87**, 458-9.

Hinck, A. P. (2012). Structural studies of the TGF-betas and their receptors - insights into

evolution of the TGF-beta superfamily. *FEBS Lett* **586**, 1860-70.

Ho, T. W., Bristol, L. A., Coccia, C., Li, Y., Milbrandt, J., Johnson, E., Jin, L., Bar-Peled, O., Griffin, J. W. and Rothstein, J. D. (2000). TGFbeta trophic factors differentially modulate motor axon outgrowth and protection from excitotoxicity. *Exp Neurol* **161**, 664-75.

Howie, S. and Fisher, C. E. (2008). Shh and Gli Signalling in Development: Springer London, Limited.

Hsu, R. J., Lin, C. C., Su, Y. F. and Tsai, H. J. (2011). dickkopf-3-related gene regulates the expression of zebrafish myf5 gene through phosphorylated p38a-dependent Smad4 activity. *J Biol Chem* **286**, 6855-64.

Hua, H. and Sarvetnick, N. (2007). Expression of Id1 in adult, regenerating and developing pancreas. *Endocrine* **32**, 280-6.

Itasaki, N. and Hoppler, S. (2010). Crosstalk between Wnt and bone morphogenic protein signaling: a turbulent relationship. *Dev Dyn* **239**, 16-33.

Iwatsuki, K., Liu, H. X., Gronder, A., Singer, M. A., Lane, T. F., Grosschedl, R., Mistretta, C. M. and Margolskee, R. F. (2007). Wnt signaling interacts with Shh to regulate taste papilla development. *Proc Natl Acad Sci U S A* **104**, 2253-8.

Jensen, J. (2004). Gene regulatory factors in pancreatic development. *Dev Dyn* **229**, 176-200.

Jia, S., Ren, Z., Li, X., Zheng, Y. and Meng, A. (2008). smad2 and smad3 are required for mesendoderm induction by transforming growth factor-beta/nodal signals in zebrafish. *J Biol Chem* **283**, 2418-26.

Jia, S., Wu, D., Xing, C. and Meng, A. (2009). Smad2/3 activities are required for induction and patterning of the neuroectoderm in zebrafish. *Dev Biol* **333**, 273-84.

Katsuno, M., Adachi, H., Banno, H., Suzuki, K., Tanaka, F. and Sobue, G. (2011). Transforming growth factor-beta signaling in motor neuron diseases. *Curr Mol Med* **11**, 48-56.

Kim, H. A., Koo, B. K., Cho, J. H., Kim, Y. Y., Seong, J., Chang, H. J., Oh, Y. M., Stange, D. E., Park, J. G., Hwang, D. et al. (2012). Notch1 counteracts WNT/beta-catenin signaling through chromatin modification in colorectal cancer. *J Clin Invest* **122**, 3248-59.

Kimelman, D. (2006). Mesoderm induction: from caps to chips. *Nat Rev Genet* **7**, 360-72.

Kimmel, C. B., Ballard, W. W., Kimmel, S. R., Ullmann, B. and Schilling, T. F. (1995). Stages of embryonic development of the zebrafish. *Dev Dyn* **203**, 253-310.

Kodjabachian, L. (2001). Morphogen gradients: nodal enters the stage. *Curr Biol* **11**, R655-8.

Komiya, Y. and Habas, R. (2008). Wnt signal transduction pathways. *Organogenesis* **4**, 68-75.

Korzh, V., Sleptsova, I., Liao, J., He, J. and Gong, Z. (1998). Expression of zebrafish bHLH genes ngn1 and nrd defines distinct stages of neural differentiation. *Dev Dyn* **213**, 92-104.

Krieglstein, K., Strelau, J., Schober, A., Sullivan, A. and Unsicker, K. (2002). TGF-beta and the regulation of neuron survival and death. *J Physiol Paris* **96**, 25-30.

Lammert, E., Cleaver, O. and Melton, D. (2001). Induction of pancreatic differentiation by signals from blood vessels. *Science* **294**, 564-7.

Lan, H. Y. (2011). Diverse roles of TGF-beta/Smads in renal fibrosis and inflammation. *Int J Biol Sci* **7**, 1056-67.

Langenfeld, E. M. and Langenfeld, J. (2004). Bone morphogenetic protein-2 stimulates angiogenesis in developing tumors. *Mol Cancer Res* **2**, 141-9.

Laux, D. W., Febbo, J. A. and Roman, B. L. (2011). Dynamic analysis of BMP-responsive smad activity in live zebrafish embryos. *Dev Dyn* **240**, 682-94.

Litingtung, Y. and Chiang, C. (2000). Specification of ventral neuron types is mediated by an antagonistic interaction between Shh and Gli3. *Nat Neurosci* **3**, 979-85.

Liu, X., Sun, Y., Constantinescu, S. N., Karam, E., Weinberg, R. A. and Lodish, H. F. (1997). Transforming growth factor beta-induced phosphorylation of Smad3 is required for growth inhibition and transcriptional induction in epithelial cells. *Proc Natl Acad Sci U S A* **94**, 10669-74.

Liu, Z. and Habener, J. F. (2010). Wnt signaling in pancreatic islets. *Adv Exp Med Biol* **654**, 391-

419.

Lopez-Rovira, T., Chalaux, E., Massague, J., Rosa, J. L. and Ventura, F. (2002). Direct binding of Smad1 and Smad4 to two distinct motifs mediates bone morphogenetic protein-specific transcriptional activation of Id1 gene. *J Biol Chem* **277**, 3176-85.

Luo, Y. J. and Su, Y. H. (2012). Opposing nodal and BMP signals regulate left-right asymmetry in the sea urchin larva. *PLoS Biol* **10**, e1001402.

Ma, E. Y. and Raible, D. W. (2009). Signaling pathways regulating zebrafish lateral line development. *Curr Biol* **19**, R381-6.

Macia, J., Widder, S. and Sole, R. (2009). Specialized or flexible feed-forward loop motifs: a question of topology. *BMC Syst Biol* **3**, 84.

Marcelle, C., Stark, M. R. and Bronner-Fraser, M. (1997). Coordinate actions of BMPs, Wnts, Shh and noggin mediate patterning of the dorsal somite. *Development* **124**, 3955-63.

Maretto, S., Cordenonsi, M., Dupont, S., Braghetta, P., Broccoli, V., Hassan, A. B., Volpin, D., Bressan, G. M. and Piccolo, S. (2003). Mapping Wnt/beta-catenin signaling during mouse development and in colorectal tumors. *Proc Natl Acad Sci U S A* **100**, 3299-304.

Miazga, C. M. and McLaughlin, K. A. (2009). Coordinating the timing of cardiac precursor development during gastrulation: a new role for Notch signaling. *Dev Biol* **333**, 285-96.

Miguez, D. G., Gil-Guinon, E., Pons, S. and Marti, E. (2013). Smad2 and Smad3 cooperate and antagonize simultaneously in vertebrate neurogenesis. *J Cell Sci*.

Moro, E., Gnugge, L., Braghetta, P., Bortolussi, M. and Argenton, F. (2009). Analysis of beta cell proliferation dynamics in zebrafish. *Dev Biol* **332**, 299-308.

Moro, E., Ozhan-Kizil, G., Mongera, A., Beis, D., Wierzbicki, C., Young, R. M., Bournele, D., Domenichini, A., Valdivia, L. E., Lum, L. et al. (2012). In vivo Wnt signaling tracing through a transgenic biosensor fish reveals novel activity domains. *Dev Biol* **366**, 327-40.

Moro, E., Vettori, A., Porazzi, P., Schiavone, M., Rampazzo, E., Casari, A., Ek, O., Facchinello, N., Astone, M., Zancan, I. et al. (2013). Generation and application of signaling pathway reporter lines in zebrafish. *Mol Genet Genomics* **288**, 231-42.

Moser, M. and Patterson, C. (2005). Bone morphogenetic proteins and vascular differentiation: BMPing up vasculogenesis. *Thromb Haemost* **94**, 713-8.

Nakashima, A., Katagiri, T. and Tamura, M. (2005). Cross-talk between Wnt and bone morphogenetic protein 2 (BMP-2) signaling in differentiation pathway of C2C12 myoblasts. *J Biol Chem* **280**, 37660-8.

Nasevicius, A. and Ekker, S. C. (2000). Effective targeted gene 'knockdown' in zebrafish. *Nat Genet* **26**, 216-20.

Ninov, N., Borius, M. and Stainier, D. Y. (2012). Different levels of Notch signaling regulate quiescence, renewal and differentiation in pancreatic endocrine progenitors. *Development* **139**, 1557-67.

Norgaard, G. A., Jensen, J. N. and Jensen, J. (2003). FGF10 signaling maintains the pancreatic progenitor cell state revealing a novel role of Notch in organ development. *Dev Biol* **264**, 323-38.

Oliver, T. G., Grasfeder, L. L., Carroll, A. L., Kaiser, C., Gillingham, C. L., Lin, S. M., Wickramasinghe, R., Scott, M. P. and Wechsler-Reya, R. J. (2003). Transcriptional profiling of the Sonic hedgehog response: a critical role for N-myc in proliferation of neuronal precursors. *Proc Natl Acad Sci U S A* **100**, 7331-6.

Papadopoulou, S. and Edlund, H. (2005). Attenuated Wnt signaling perturbs pancreatic growth but not pancreatic function. *Diabetes* **54**, 2844-51.

Park, C., Lavine, K., Mishina, Y., Deng, C. X., Ornitz, D. M. and Choi, K. (2006). Bone morphogenetic protein receptor 1A signaling is dispensable for hematopoietic development but essential for vessel and atrioventricular endocardial cushion formation. *Development* **133**, 3473-84.

Patten, I. and Placzek, M. (2002). Opponent activities of Shh and BMP signaling during floor plate induction in vivo. *Curr Biol* **12**, 47-52.

Pauls, S., Zecchin, E., Tiso, N., Bortolussi, M. and Argenton, F. (2007). Function and regulation of zebrafish nkx2.2a during development of pancreatic islet and ducts. *Dev Biol* **304**, 875-90.

Piedra, M. E. and Ros, M. A. (2002). BMP signaling positively regulates Nodal expression during left right specification in the chick embryo. *Development* **129**, 3431-40.

Pogoda, H. M. and Meyer, D. (2002). Zebrafish Smad7 is regulated by Smad3 and BMP signals. *Dev Dyn* **224**, 334-49.

Prado, C. L., Pugh-Bernard, A. E., Elghazi, L., Sosa-Pineda, B. and Sussel, L. (2004). Ghrelin cells replace insulin-producing beta cells in two mouse models of pancreas development. *Proc Natl Acad Sci U S A* **101**, 2924-9.

Pyati, U. J., Cooper, M. S., Davidson, A. J., Nechiporuk, A. and Kimelman, D. (2006). Sustained Bmp signaling is essential for cloaca development in zebrafish. *Development* **133**, 2275-84.

Roelink, H., Porter, J. A., Chiang, C., Tanabe, Y., Chang, D. T., Beachy, P. A. and Jessell, T. M. (1995). Floor plate and motor neuron induction by different concentrations of the amino-terminal cleavage product of sonic hedgehog autoproteolysis. *Cell* **81**, 445-55.

Ronneberger, O., Liu, K., Rath, M., Ruebeta, D., Mueller, T., Skibbe, H., Drayer, B., Schmidt, T., Filippi, A., Nitschke, R. et al. (2012). ViBE-Z: a framework for 3D virtual colocalization analysis in zebrafish larval brains. *Nat Methods* **9**, 735-42.

Roy, A., Haldar, S., Basak, N. P. and Banerjee, S. (2014). Molecular cross talk between Notch1, Shh and Akt pathways during erythroid differentiation of K562 and HEL cell lines. *Exp Cell Res* **320**, 69-78.

Sasaki, H., Hui, C., Nakafuku, M. and Kondoh, H. (1997). A binding site for Gli proteins is essential for HNF-3beta floor plate enhancer activity in transgenics and can respond to Shh in vitro. *Development* **124**, 1313-22.

Schafer, M., Kinzel, D., Neuner, C., Schartl, M., Volff, J. N. and Winkler, C. (2005). Hedgehog and retinoid signalling confines nkx2.2b expression to the lateral floor plate of the zebrafish trunk. *Mech Dev* **122**, 43-56.

Schier, A. F., Neuhauss, S. C., Harvey, M., Malicki, J., Solnica-Krezel, L., Stainier, D. Y., Zwartkruis, F., Abdelilah, S., Stemple, D. L., Rangini, Z. et al. (1996). Mutations affecting the development of the embryonic zebrafish brain. *Development* **123**, 165-78.

Schmidt, R., Strahle, U. and Scholpp, S. (2013). Neurogenesis in zebrafish - from embryo to adult. *Neural Dev* **8**, 3.

Schulte-Merker, S., Lee, K. J., McMahon, A. P. and Hammerschmidt, M. (1997). The zebrafish organizer requires chordino. *Nature* **387**, 862-3.

Schwend, T., Loucks, E. J. and Ahlgren, S. C. (2010). Visualization of Gli activity in craniofacial tissues of hedgehog-pathway reporter transgenic zebrafish. *PLoS One* **5**, e14396.

Schwitzgebel, V. M. (2001). Programming of the pancreas. *Mol Cell Endocrinol* **185**, 99-108.

Shimojo, H., Ohtsuka, T. and Kageyama, R. (2008). Oscillations in notch signaling regulate maintenance of neural progenitors. *Neuron* **58**, 52-64.

Slack, J. M. (1995). Developmental biology of the pancreas. *Development* **121**, 1569-80.

Song, J. (2007). EMT or apoptosis: a decision for TGF-beta. *Cell Res* **17**, 289-90.

Stipursky, J. and Gomes, F. C. (2007). TGF-beta1/SMAD signaling induces astrocyte fate commitment in vitro: implications for radial glia development. *Glia* **55**, 1023-33.

Sugimura, R. and Li, L. (2010). Noncanonical Wnt signaling in vertebrate development, stem cells, and diseases. *Birth Defects Res C Embryo Today* **90**, 243-56.

Tapia-Gonzalez, S., Giraldez-Perez, R. M., Cuartero, M. I., Casarejos, M. J., Mena, M. A., Wang, X. F. and Sanchez-Capelo, A. (2011). Dopamine and alpha-synuclein dysfunction in Smad3 null mice. *Mol Neurodegener* **6**, 72.

Tehrani, Z. and Lin, S. (2011). Antagonistic interactions of hedgehog, Bmp and retinoic acid signals control zebrafish endocrine pancreas development. *Development* **138**, 631-40.

ten Dijke, P. and Hill, C. S. (2004). New insights into TGF-beta-Smad signalling. *Trends Biochem*

Sci **29**, 265-73.

Thisse, C., Thisse, B., Schilling, T. F. and Postlethwait, J. H. (1993). Structure of the zebrafish snail1 gene and its expression in wild-type, spadetail and no tail mutant embryos. *Development* **119**, 1203-15.

Town, T., Laouar, Y., Pittenger, C., Mori, T., Szekely, C. A., Tan, J., Duman, R. S. and Flavell, R. A. (2008). Blocking TGF-beta-Smad2/3 innate immune signaling mitigates Alzheimer-like pathology. *Nat Med* **14**, 681-7.

Uwe, U. and Thomas, A. (2013). The Role of Smad Proteins for Development, Differentiation and Dedifferentiation of Neurons.

Veien, E. S., Rosenthal, J. S., Kruse-Bend, R. C., Chien, C. B. and Dorsky, R. I. (2008). Canonical Wnt signaling is required for the maintenance of dorsal retinal identity. *Development* **135**, 4101-11.

Villapol, S., Logan, T. T. and Symes, A. J. (2013). Role of TGF-Î² Signaling in Neurogenic Regions After Brain Injury.

Wahl, M. B., Deng, C., Lewandoski, M. and Pourquie, O. (2007). FGF signaling acts upstream of the NOTCH and WNT signaling pathways to control segmentation clock oscillations in mouse somitogenesis. *Development* **134**, 4033-41.

Wang, Z., Li, Y., Banerjee, S. and Sarkar, F. H. (2009). Emerging role of Notch in stem cells and cancer. *Cancer Lett* **279**, 8-12.

Watabe, T. and Miyazono, K. (2009). Roles of TGF-beta family signaling in stem cell renewal and differentiation. *Cell Res* **19**, 103-15.

Wen, S., Li, H. and Liu, J. (2009). Dynamic signaling for neural stem cell fate determination. *Cell Adh Migr* **3**, 107-17.

Wierup, N., Yang, S., McEvilly, R. J., Mulder, H. and Sundler, F. (2004). Ghrelin is expressed in a novel endocrine cell type in developing rat islets and inhibits insulin secretion from INS-1 (832/13) cells. *J Histochem Cytochem* **52**, 301-10.

Wilson, M. E., Scheel, D. and German, M. S. (2003). Gene expression cascades in pancreatic development. *Mech Dev* **120**, 65-80.

Yan, X., Liu, Z. and Chen, Y. (2009). Regulation of TGF-beta signaling by Smad7. *Acta Biochim Biophys Sin (Shanghai)* **41**, 263-72.

Yasunaga, M., Oumi, N., Osaki, M., Kazuki, Y., Nakanishi, T., Oshimura, M. and Sato, K. (2011). Establishment and characterization of a transgenic mouse model for in vivo imaging of Bmp4 expression in the pancreas. *PLoS One* **6**, e24956.

Yee, N. S., Lorent, K. and Pack, M. (2005). Exocrine pancreas development in zebrafish. *Dev Biol* **284**, 84-101.

Zecchin, E., Mavropoulos, A., Devos, N., Filippi, A., Tiso, N., Meyer, D., Peers, B., Bortolussi, M. and Argenton, F. (2004). Evolutionary conserved role of ptf1a in the specification of exocrine pancreatic fates. *Dev Biol* **268**, 174-84.

Zhang, Y., Zhang, Z., Zhao, X., Yu, X., Hu, Y., Geronimo, B., Fromm, S. H. and Chen, Y. P. (2000). A new function of BMP4: dual role for BMP4 in regulation of Sonic hedgehog expression in the mouse tooth germ. *Development* **127**, 1431-43.

Zhou, Y., Cashman, T. J., Nevis, K. R., Obregon, P., Carney, S. A., Liu, Y., Gu, A., Mosimann, C., Sondalle, S., Peterson, R. E. et al. (2011). Latent TGF-beta binding protein 3 identifies a second heart field in zebrafish. *Nature* **474**, 645-8.